

Fundamental study on co-gasification of biomass with coal

KIHEDU, Joseph

Fundamental study on co-gasification of biomass with coal

バイオマスと石炭の共ガス化に関する基礎的研究

KIHEDU, Joseph

Department of Mechanical Science and Engineering
Graduate School of Engineering
Nagoya University
March 2013

CONTENTS

1	Introduction	1
1.1	Biomass and coal	1
1.1.1	Resources and utilization	1
1.1.2	Basic properties	3
1.2	Biomass and coal gasification	6
1.2.1	Fundamentals of gasification process	6
1.2.2	Co-gasification of biomass and coal	7
1.2.3	Salient features of the packed bed gasification	8
1.3	Objectives of this study	10
1.4	Outlines of the thesis	11
	References	12
2	Effects of gasifying agents on biomass gasification; thermo-gravimetric basis	16
2.1	Introduction	16
2.2	Experimental methods	17
2.2.1	Properties of the sample	17
2.2.2	Gasification and pyrolysis experiments	17
2.2.3	Morphology investigation by Scanning Electron Microscope (SEM)	18
2.3	Results and discussion	19
2.3.1	Conversion behaviors	19
2.3.2	Morphology changes	22
2.4	Summary	26
	References	27
3	Co-gasification of biomass with coal; thermo-gravimetric basis	29
3.1	Introduction	29
3.2	Experimental methods	30
3.2.1	Properties of the samples	30
3.2.2	Gasification experiments	30
3.2.3	Analysis of conversion and extent of synergy	32
3.2.4	Morphology investigation by Scanning Electron Microscope (SEM)	33
3.3	Results and discussion	34
3.3.1	Conversion behaviors during co-gasification of cedar with coal	34
3.3.2	The extent of synergy	36
3.4	Elucidating the synergy mechanism	38
3.4.1	Flue gas evolution and hydrogen transfer mechanism	39

3.4.2	Co-gasification of simulated ligno-cellulosic biomass with coal	42
3.5	Morphology changes during co-gasification process	46
3.5.1	Morphology changes in biomass and coal blends	46
3.5.2	Morphology changes in simulated biomass and coal blends	49
3.6	Summary	54
	References	56
4	Gasification of biomass in the auto-thermal packed bed reactor	59
4.1	Introduction	59
4.2	Experimental methods	59
4.2.1	Properties of the sample	59
4.2.2	Experimental set-up	60
4.2.3	Gasification and tar sampling procedures	62
4.2.4	Analysis of performance factors	64
4.3	Results and discussion	65
4.3.1	Temperature and gas compositions during downdraft gasification	65
4.3.2	Temperature and gas compositions during updraft gasification	68
4.3.3	Tar contents and performance factors	70
4.3.4	Tar reduction by steam injection	72
4.4	Summary	73
	References	74
5	Co-gasification of biomass and coal in the auto-thermal packed bed reactor	75
5.1	Introduction	75
5.2	Experimental methods	76
5.2.1	Properties of the samples	76
5.2.2	Improved experimental set-up and stoichiometric air ratio	77
5.2.3	Gasification and tar sampling procedures	79
5.2.4	Analysis of performance factors and synergetic aspects	81
5.3	Results and discussion	82
5.3.1	Temperature and gas compositions during biomass gasification	82
5.3.2	Temperature and gas compositions during co-gasification	85
5.3.3	Temperature and gas inside the reactor	87
5.3.4	Tar contents and performance factors	91
5.4	Summary	95
	References	95
6	Conclusions	97
	Acknowledgements	100

Chapter 1

Introduction

1.1 Biomass and coal

1.1.1 Resources and utilization

Biomass and coal, both are carbonaceous solid fuels. Biomass is an organic resource available as plant or animal matters and the related waste streams [1]. Specifically, biomass includes forest products, agricultural wastes, municipal and industrial organic wastes. On the other hand, coal originates from fossilized bio-resources which, in millions of years, went through geological alteration covering compression and heating however spared from bio-degradation and oxidation [2]. According to coal development under these processes, low to high rank coal are available as peat, lignite, sub-bituminous, bituminous and anthracite.

Biomass is the earliest energy source for humankind. So far, biomass still accounts for 14% of the world's primary energy consumption and 35% in developing countries [3]. Figure 1-1(a) shows that Tanzania depends on biomass by 90% [4]. In 2009, biomass contributed about 1,500 million tons of oil equivalent (Mtoe) out of 12,000 Mtoe total world energy consumption as shown in Figure 1-2 [5]. Biomass is used for domestic and industrial heating through combustion. CO₂ produced during combustion can be consumed during photosynthesis to reproduce biomass. Therefore biomass is a renewable energy source and biomass utilization can be considered to be carbon neutral [6].

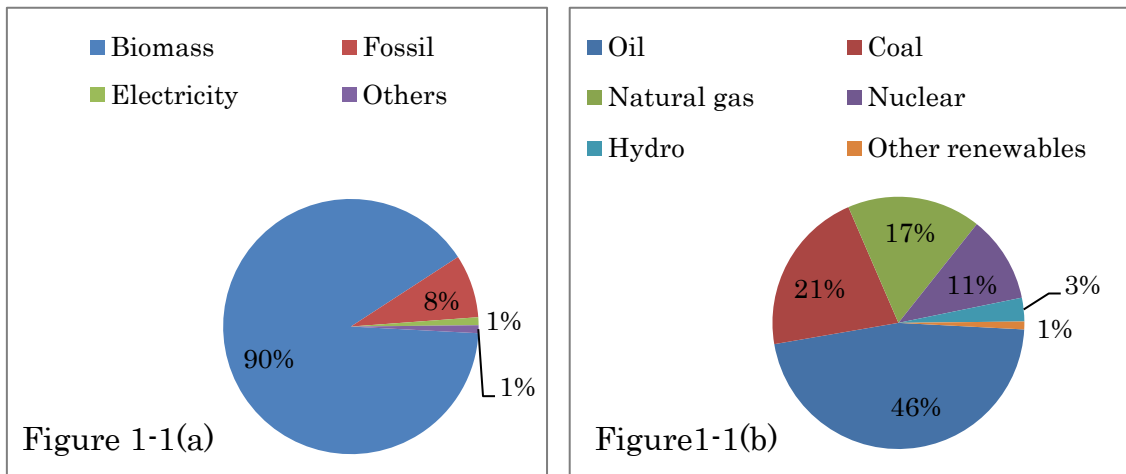


Figure 1-1. Primary energy consumption in (a) Tanzania [4] (b) Japan [5,7]

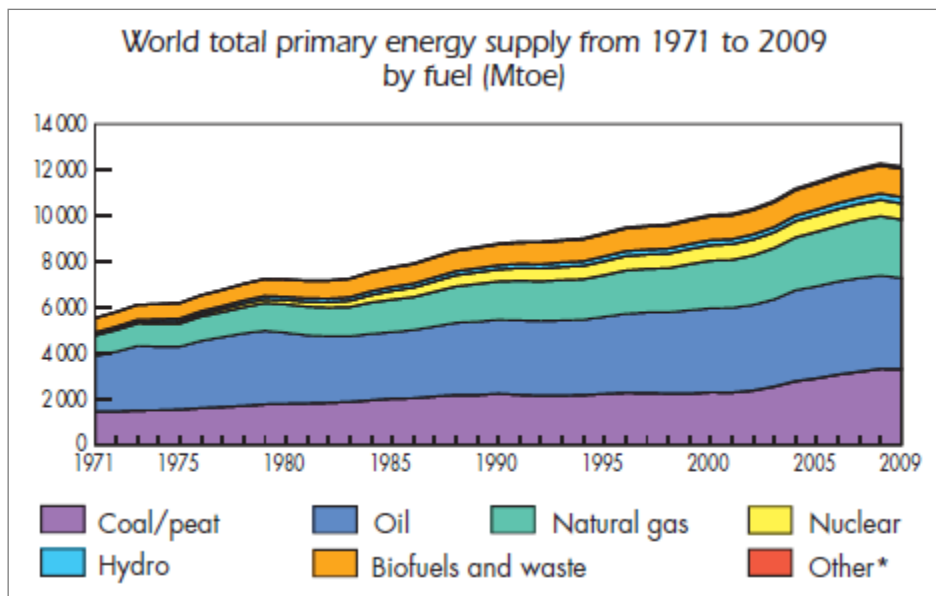


Figure 1-2. World energy consumption in million tons of oil equivalent (Mtoe) [4]

Proved coal reserves are estimated to be about 890 trillion tones while reserve to production ratio shows that these reserves will last for 102 years [7]. Coal consumption was around 139 quadrillion Btu in 2008. Coal contributes to about 28% of the total energy consumption and 37% for power generation. Coal is mainly utilized for power generation but also in steel industry. The U.S. as the world's

largest electricity consumer depends on coal contribution of about 48% for power production [7]. Japan, the second largest steel producer, consumed 4.9 quadrillion Btu coal in 2008 [5,7]. This is equivalent to 21% of the total Japan's primary energy consumption (see Figure 1-1(b)). Figure 1-2 suggests that despite of the call to shift to the renewable energy, the global energy demand continues to depend on coal.

In addition to combustion, solid biomass or coal can be converted to gas or oil through various thermal-chemical methods. Gasification, for example, allows processing a wide range of biomass feedstock at a higher efficiency. As opposed to direct combustion, gasification offers opportunity for gas cleaning to reduce H₂S, COS, HCN and NH₃ which are unfriendly to the environment [2].

1.1.2 Basic properties

Plant biomass is mainly composed up of lignin and holocellulose in addition to xylan [8,9]. Between the plant cell walls, the *vacuole* appear as hollow section of the cell while *plasmodesmata* are the small holes which interconnects the two adjacent cells. Plant cell structure is reinforced by primary wall composed of lignin while secondary wall is rich in cellulose (Figure 1-3). Compositions of lignin and cellulose are crucial factors in biomass reactivity [10,11,12]. Biomass with high cellulose content is relatively more reactive than biomass with higher lignin content [11,13]. Hemicellulose decomposes at lower temperatures around 250 °C to 300 °C. Cellulose decomposes fast between 300 °C and 400 °C while lignin decomposes slowly from 250 °C to 500 °C [11,13,14]. Yang *et al.*, argued on even wider decomposition temperature range for lignin, extending from 100 °C to 900 °C [12].

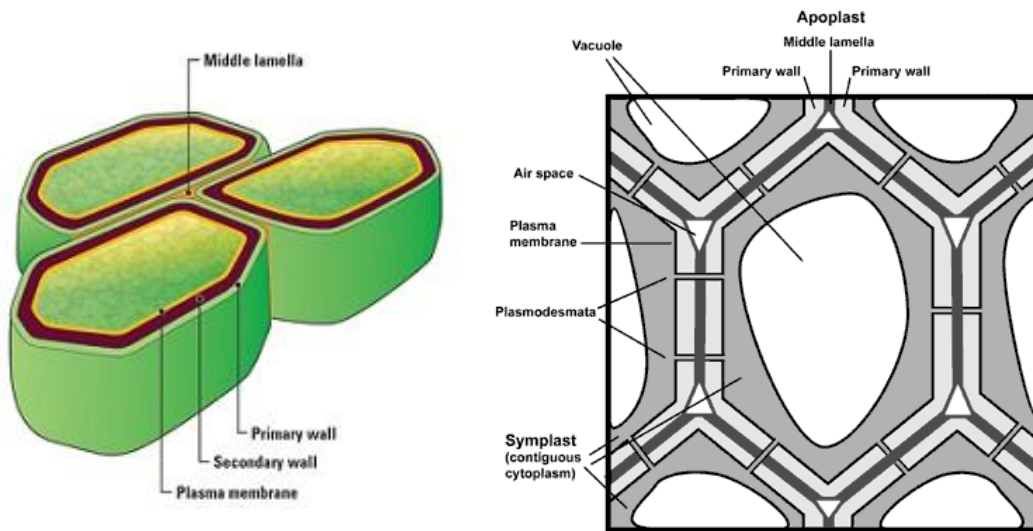


Figure 1-3. Plant biomass cell structure [9]

In comparison to coal, biomass generally has higher volatile contents, lower ash contents and negligible sulfur contents. Volatile matter consists of aliphatic carbon atoms that are driven off when solid fuels are heated to around 500°C in the absence of air. Having higher volatile contents, biomass produced more tar while no tar is given off by anthracite [15]. Ash and moisture contents reduce the heating value, raise transportation payload and affect boiler or gasifier performance [16]. Sulfur is probably the most important contaminant in coal as it leads into production of SO₂, H₂S and COS. Van Krevelen diagram [17] shows that biomass has higher hydrogen to carbon and oxygen to carbon ratios in comparison to coal as shown in Figure 1-4.

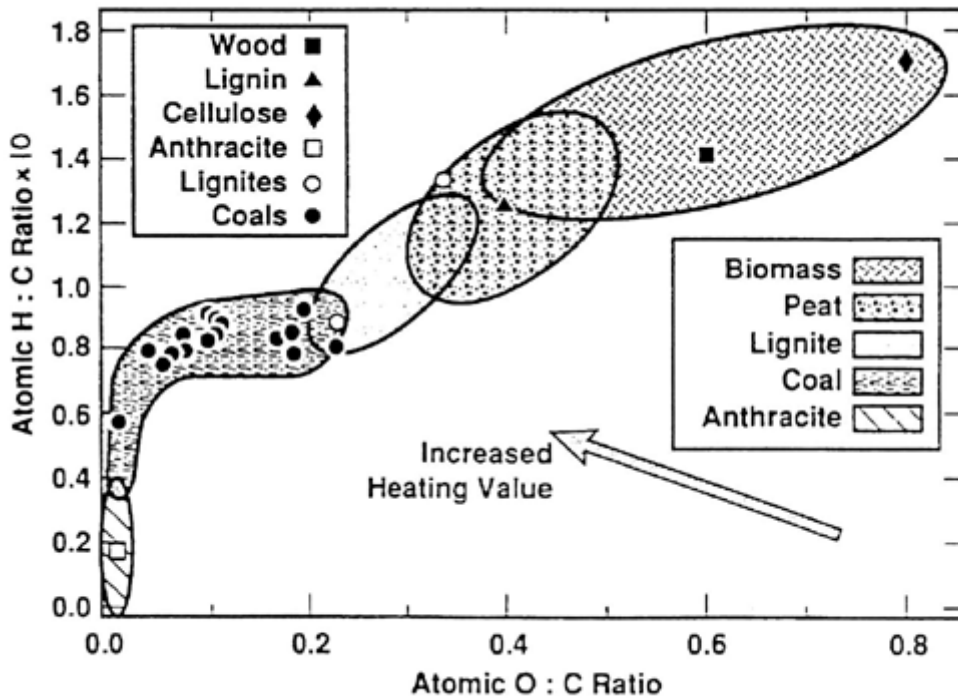


Figure 1-3. Van Krevelen diagram [17]

Heating values of coal tend to increase with ranking while moisture contents decrease as shown in Table 1-1 [15]. Therefore coal with high moisture and ash contents are considered to be low grade coal. Peat is the lowest ranked coal composed of vegetable material containing roots of living things. Lignite is brown, soft and it has high moisture content. Anthracite is black, hard and virtually has no moisture content. Coal as organic deposit is made up of three organic grains known as macerals namely; liptinite, vitrinite and inertinite [2]. Liptinites are dark gray and hydrogen-rich macerals originating from plant pollens and resins. Vitrinite are light gray in color and hails from wood and bark. Inertinite are oxidation product, or say, fossil charcoal which is rich in carbon.

Table 1-1. Typical coal compositions [15]

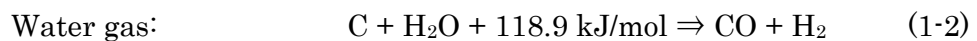
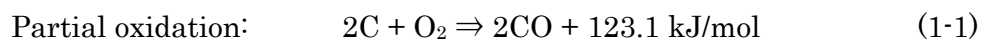
	Heat value (MJ/kg)	Moisture (%)	Fixed carbon (%)	Ash (%)	Sulfur (%)
Anthracite	Up to 32	< 15	85 - 98	10 - 20	0.6 - 0.8
Bituminous	24 - 28	2 - 15	45 - 85	3 - 12	0.7 - 4.0
Sub-bituminous	22 - 24	10 - 45	35 - 45	≤ 10	< 2
Lignite	8 - 10	30 - 60	25 - 35	10 - 50	0.4 - 1.0

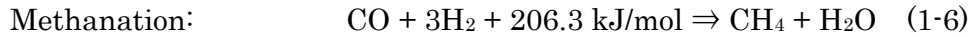
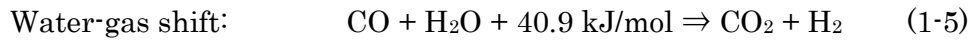
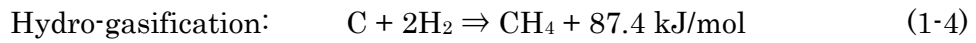
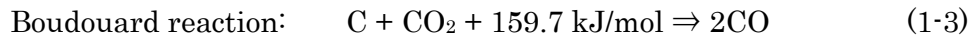
1.2 Biomass and coal gasification

1.2.1 Fundamentals of gasification

Gasification refers to a process of converting carbonaceous materials to a combustible synthetic gas (syngas), composed of H₂ and CO. In contrast to combustion, gasification process operates with sub-stoichiometric conditions. Therefore oxygen supply during gasification is limited to approximately 35% of that required for complete combustion [2]. This process involves reaction of carbon with air, enriched air, oxygen, steam or carbon dioxide. Gasification by using air leads to dilution of syngas heating value by high nitrogen composition [16]. In addition to that, nitrogen needs sensible heat to raise it to the gasification reaction temperature.

Typical gasification reactions are shown as Equation (1-1) to Equation (1-6) below. For the case self-heated i.e. auto-thermal gasification process, energy balance for exothermic reactions (Equation 1-1, 1-4, 1-5) and endothermic reactions (Equation 1-2, 1-3, 1-6) is necessary. Reaction 1-2 requires high temperature while reaction 1-4 occurs at high pressures [2].





Theoretically, gasification process can be split into three main sequential processes; drying, pyrolysis and char reduction. Thus during gasification, firstly moisture is released, then volatile matters are evolved and finally the residual char is reduced. It can be noted that decomposed volatiles can form gases or can undergo condensation and polymerization to form tar [2]. Tar refers to oxygenated aromatic constituents which can condense at low temperatures. Therefore in case of syngas application in engine, tar can get deposited to cause engine troubles [16]. Tar is also detrimental to performance of fuel cell and even to gasification catalysts. In addition to that, tar formation represents low conversion to gas and hence low gasification efficiency.

1.2.2 Co-gasification of biomass and coal

Biomass energy qualifies for Renewables Obligation and Climate Change benefits [18]. However, one of the most important barriers to an accelerated penetration of biomass conversion technologies is that of inadequate supply in some regions. In Germany, all industrial wood waste and other wood residues are consumed completely and there is no other clean biomass available to increase the contribution of biomass energy [19]. In addition to that, biomass has low energy density. During gasification, biomass generates syngas with high tar content than

coal gasification as shown in Table 1-2 [2]. On the other side, coal is not a renewable energy. Also, coal is less reactive than biomass therefore requires higher reaction temperature (Table 1-2).

Table 1-2. Comparison of biomass and coal gasification [2]

	Biomass gasification	Coal gasification
Gas heating value (MJ/m ³ _N)	3 – 8	4 – 12
Tar generation (g/m ³ _N)	5 - 30	5 - 30
Reaction temperature (°C)	700 - 1200	900 - 1500
Syngas contaminants	Fly ash, NH ₃ , HCN	Fly ash, SO _x , H ₂ S, COS

To effectively exploit biomass as renewable energy while overcoming its potential unreliability by supplementary reliable coal supply, co-processing of biomass and coal is considered [6,20]. Further advantages of co-gasification consist of the reduction of overall energy production cost. Since hydrogen to carbon ratio in biomass and coal is much different [17], unexpected reactivity improvement or limitation under co-processing can occur. Various researchers have reported that reactivity improvement is associated with solid or gaseous interactions or due to catalytic effect of inherent mineral matters [20,21,22]. However, other research works indicate that there are neither significant interactions nor conversion synergy during co-gasification of biomass with coal [23,24,25].

1.2.3 Salient features of the packed bed gasification

Various gasifiers have been designed and tested. However, in this study we have used packed bed gasifier which has a simple structure and is characterized by simple operation and maintenance. Usually, the packed bed can be operated by

using downdraft or updraft modes. These modes are named from the directions of gas flow inside the upright standing reactor that is either downwards or upwards (Figure 1-5). Downdraft and updraft operation modes for biomass gasification in the packed bed reactor have extensively been reported [26,27,28]. Under both of the operation modes, if the solid fuel is fed from the top of the reactor, then reaction zones in a top to bottom arrangement are; drying, pyrolytic reactions and char reduction zone [26]. In addition to these reaction zones, during auto-thermal gasification process, combustion zone would occur either at the top or at the bottom of the packed bed during downdraft or updraft gasification, respectively.

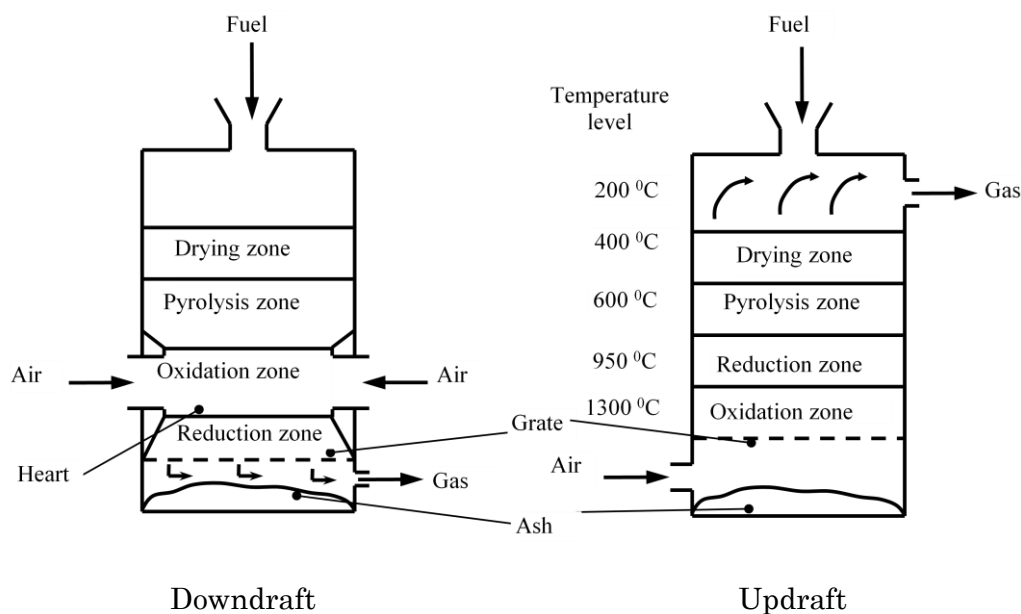


Figure 1-5: Schematic diagrams of downdraft and updraft gasifiers [29].

To understand the packed bed gasification process, various researchers have embarked on investigating various parameters. Most of researchers have preferred to work with downdraft gasification rather than updraft gasification [26,27,28]. This is due to relatively lower tar generation during downdraft gasification under

which further tar cracking occurs as product gasses pass through the high temperature reduction zone packed with charred biomass [30]. As opposed to that, pre-mature escaping of product gasses under updraft gasification results into high tar content of the syngas. However, updraft gasification produces syngas with favorably slightly higher syngas lower heating value (LHV).

1.3 Objectives of this study

In pursuit of renewable energy utilization and the need to meet the energy demand by using the abundant coal, co-gasification is considered [6,20,21]. However, when biomass and coal are co-gasified, the resulting behaviors covering occurrence of synergy and mechanism of interaction, have not clearly been understood [20,31]. So far, not only correlating results but also controversial findings have been reported rendering co-gasification behavior inconclusive unless for specific experimental conditions, parameter analyzed, techniques or samples used. Therefore, it is important that the occurrence of synergy, if any, be confirmed, quantified and the underlying mechanism be discussed in details.

The objective of this research is to investigate co-gasification characteristics of biomass and coal. Thermo-gravimetical methods have been used to study conversion characteristics, gas evolution and morphology changes. Also, the packed bed reactor has been used for investigating gas compositions, temperature variations and tar contents. Syngas LHV, cold gas efficiency and carbon conversion were also analyzed. In addition, this study realizes improvement of gasification method targeting at tar reduction and syngas LHV enhancement.

1.4 Outline of the thesis

Chapter 1 presents the introduction and background of the research. This chapter presents the review of the previous studies and the objectives of this research.

Chapter 2 discusses on effect of gasification agents, i.e. CO₂ and steam, on gasification of biomass based on thermo-gravimetric methods. It presents conversion ratios and morphology changes during biomass gasification. Pyrolysis conducted in N₂ atmosphere provides the basis for realizing the effects of gasification agents. Results obtained from this chapter, provide the basis for selection of gasifying agent for investigation of co-gasification characteristics in Chapter 3.

Chapter 3 deliberates on thermo-gravimetric characteristics for co-gasification of biomass with coal. Results presented on this chapter include conversion ratios, gas evolution and morphology changes during co-gasification process. The differences between co-gasification conversion and the average conversion calculated from separate biomass gasification and coal gasification are discussed. The contribution of volatile interaction and catalytic effects of alkali and alkaline earth metals (AAEM) is shown by using simulated biomass, i.e. acid washed cellulose [32] that has high volatile matter and Na rich lignin chemicals.

Chapter 4 covers on downdraft and updraft gasification of biomass by using the packed bed reactor. Analyses performed include syngas compositions, tar generation as well as temperature profiles and gas concentration in the reactor. In addition to that, syngas LHV, cold gas efficiency and carbon conversion are also presented.

Chapter 5 features on co-gasification of biomass with coal in the packed bed gasifier. With the aim of improving gas LHV and reducing tar generation, the packed bed gasifier was modified to allow combination of downdraft and updraft gasification, i.e. counter-flow gasification. Then biomass gasification and co-gasification of biomass with coal were conducted. Results discussed in this chapter include gas composition, temperature variations, tar contents, Syngas LHV, cold gas efficiency and carbon conversion.

Chapter 6 summarizes conclusions drawn from chapter 2, 3, 4 and 5.

References

- [1] Balat M, Ayar G, Biomass energy in the world, use of biomass and potential trends. *Energy Sources*, 2005, 27, 931-940.
- [2] Rezaiyan J, Cheremisinoff NP, *Gasification technologies; a primer for engineers and scientists*. Boca Raton: Taylor and Francis, 2005.
- [3] *Key World Energy Statistics*, International Energy Agency, 2011.
- [4] Mkilaha ISN, Nzali AH, *Energy crisis and the Tanzanian economy*. Commission for Science and Technology, 2007.
- [5] *International Energy Outlook*, U.S. Energy Information Administration, 2011.
- [6] Howaniec N, Smolinski A, Stanczyk K, Pichlack M. Steam co-gasification. *International Journal of Hydrogen Energy*, 2011, 26, 14455-14463.
- [7] *Statistical Review of World Energy*, BP, 2012.
- [8] L. Salmén, "Micromechanical understanding of the cell-wall structure," *Comptes Rendus Biologies*, 2004, 327, 873-880.
- [9] Somerville C, Bauer S, Brininstool G, Facette M, Hamann T, Milne J, Osborne

- E, Paredez A, Persson S, Raab T, Towards a Systems Approach to Understanding Plant Cell Walls. *Science*, 2004, 306, 2206–2211.
- [10] Gani A, Naruse I, Effect of cellulose and lignin content on pyrolysis and combustion characteristics for several types of biomass. *Renewable Energy*, 2007, 32, 649-661.
- [11] Lv D, Xu M, Liu X, Zhan Z, Li Z, Yao H, Effect of cellulose, lignin, alkali and alkaline earth metallic species on biomass pyrolysis and gasification. *Fuel Processing Technology*, 2009, 91, 903-909.
- [12] Yang H, Yan R, Chen H, Lee DH, Zheng C, Characteristics of hemicellulose, cellulose and lignin pyrolysis. *Fuel*, 2007, 86, 1781-1788.
- [13] Gottipati R, Mishra S, A kinetic study on pyrolysis and combustion characteristics of oil cakes: Effect of cellulose and lignin content. *Journal of Fuel Chemistry and Technology*, 2011, 39, 265-270.
- [14] Haykiri-Acma H, Yaman S, Kucukbayrak S, Comparison of the thermal reactivities of isolated lignin and holocellulose during pyrolysis. *Fuel Processing Technology*, 2010, 91, 759-764.
- [15] Bowen BH, Irwin MW, Coal Characteristics. CCTR Basic Facts File # 8, Indiana Center for Coal Technology Research. 2008.
- [16] Kumar A, Jones DD, Hanna MA, Thermochemical Biomass Gasification: A Review of the Current Status of the Technology. *Energies* 2009, 2, 556-581.
- [17] Van Krevelen DW, Organic Chemistry – old and new. *Organic Chemistry*, 1984, 6, 1-10.
- [18] Cleaner Coal Technology Programme (CCTP), Waste or biomass co-gasification with coal. Technology Status Report 017, DTI/Pub URN 02/787,

London, UK.

- [19] Pinto F, Franco C, Andre RN, Tavares C, Dias M, Gulyurtlu I, Cabrita I, Effect of experimental conditions on co-gasification of coal, biomass and plastics wastes with air/steam mixtures in a fluidized bed system. *Fuel*, 2003, 82, 1967–1976.
- [20] Sonobe T, Worasuwanarak N, Pipatmanomai S. Synergies in co-pyrolysis of Thai lignite and corncob. *Fuel Processing Technology* 2008, 89, 1371-1378.
- [21] Zhu W, Song W, Lin W, Catalytic gasification of char from co-pyrolysis of coal and biomass. *Fuel Processing Technology*, 2008, 89, 890-896.
- [22] Haykiri-Acma H, Yaman S. Interaction between biomass and different rank coals during co-pyrolysis. *Renewable Energy*, 2010, 35, 288-292.
- [23] Pan YG, Velo E, Roca X, Manya JJ, Puigjaner L. Fluidized-bed co-gasification of residual biomass/poor coal blends for fuel gas production. *Fuel* 2000, 79, 1317-1326.
- [24] Kastanaki E, Vamvuka D, Grammelis P, Kakaras E. Thermogravimetric studies of the behavior of lignite–biomass blends during devolatilization. *Fuel Processing Technology*, 2002, 77, 159-166.
- [25] Meesri C, Moghtaderi B. Lack of synergetic effects in the pyrolytic characteristics of woody biomass/coal blends under low and high heating rate regimes. *Biomass Bioenergy*, 2002, 23, 55-66.
- [26] Bunt JR, Waanders FB. Identification of the reaction zones occurring in a commercial-scale Sasol–Lurgi FBDB gasifier. *Fuel*, 2008, 87, 1814–1823.
- [27] Pérez JF, Melgar A, Benjumea PN. Effect of operating and design parameters on the gasification/combustion process of waste biomass in fixed bed

- downdraft reactors: An experimental study. *Fuel*, 2012, 96, 487–496.
- [28] Simone M, Barontini F, Nicoletta C, Tognotti L, Gasification of pelletized biomass in a pilot scale downdraft gasifier, *Bioresour Technol*, 2012, 116, 403-412.
- [29] Fock F, Kirstine PB, Thomsen KPB, Houbak N, Henriksen U, Modelling a biomass gasification system by means of engineering equation solver. SIMS Conference, 2000, Technical University of Denmark, Denmark.
- [30] Brandt P, Larsen E, Henriksen U, High tar reduction in a two-stage gasifier. *Energy and Fuels*, 2000, 14, 816-819.
- [31] Xu Q, Pang S, Levi T. Reaction kinetics and producer gas compositions of steam gasification of coal and biomass blend chars, part 1: Experimental investigation. *Chemical Engineering Science* 2011, 66, 2141-2148.
- [32] Sigma-Aldrich, product number 22182, http://www.sigmaaldrich.com/catalog/search?interface=All_JA&term=cellulose&lang=ja®ion=JP&focus=product&N=0 accessed on December 6, 2012.

Chapter 2

Effects of gasifying agents on biomass gasification; thermo-gravimetric basis

2.1 Introduction

Biomass gasification characteristics depend on various factors such as gasifying agents, chemical compositions, reaction temperature, residence time and morphology of the fuel particles [1,2,3]. Regarding chemical compositions, cellulose and lignin affect decomposition behavior as detailed in section 1.1.2. The effects of temperature, residence time and morphology have been reported elsewhere [3,4,5]. Gasifying agents affect surface and intrinsic char reduction reactions. These reactions proceed very slowly, except at very high temperature, therefore appropriate choice of gasifying agent is an important factor for gasification process. Gasifying agents can build-up a competitive but also inhibitive medium, therefore enhance or hinder the gasification reactions [1,6,7].

This chapter discusses on effects of gasification agents, i.e. CO₂ and steam, on conversion ratios and morphology changes during biomass gasification. To realize such effects, pyrolytic characteristics of biomass in N₂ atmosphere are taken as the basis for comparison of CO₂ and steam gasification environments. As such, pyrolysis refers to thermal decomposition of solid fuels taking place within non-reactive medium while gasification uses a sub-stoichiometric medium [2,8]. Results obtained from this chapter, provide the basis for selection of gasifying agent for investigation of co-gasification characteristics in Chapter 3.

2.2 Experimental methods

2.2.1 Properties of the sample

Japanese cedar (*cryptomeria japonica*) was milled to 150 μm and stored in a desiccator to avoid moisture contamination. Proximate analysis and ultimate analysis of Japanese cedar are shown in Table 2-1 while ash analysis is presented in Table 2-2.

Table 2-1. Proximate analysis and ultimate analysis for cedar

Proximate analysis (wt %)				Ultimate analysis (wt %)				
As received	Dry basis			Dry ash free basis				Balance
Moisture	VM ^a	FC ^b	Ash	C	H	N	S	O
3.90	82.09	15.79	2.13	47.56	5.66	0.27	-	46.51

^aVM represents volatile matter

^bFC represents fixed carbon

Table 2-2. Ash analysis for cedar

	SiO ₂	Al ₂ O ₃	CaO	TiO ₂	Fe ₂ O ₃	MgO	Na ₂ O	K ₂ O	P ₂ O ₅	SO ₃
wt %	24.51	4.67	25.99	0.26	4.98	5.89	3.13	19.13	1.66	3.32

2.2.2 Gasification and pyrolysis experiments

Gasification or pyrolysis of about 10 mg samples was conducted by using Shimadzu Thermo-Gravimetric Analyzer (TGA) in a top-bottom setting of gasifying agent and a platinum sample pan. Heating rate from ambient temperature to 1,000 °C was set at 20 °C/min, however holding at 107 °C for 10 min to ensure complete removal of moisture contents. In order to counter check for replicability of the results, gasification experiments were also conducted at 5 °C/min. Under both

heating rate conditions, when 1,000 °C was attained, constant temperature gasification was allowed to proceed until no mass loss was observed.

During steam gasification, WORKlab water pump was used to supply distilled water to a steam generator set at 300 °C. To avoid steam condensation within TGA reactor at lower temperature ranges, only N₂ at 150 mL_N/min was supplied from ambient temperature to 200 °C. Thereafter, N₂ flow was reduced to 75 mL_N/min, however the remaining 75 mL_N/min was maintained as purge gas and steam carrier throughout the gasification process. Meanwhile, 75 mL_N/min of gasifying agent was supplied to allow gasification reactions to proceed. For rational comparison basis with steam gasification case, CO₂ was also introduced at 200 °C. During pyrolysis, N₂ at 150 mL_N/min was supplied throughout the experiment.

Conversion X (wt %) was derived from mass decomposition during gasification or pyrolysis as follows;

$$X = 1 - m/m_o \quad (2-1)$$

where m and m_o (both in g) represent mass of the sample on d.a.f. basis at a certain temperature and at initial condition, respectively.

2.2.3 Morphology investigation by Scanning Electron Microscope (SEM)

Raw samples for morphology investigation were dried in Yamato constant temperature oven set at 60 °C for 24 hours. Other samples were partially gasified or pyrolyzed to 700 °C or to 900 °C at 20 °C/min. Residues from partial gasification at these temperature ranges were considered to have consistent morphology, well developed shapes and contain significant amount of combustible contents rather than ash. During partial gasification or pyrolysis, temperature profile as well as

flow rates for gasifying agents and/or N₂ respectively, were similar to those applied during complete gasification or pyrolysis experiments. When the target temperature was attained during partial gasification, heating and supply of CO₂ or steam was terminated. For the case of pyrolysis, heating was terminated after holding the sample at 1,000 °C for 10 minutes. Residues after partial gasification or pyrolysis were allowed to cool under 150 mL_N/min supply of N₂.

Before SEM investigation, dried or partially gasified samples were carbon coated in order to improve their visibility for SEM. SEM images of the residues were taken at 300 times magnification however 1,500 times magnification was preferred for unveiling more visible surface structures. It can be noted that due to high temperature and possible presence of residual steam or CO₂ during gasification, it is most likely that further conversion of the residues occurred at initial stage of the cooling process to affect their morphology.

2.3 Results and discussion

2.3.1 Conversion behaviors

Conversion was calculated from mass decomposition data by using Equation 2-1. Figure 2-1 shows conversion characteristics during gasification and pyrolysis experiments at 20 °C/min. It was observed that initial conversion of cedar is marked by fast decomposition of volatile matters that ended-up at around 500 °C during pyrolysis, CO₂ gasification and steam gasification, respectively. At these temperatures, corresponding conversions were 65%, 69% and 72%. These results suggest slight effect of gasifying agent during volatile matter decomposition, steam being more favorable. The observed conversion, however, is less than the total

volatile matter content which accounts for 82% of cedar d.a.f. weight (Table 2-1). This difference is due to slower decomposition of lignin which require even higher decomposition temperature [4,9]. Therefore, even under pyrolytic conditions, cedar continue to decompose slowly at higher temperatures.

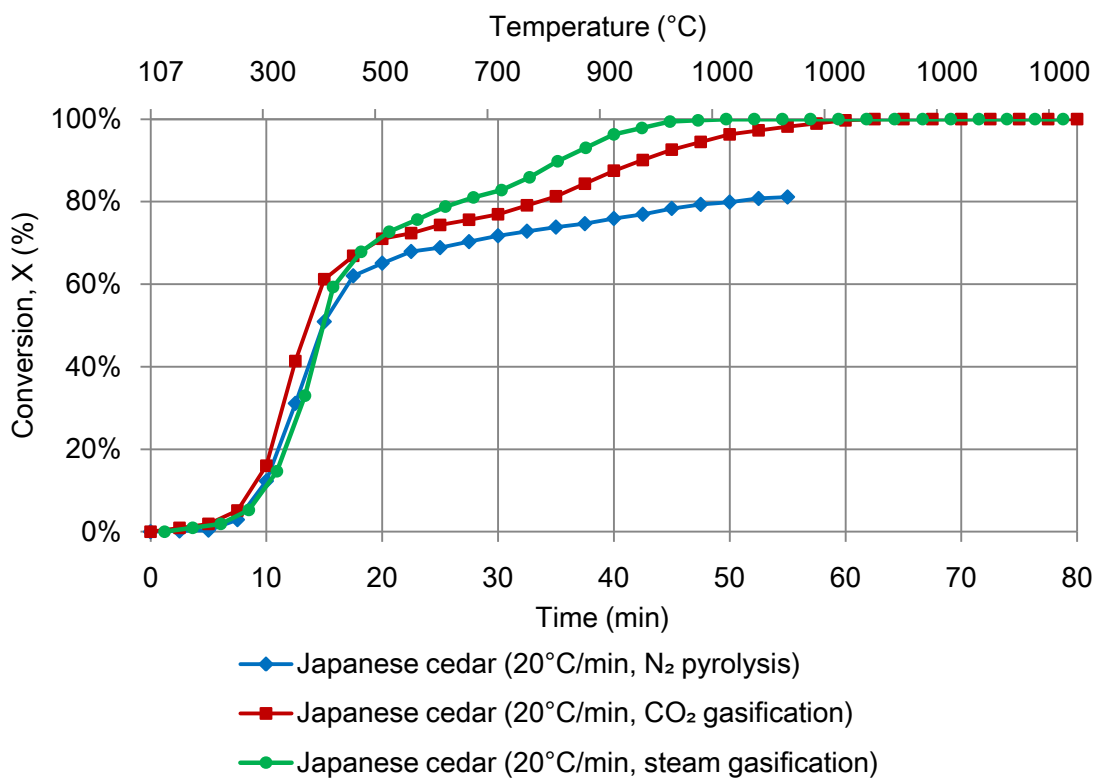


Figure 2-1. Conversion characteristics of cedar during N₂ pyrolysis, CO₂ gasification and steam gasification at 20 °C/min.

Char gasification stage under CO₂ and steam environment is marked by slow conversion starting from around 750 °C (Figure 2-1). When 1,000 °C was attained, conversion was 92% and 99% for CO₂ gasification and steam gasification, respectively. Under CO₂ gasification, 100% conversion was attained 20 minutes later after constant temperature gasification at 1,000 °C. Apparently, cedar reacts

faster under steam gasification than under CO₂ environment during char reduction. This result corresponds to drastic changes during biomass gasification observed by Dufour *et al.* [3] and steam affinity to char gasification reported by Fushimi et al [7]. On the other side, the observed slow CO₂ gasification can be associated with slower C-CO₂ reactions [10] rather than inhibition by higher concentration of CO which is not likely to occur under TGA conditions used [1,7].

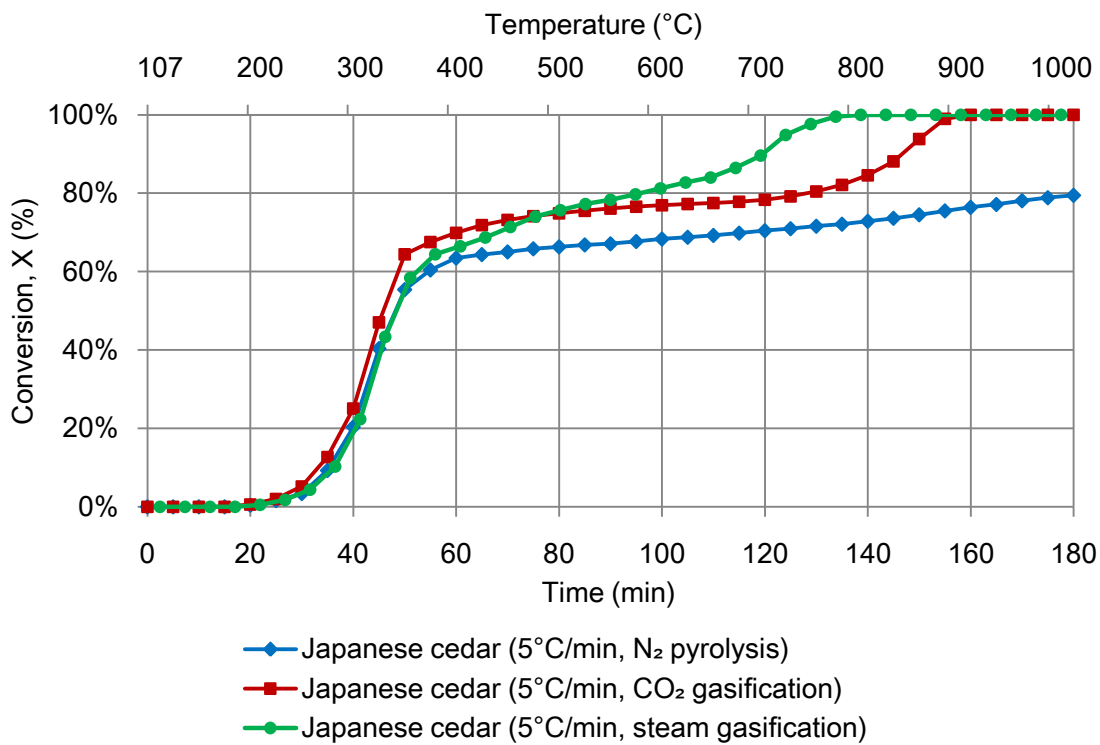


Figure 2-2. Conversion characteristics of cedar during N₂ pyrolysis, CO₂ gasification and steam gasification at 5 °C/min.

Figure 2-2 shows conversion during slow pyrolysis, CO₂ gasification and steam gasification at 5 °C/min. This figure shows almost similar conversion trends for pyrolysis as presented in Figure 2-1. However, as a result of longer residence

time, char gasification occurs at lower temperatures under CO₂ and steam environment [1,6,11]. Nevertheless, enhanced reactivity of biomass during steam gasification was confirmed.

2.3.2 Morphology changes

Investigation of morphology change included raw samples as well as partially gasified samples. Figure 2-3(a) and Figure 2-3(b) show SEM images of raw Japanese cedar woody particle in longitudinal and cross-sectional views, respectively. Cedar morphology shows fiber based structure with multiple tube-like cells [8,9].

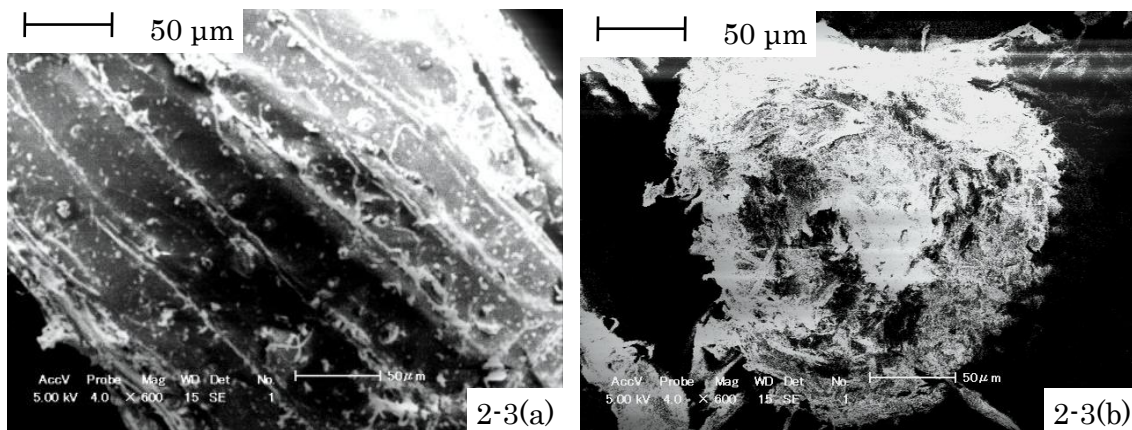


Figure 2-3. SEM images of raw cedar particles; (a) longitudinal view, (b) cross-sectional view.

After partial gasification under CO₂ environment, cedar particles reveals slight morphological changes as shown in Figure 2-4. Figure 2-4(a) shows SEM images of Japanese cedar particle gasified to 700 °C under CO₂ environment. A magnified surface image was taken from the solid rectangular boundary inset in

this figure, is presented in Figure 2-4(b). In comparison to the raw cedar presented in Figure 2-3(a), notable changes include slight fiber shrinkage and appearance of the *plasmodesmata* [12,13] seen as round marks. These changes correspond to about 75% conversion attained by cedar at 700 °C (Figure 2-1).

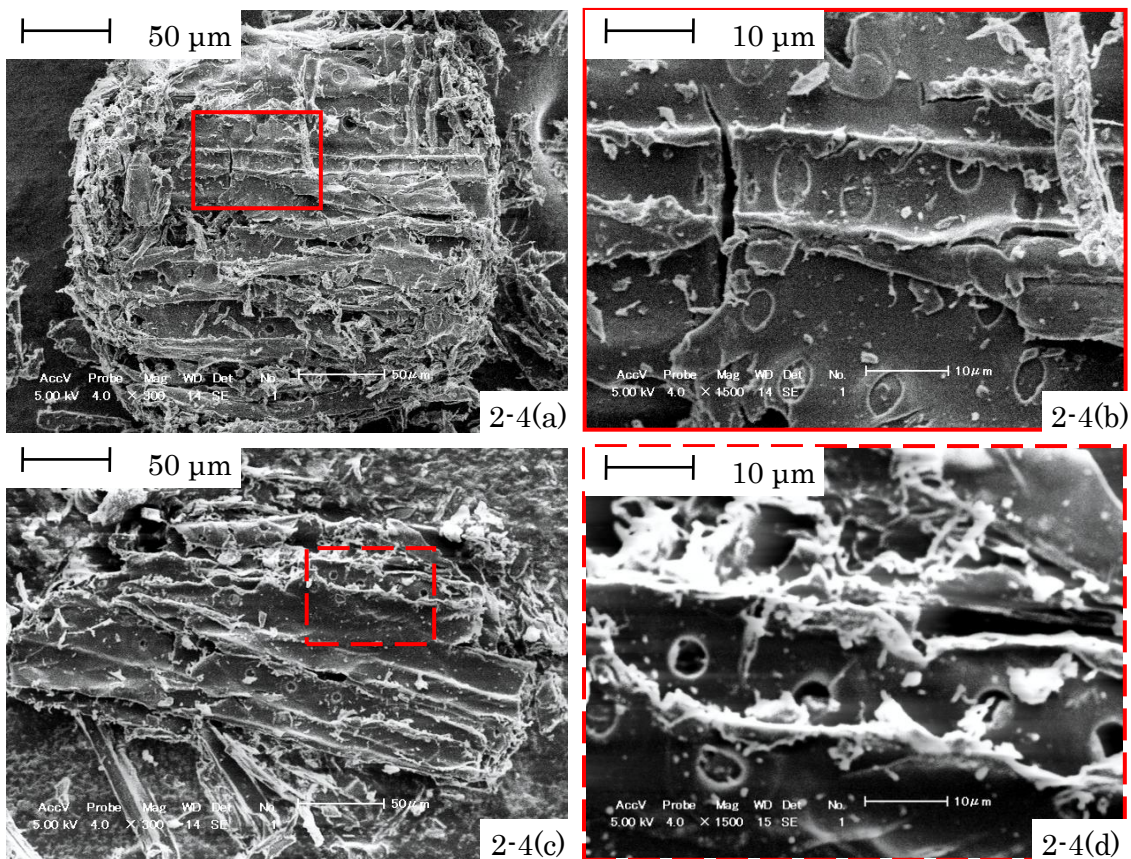


Figure 2-4. SEM images of cedar particles after CO₂ gasification; (a) particle morphology at 700 °C (b) magnified surface from solid boundary inset (c) particle morphology at 900 °C (d) magnified surface from dashed boundary inset.

Up on further CO₂ gasification to 900 °C, further changes in cedar were observed. Figure 2-4(c) shows morphology of cedar particle and its magnified surface structure drawn from the dashed rectangular boundary inset is depicted in

Figure 2-4(d). At this stage, *plasmodesmata* appear as perforated holes. The associated changes on cedar morphology are equivalent to conversion of about 88% (Figure 2-1). Fast conversion observed from 700 °C, 900 °C and above can be associated with further porosity, suggested by these images, favoring diffusion of the gasifying agent and resulting to enhanced intrinsic gasification reactions [10].

During steam gasification, morphology changes are relatively faster compared to CO₂ gasification. After steam gasification to 700 °C under environment, cedar particle clearly shows *plasmodesmata* holes in addition to fiber shrinkage as shown in Figure 2-5(a). The cross-sectional view of the cedar particle prepared under the similar conditions, reveal *vacuoles* [12,13] visible as hollow sections between the fibers in Figure 2-5(b). Cedar attains around 83% conversion at this stage (Figure 2-1). Figure 2-5(c) depicts the morphology of cedar gasified to 900 °C whereas Figure 2-5(d) portrays magnified image drawn from dashed rectangular boundary inset in Figure 2-5(c). These images demonstrate remarkable changes in cedar morphology between 700 °C and 900 °C where corresponding conversion rises from 83% to 96% (Figure 2-1). In the latter case, the residue could likely be composed of mainly ash rather than combustible content. These figures also suggest that enhanced gasification observed from 750 °C onwards, is contributed by porosity of well developed cedar char matrix at these stages favoring diffusion of the gasifying agent and intrinsic gasification reactions [11].

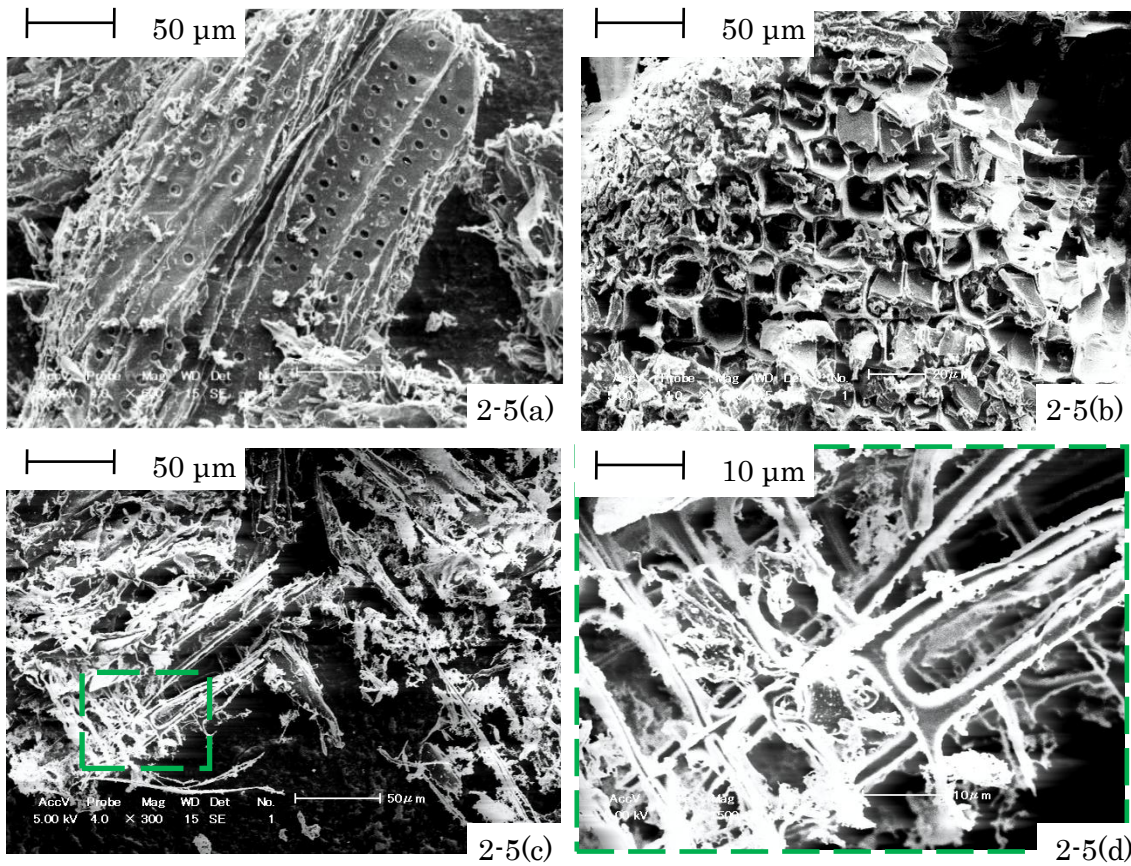


Figure 2-5. SEM images of cedar particles after steam gasification; (a) longitudinal view at 700 °C (b) cross-sectiona view at 700 °C (c) particle morphology at 900 °C (d) magnified surface taken from dashed boundary inset.

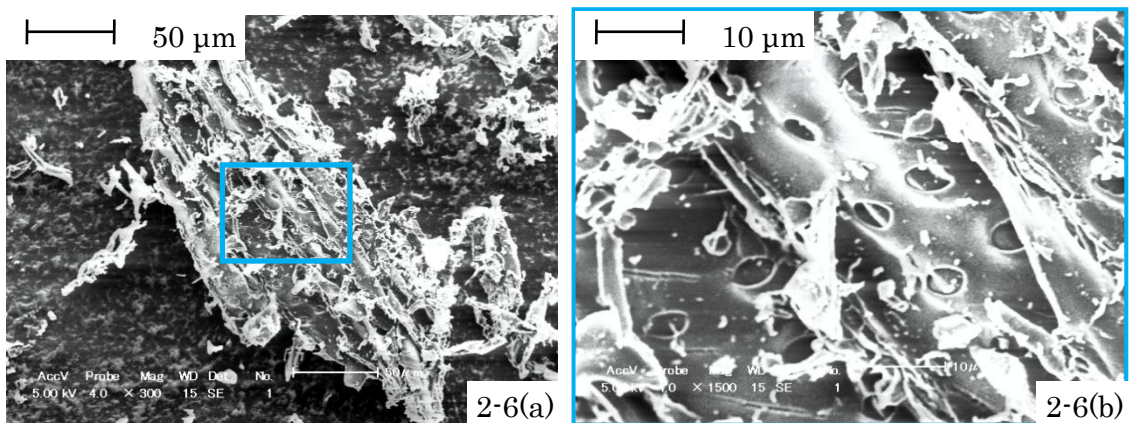


Figure 2-6. SEM images of cedar after N₂ pyrolysis to 1,000 °C and 10 minutes hold; (a) particle morphology (b) magnified surface taken from solid boundary inset.

SEM images of cedar char particles prepared under N₂ pyrolysis conditions are presented in Figure 2-6. These char were pyrolyzed at 20 °C/min to 1,000 °C and subsequently held at the same temperature for 10 minutes as detailed in section 2.2.3. Despite of the higher temperature in addition to longer residence time, by then cedar reaches about 82% conversion. This conversion is almost similar to that attained at 700 °C during steam gasification. As a result, morphology of these chars appears to resemble the residues from steam gasification presented in Figure 2-5(a).

2.4 Summary

In this chapter, gasification characteristics of Japanese cedar as a typical biomass sample were investigated. The results obtained show effects of CO₂ and steam, as gasifying agents, on conversion and morphology changes in comparison to N₂ pyrolysis. Summary of the results obtained is as follows;

- Biomass gasification can be classified into three stage;
 - Fast volatile decomposition that end-up at about 500 °C,
 - Slow volatile decomposition that start around 500 °C, and
 - Char reduction stage which occurs above 750 °C
- Biomass gasification is faster under steam environment than under CO₂ environment especially during char reduction stage.
- Morphology changes during gasification of biomass occur as follows ;
 - Decomposition volatile matters relieves biomass cells of its secondary walls,
 - Upon further decomposition, features on its primary walls such as *plasmodesmata* are embodied, and
 - Hence, the remaining char will be reduced, leaving the ash.

- During gasification, enhanced conversion of biomass which occurs above 750 °C is contributed by porosity of well developed cedar char matrix favoring diffusion of the gasifying agent and intrinsic gasification reactions.
- Subject to the observation of the synergy, steam was chosen as gasifying agent for investigation of co-gasification characteristics in Chapter 3.

References

- [1] Roberts DG, Harris DJ. Char gasification in mixtures of CO₂ and H₂O: Competition and inhibition. *Fuel*, 2007, 86, 2672-2678.
- [2] Lv D, Xu M, Liu X, Zhan Z, Li Z, Yao H, Effect of cellulose, lignin, alkali and alkaline earth metallic species on biomass pyrolysis and gasification. *Fuel Processing Technology*, 2009, 91, 903-909.
- [3] Dufour A, Girods P, Masson E, Rogaume Y, Zoulalian A, Synthesis gas production by biomass pyrolysis: Effect of reactor temperature on product distribution. *International Journal of Hydrogen Energy*, 2009, 34, 1726-1734.
- [4] Gani A, Naruse I. Effect of cellulose and lignin content on pyrolysis and combustion characteristics for several types of biomass. *Renewable Energy*, 2007, 32, 649-661.
- [5] Blasi C. Combustion and gasification rates of lignocellulosic chars. *Progress in Energy Combustion Science* 2009, 35, 121-140.
- [6] Keown DM, Hayashi J-I, Li C-Z, Drastic changes in biomass char structure and reactivity upon contact with steam. *Fuel*, 2008, 87, 1127-1132.
- [7] Fushimi C, Wada T, Tsutsumi A. Inhibition of steam gasification of biomass char by hydrogen and tar. *Biomass Bioenergy*, 2011, 35, 179-185.

- [8] Sonobe T, Worasuwanarak N, Pipatmanomai S. Synergies in co-pyrolysis of Thai lignite and corncob. *Fuel Processing Technology* 2008, 89, 1371-1378.
- [9] Yang H, Yan R, Chen H, Lee DH, Zheng C, Characteristics of hemicellulose, cellulose and lignin pyrolysis. *Fuel*, 2007, 86, 1781-1788.
- [10] Mitsuoka K, Hayashi S, Amano H, Kayahara K, Sasaoaka E, Uddin A. Gasification of woody biomass char with CO₂: The catalytic effects of K and Ca species on char gasification reactivity. *Fuel Processing Technology*, 2011, 92, 26-31.
- [11] Xu Q, Pang S, Levi T. Reaction kinetics and producer gas compositions of steam gasification of coal and biomass blend chars, part 1: Experimental investigation. *Chemical Engineering Science* 2011, 66, 2141-2148.
- [12] L. Salmén, “Micromechanical understanding of the cell-wall structure,” *Comptes Rendus Biologies*, 2004, 327, 873-880.
- [13] Somerville C, Bauer S, Brininstool G, Facette M, Hamann T, Milne J, Osborne E, Paredez A, Persson S, Raab T, Towards a Systems Approach to Understanding Plant Cell Walls. *Science*, 2004, 306, 2206–2211.

Chapter 3

Co-gasification of biomass with coal; thermo-gravimetric basis

3.1 Introduction

Enhanced reactivity of biomass and coal blends has been widely linked to catalytic effects of alkali and alkaline earth metal (AAEM) contents in biomass [1,2,3]. Such effects are significant at higher conversion stages of coal and biomass blend char where virtual concentration of AAEM is likely higher. Similar effect is notable if gasification behavior of acid washed biomass char is compared with that of calcium or potassium loaded char [2,3]. On the other side, coal and especially low quality coal such as lignite, also have significant amount of metal contents with the similar catalytic effect [4]. However, demineralization of coal is reported to increase synergetic effects during co-pyrolysis of coal and petroleum residues [5]. Therefore, contribution of interactions between biomass volatiles or other hydrogen donors with coal through hydrogen transfer has been proposed [4,5,6].

So far, not only correlating results but also controversial findings have been reported rendering discussion on co-gasification inconclusive [7,8]. Therefore, it is important that the occurrence of synergy, if any, be confirmed, quantified and the underlying mechanism be discussed. This chapter compares co-gasification behavior with the average behavior calculated from the separate biomass gasification and coal gasification. Although steam gasification indicated better performance than CO₂ gasification in Chapter 2, occurrence of synergy has to be confirmed. The contribution of volatile interaction and catalytic effects of AAEM are realized by comparing co-gasification behavior of coal with acid washed cellulose [9] that has

high volatile matter and Na rich lignin.

3.2 Experimental methods

3.2.1 Properties of the samples

Japanese cedar (*cryptomeria japonica*) and coal were milled to 150 μm and stored in a desiccator to avoid moisture contamination. Microcrystalline acid washed cellulose prepared by Sigma-Aldrich Chemie GmbH, and lignin made by Kanto Chemical Co. Inc, were used as artificial biomass constituents. Proximate analysis, ultimate analysis and ash analysis for these samples are shown in Table 3-1. For the case of co-gasification, the basic blending ratio was taken to be 50% biomass and 50% coal in dry and ash free (d.a.f.) mass basis. Other biomass to coal ratio used are 80%:20%, 60%:40%, 40%:60% and 20%:80%. In reference to cellulose and lignin contents in Japanese cedar [10,11], simulated biomass was made by mixing cellulose and lignin at 70% and 30% dry and ash free (d.a.f.) mass basis.

3.2.2 Gasification experiments

Gasification of about 10 mg samples was conducted by using Shimadzu Thermo-Gravimetric Analyzer (TGA). To investigate gas evolution synergy, micro gas chromatograph (Agilent 3000A), was connected to the TGA to analyze flue gas concentration. Heating rate from ambient temperature to 1,000 $^{\circ}\text{C}$ was set at 20 $^{\circ}\text{C}/\text{min}$, however holding at 107 $^{\circ}\text{C}$ for 10 min to ensure complete removal of moisture contents from the samples. When 1,000 $^{\circ}\text{C}$ was attained, constant temperature gasification was allowed to proceed until no mass loss was observed.

Table 3-1. Proximate, ultimate and ash analysis of the samples

Sample			Cedar	Coal	Lignin	Cellulose
Proximate analysis (wt %)	As received	Moisture	3.90	2.00	2.23	4.96
	Dry basis	VM ^c	82.09	30.30	38.62	85.14
		FC ^d	15.79	56.00	55.64	14.86
		Ash	2.13	13.60	5.74	<0.01
Ultimate analysis (wt %)	Dry and ash free basis	C	47.56	80.97	60.58	45.34
		H	5.66	1.47	5.14	6.97
		N	0.27	9.32	0.27	0.08
		S	-	0.45	-	-
	Balance	O	46.51	7.79	33.99	51.39
Ash analysis (ash wt %)		SiO ₂	24.51	65.90	10.05	-
		Al ₂ O ₃	4.67	22.90	1.33	-
		CaO	25.99	1.08	0.44	-
		TiO ₂	0.26	1.37	<0.01	-
		Fe ₂ O ₃	4.98	4.58	0.15	-
		MgO	5.89	0.79	0.81	-
		Na ₂ O	3.13	0.47	47.18	-
		K ₂ O	19.13	1.37	1.17	-
		P ₂ O ₅	1.66	0.31	<0.01	-
		MnO	-	0.03	-	-
		V ₂ O ₅	-	0.07	-	-
	SO ₃	3.32	0.62	32.25	-	

^cVM represents volatile matter

^dFC represents fixed carbon

Since occurrence of synergy has to be confirmed under steam or CO₂ gasification, co-gasification under both environment were conducted before selecting one gasification agent for further analysis. During steam gasification, WORKlab water pump was used to supply distilled water to a steam generator set at 300 °C. To avoid steam condensation within TGA reactor at lower temperature ranges, only N₂ at 150 mL_N/min was supplied from ambient temperature to 200 °C.

Thereafter, N₂ flow was reduced to 75 mL_N/min, and steam at 75 mL_N/min was supplied to allow gasification reactions to proceed. For rational comparison basis with steam gasification case, CO₂ was also introduced at 200 °C. It can be noted that N₂ supplied at 75 mL_N/min was maintained throughout the gasification process as purging gas and as a steam carrier.

3.2.3 Analysis of conversion and extent of synergy

Conversion X (wt %) was derived from mass decomposition data by TGA as follows;

$$X = 1 - m/m_o \quad (3-1)$$

where m and m_o (both in g) represent mass of the sample on d.a.f. basis at a certain gasification temperature and at initial condition, respectively.

Average conversion X_{avg} (wt %) was calculated from conversion for cedar, lignin or cellulose X_{bio} and conversion of coal X_{col} multiplied with mass ratio of the respective sample in the blend;

$$X_{avg} = (X_{bio} \times m_{bio}/m_{bld}) + (X_{col} \times m_{col}/m_{bld}) \quad (3-2)$$

where m_{col} and m_{bld} (both in g) represents initial d.a.f. mass of coal and the blend while m_{bio} (g) represents d.a.f. mass of cedar, lignin or cellulose.

Extent of synergy Y (%), was calculated as the difference between conversion for blend X_{bld} and the calculated average conversion X_{avg} at the same temperature;

$$Y = X_{bld} - X_{avg} \quad (3-3)$$

3.2.4 Morphology investigation by Scanning Electron Microscope (SEM)

Samples for morphology investigation were partially gasified to 550 °C and 800 °C. Residues from partial gasification at these temperature ranges were considered to have consistent morphology, well developed shapes and contain significant amount of combustible contents rather than ash. During partial gasification, temperature profile as well as flow rates for N₂ and steam were similar to those applied during complete gasification experiments. However, when the target temperature was attained, heat supply and steam supply was terminated. Mean while the residues were allowed to cool under 150 mL_N/min supply of N₂. Due to high temperature and possible presence of residual steam, it is most likely that further conversion of the residues occurred at initial stage of the cooling process to affect their morphology.

Before SEM investigation, dried or partially gasified samples were carbon coated in order to improve their visibility for SEM. SEM images of the residues were taken at 300 times magnification however 1,500 times magnification was preferred for unveiling more visible surface structures. It can be noted that due to high temperature and possible presence of residual steam or CO₂ during gasification, it is most likely that further conversion of the residues occurred at initial stage of the cooling process to affect their morphology.

3.3 Results and discussion

3.3.1 Conversion behaviors during co-gasification of cedar with coal

From TGA mass decomposition data of Japanese cedar, coal and their blends, conversion were calculated by using Equation 3-1 while the average conversions were deduced by using Equation 3-2. Conversion characteristics under CO₂ gasification and steam gasification, are presented Figure 3-1(a) and Figure 3-1(b), respectively. Conversion behaviors of cedar presented in these figures are similar to those presented in Chapter 2 therefore they will not be discussed here.

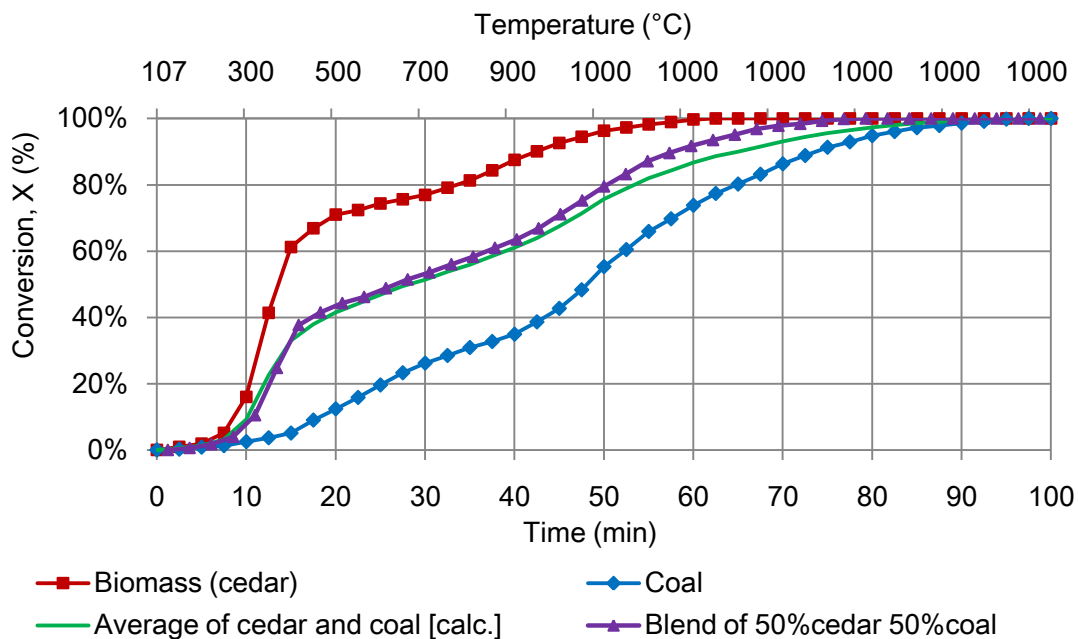


Figure 3-1(a). Conversion characteristics of cedar, coal and their blend during CO₂ gasification.

For the case of CO₂ co-gasification (Figure 3-1 (a)), it was observed that the initial conversion for cedar and coal blend is marked by evolution of volatile matters that ended-up at and 450 °C. Volatile matter evolution in coal was relatively slow

and extended to 700 °C. The corresponding conversions at these stages are 38% and 26% for the blend and coal, respectively. Intermediate conversions marked by slow conversion proceeded to 35% at 700 °C and 63% at 900 °C for the blend and coal cases, correspondingly. Volatile evolution in coal is governed by distribution of weak bonds alongside chains, hydrogen rich functional groups and thermo-cracking of its large molecules which occur at elevated temperatures [12,13]. The final conversion stages at which char gasification takes place appears to be moderately faster than the intermediate conversion stage. It can be noted that co-gasification behavior is almost similar to average behavior (Figure 3-1 (a)). This result shows limited occurrence of synergy.

Conversion patterns during steam gasification are presented in Figure 3-1(b). Marked by fast initial conversions, volatile evolution for the blend and coal show almost similar trend as in steam gasification case (Figure 3-1 (a)). However intermediate and final conversion regions proceeds relatively faster. In comparison with the calculated average conversion, co-gasification characteristics shows improved trend above 400 °C and notably above 800 °C. This improvement is an indication of occurrence of synergy.

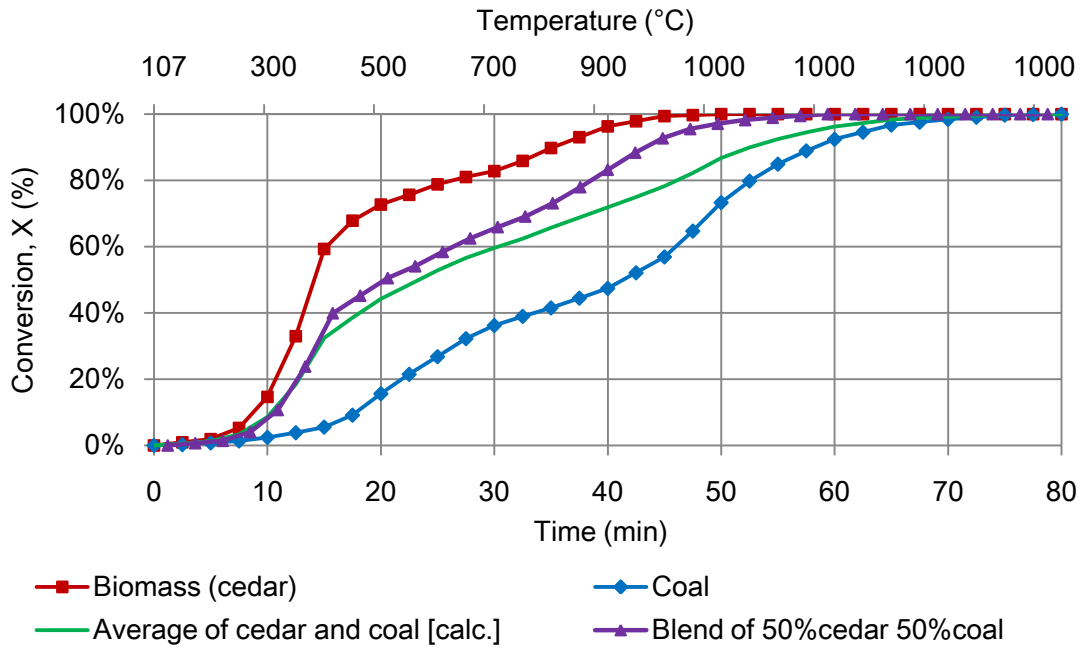


Figure 3-1(b). Conversion characteristics of cedar, coal and their blend during steam gasification.

3.3.2 The extent of synergy

Extent of the synergy throughout co-gasification processes was derived by using Equation 3-3 is shown in Figure 3-2(a). Two conversion synergetic peaks are observed, under both steam and CO₂ gasification. The first peak occurs at around 400 °C for while the other peak occurs above 800 °C. Under CO₂ gasification, both the low and high temperature synergy peaks are limited to 5% while for corresponding peaks for steam gasification are 7% and 14%, respectively. This result confirms that CO₂ environment may not be suitable for further investigation of co-gasification characteristics as discussed in Chapter 2.

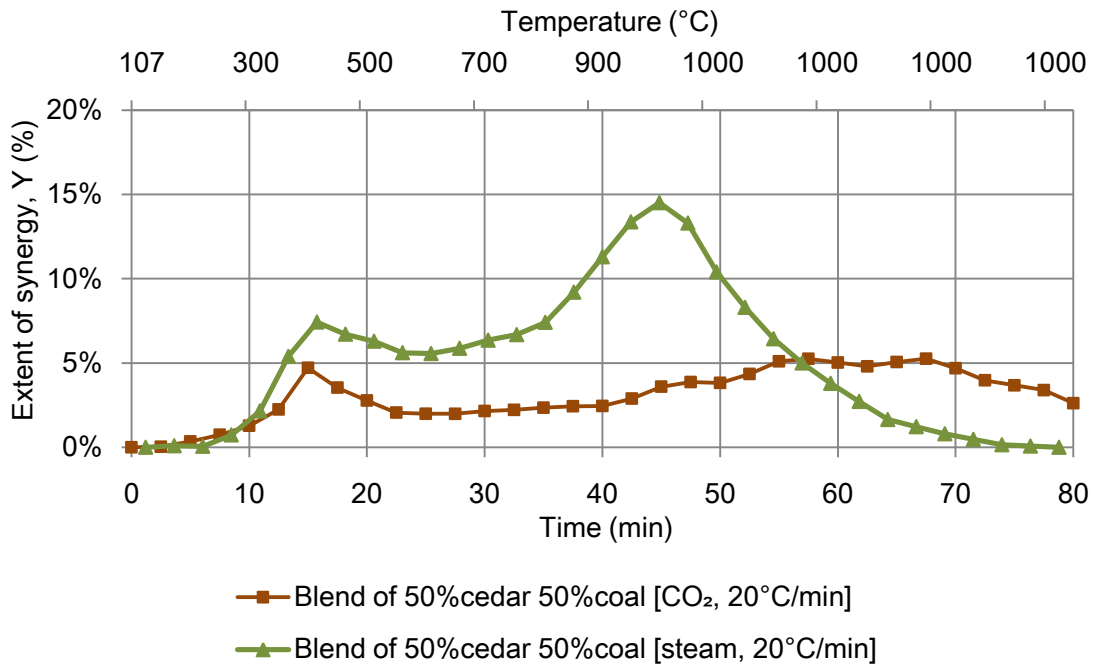


Figure 3-2(a). The extent of synergy during CO₂ and steam co-gasification of cedar and coal.

To check for the replicability of the extent of synergy under steam gasification conditions, biomass to coal was varied to 80%:20%, 60%:40%, 40%:60% and 20%:80%. The heating rate was maintained at 20 °C/min during these sets of experiments. Apparently, similar double synergetic peaks observations are replicated in Figure 3-2(b). Throughout the co-gasification process, synergy seems to be lower for the lowest and highest biomass to coal ratio, i.e. 80%:20% and 20%:80%. The higher biomass to coal ratio favors the synergy at higher temperature as reported by other researchers [2,3]. However the synergy at low temperature does not follow this tendency.

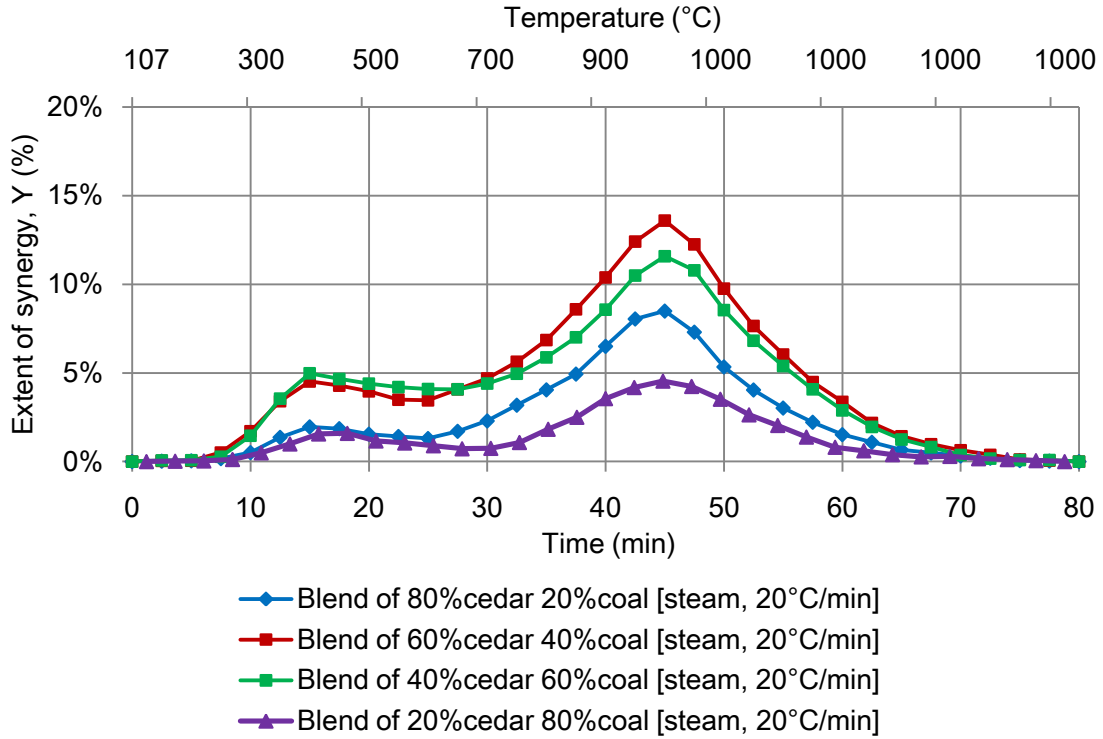


Figure 3-2(b). Effect of variation of biomass to coal ratio to the extent of synergy.

3.4 Elucidating the synergy mechanism

After quantifying the extent of synergy and realizing the two synergy peak presented in Figure 3-2(a) and Figure 3-2(b), then we have the foundation for discussing the related synergy. Many researchers have reported on catalytic effects of biomass AEMM species which dominate at higher temperatures [1,2,3]. However, low temperature synergy has not been discussed in details [4,5,14]. In addition to that, we observed this synergetic region coincides with volatile evolution. Therefore, we check if the low temperature synergy is associated to catalytic effects of AAEM and/or volatile interactions. The investigation was done by considering gas compositions as well as steam by comparison of co-gasification characteristics of coal with acid washed cellulose [9] that has high volatile matter and Na rich lignin.

3.4.1 Flue gas evolution and hydrogen transfer mechanism

Flue gas concentrations presented in this section were recorded at the steam gasification experiments presented in Figure 3-1(b). It can be noted that H₂ and CO₂ were the main gaseous products while CO composition was very low. Probably, steam presence favored water-gas shift reaction resulting into decrease in CO yield (see Equation 1-3). Meanwhile, lower concentration of H₂ and CO₂ as indicated in Figure 3-3(a) and Figure 3-3(a) is attributed to higher amount of N₂ supplied in comparison to relatively small amount of samples used.

Figure 3-3(a) shows that cedar releases higher H₂ amount between 400 °C and 700 °C in comparison to coal and the blend as observed by other researchers [4,15]. Lower H₂ releases from coal at this temperature range conform to its slow volatile evolution (Figure 3-1(b)). It was observed that below 700 °C, H₂ release from the blend was less than the average release from separate gasification of coal and cedar. However, this is not case at higher temperature ranges. It is known that H₂ evolution during steam biomass gasification is larger than its absorption [15]. The lower release of H₂ from the blend despite of the expected higher release of H₂ from biomass particle in the blend, gives an indication of volatile interactions [4,5,15,16]. This result suggests H₂ capture below 700 °C and therefore biomass served as a hydrogen donor to coal.

Figure 3-3(b) shows CO₂ release during steam gasification. Between 400 °C and 700 °C, CO₂ release from biomass and coal shows similar trends with H₂ release (Figure 3-3(a) vs. Figure 3-3(b)). However, CO₂ from the blend is significantly higher. This result demonstrates higher carbon consumption during synergetic region of the gasification process leading to higher conversions.

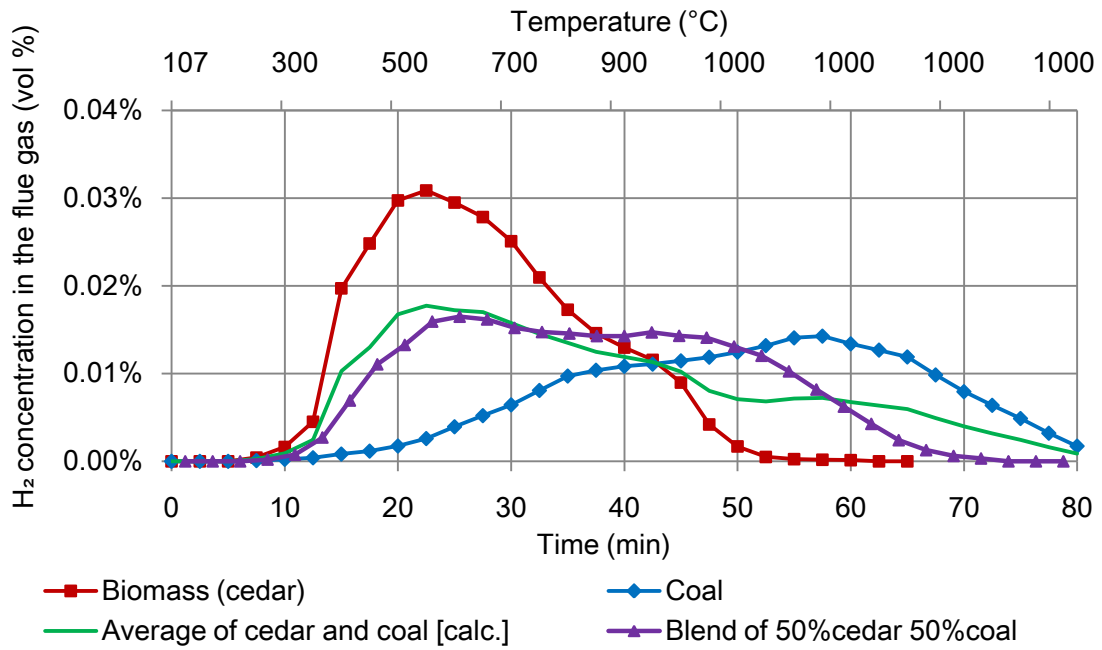


Figure 3-3(a). H₂ concentration during steam gasification of cedar, coal and the blend.

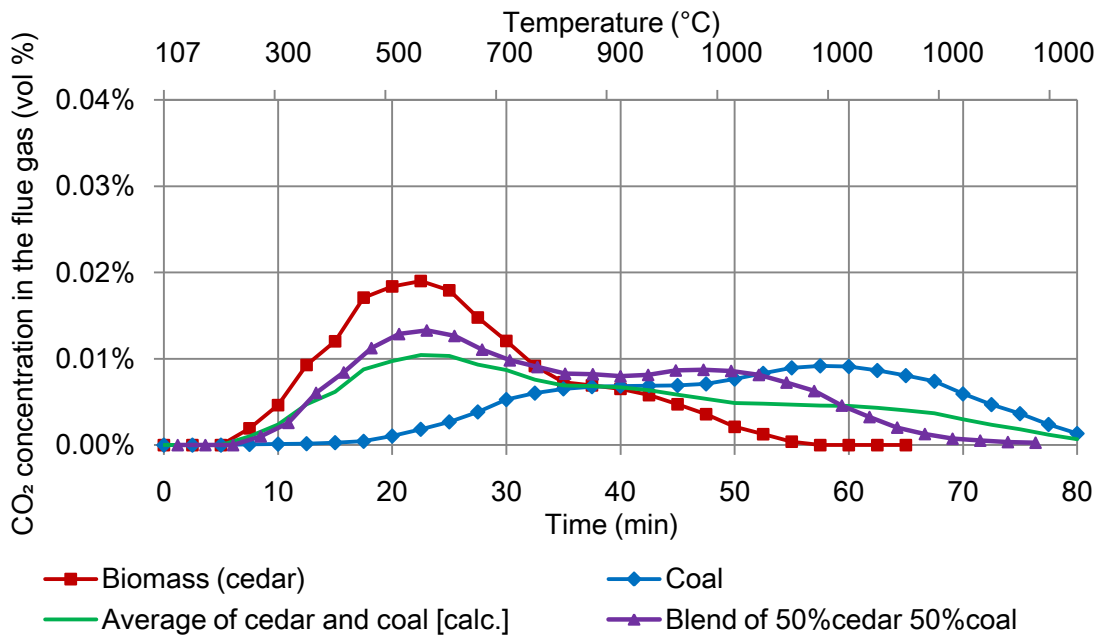
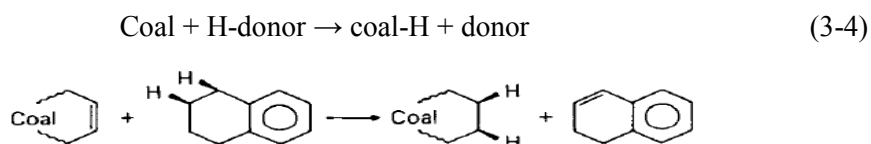


Figure 3-3(b). CO₂ concentration during steam gasification of cedar, coal and the blend.

Conversion synergy observed during co-gasification of biomass with coal, indicates enhancement of reactivity of coal particles. This phenomena result into unexpected coal consumption by gas evolution and reduction in char formation. Sulves *et al.* [14] reported that enhancement of coal conversion can be achieved if radicals produced during volatile evolution, involving bond breaking reactions are promoted, and simultaneously, the cross-linking reactions that increase char formation are decreased. Both coal and H-donor can initiate or inhibit the reaction. However, usually coal acts as the initiator of the process, enhancing the degradation of the donor, which afterwards forms intermediate radicals that act as promoters for coal conversion.

During H₂ donor-acceptor mechanism for coal comprises of destruction of valent bonds in coal followed by formation of low molecular weight compounds and poly-association of hydrogen [16,17]. Alternatively, thermally cracked O-H functional groups in coal can interact with H radicals to form new active sites and therefore enhancing coal gasification reactivity [17,18]. In addition, iron compounds in coal suffice as a catalyst for this process. Marzec and Schulten [19] observed that hydrogen transfer occurs between 340 °C and 440 °C involving coal and volatile organic compounds in the following sequence:



3.4.2 Co-gasification of simulated ligno-cellulosic biomass with coal

Although gas composition provided important clues on volatile interactions through hydrogen transfer, presence of AAEM in biomass may also have contributed to the observed synergy. In order to demarcation of the effect of the contribution of volatile interaction and catalytic effects of AAEM, acid washed cellulose [9] that has high volatile matter and Na rich lignin (Table 3-1) chemicals were used as artificial biomass components. Simulated biomass made by mixing 70% cellulose and 30% lignin as it is the case for Japanese cedar composition [10,11] was gasified and its conversion behavior compared to that of Japanese. Hence, co-gasification of coal with cellulose or lignin was done.

Conversion ratio patterns during steam gasification for Japanese cedar, cellulose, lignin and simulated biomass are presented in Figure 3-4. It was noted that cellulose gasification is characterized by sharp volatilization which occurs between 350 °C and 450 °C as reported by other researchers [1,20,21,22]. Volatilization during cellulose gasification extends to around 87% conversion, the figure which corresponds to its higher volatile contents (see Table 3-1). By the end of volatilization, slow cellulose char gasification that proceeds thereafter indicates absence of AAEM species in the blend and hence lack of catalysis. Lignin shows relatively slower volatilization limited to about 38% at 450 °C. Fast lignin char gasification occurring above 800 °C is attributed to catalytic effect of its high Na content (Table 3-1).

Gasification behavior of simulated biomass is also presented in Figure 3-4. Simulated biomass shows close correspondence to cellulose behavior between 300 °C and 450 °C. Above 800 °C, simulated biomass shows sharp conversion behavior similar to that of lignin. Gasification of simulated biomass at low and high temperature signifies the roles of volatiles from cellulose and catalysis by AAEM species in lignin, correspondingly. Simulated biomass and Japanese cedar show almost similar gasification behavior. However, cedar yields earlier volatilization at 250 °C and continuous decomposition between 450 °C and 800 °C. Above this range, simulated biomass appears to be more reactive than cedar, due to higher AAEM content in lignin.

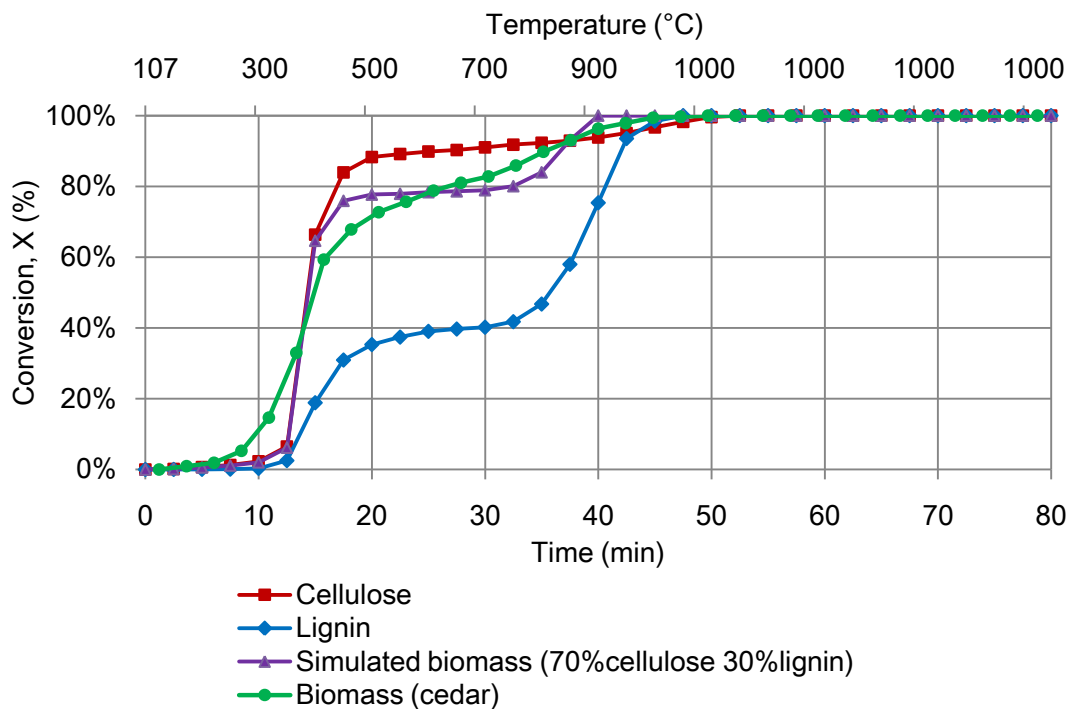


Figure 3-4. Conversion characteristics of cedar, cellulose, lignin and simulated biomass during steam gasification at 20 °C/min.

Conversion characteristics during co-gasification of coal with lignin and co-gasification of coal with cellulose are presented in (Figure 3-5(a) and Figure 3-5(b)). Lignin and cellulose behavior presented in these figures are identical to those presented in Figure 3-4 while coal behavior is identical to that presented in Figure 3-1(b). Average conversion for coal and cellulose or lignin was calculated by using Equation (3-2). On the other side, co-gasification of cellulose with coal shows only a single synergy peak between 350 °C and 450 °C (Figure 3-5(b)). No significant synergy is observed at temperatures above 800 °C for cellulose-coal co-gasification case. This result indicates that, at low temperature, synergy occurred under the influence of volatiles rather than AAEM catalysis.

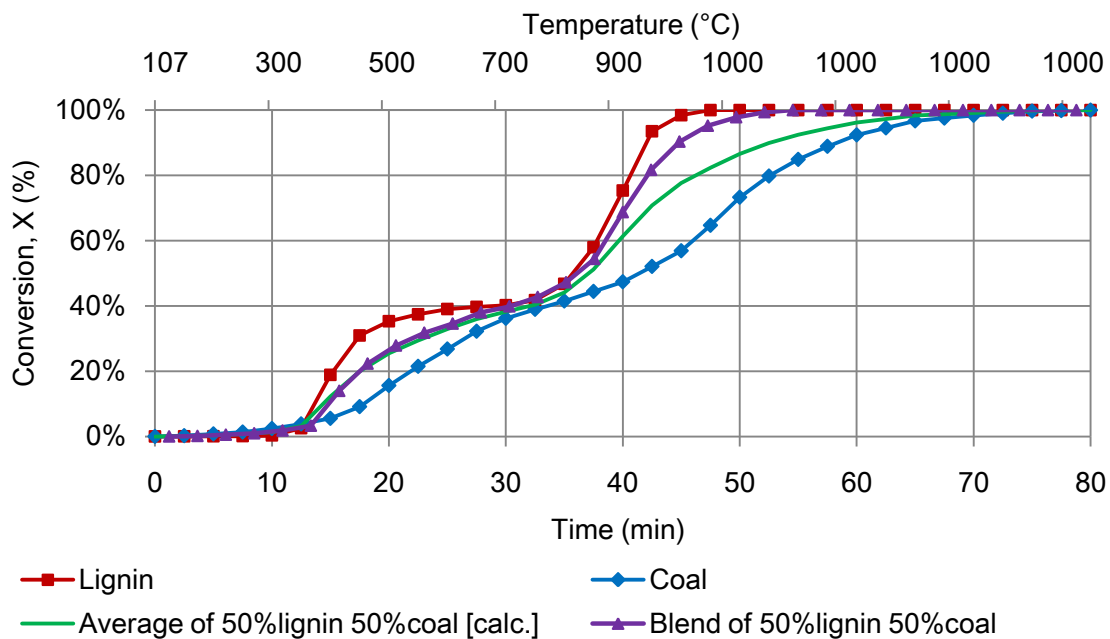


Figure 3-5(a). Conversion characteristics of lignin, coal and their blend during steam gasification.

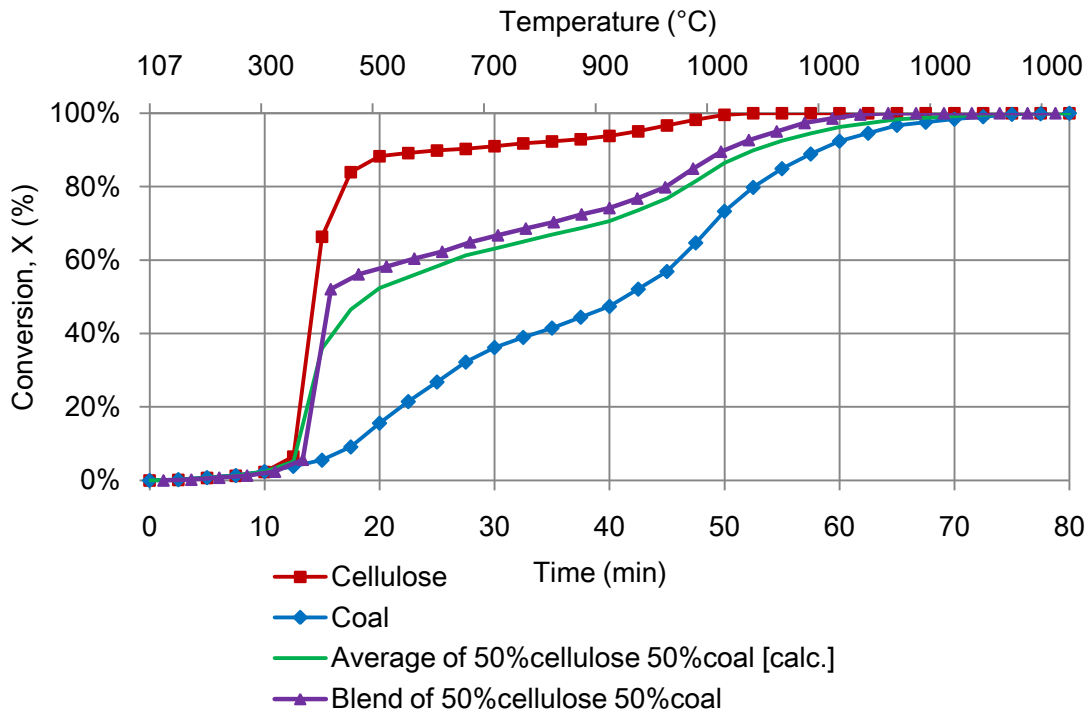


Figure 3-5(b). Conversion characteristics of lignin, coal and their blend during steam gasification.

The extent of the synergy throughout co-gasification of simulated biomass, cellulose or lignin with coal was deduced by using Equation (3-3). Co-gasification of lignin with coal shows two synergy peaks while single synergy peak occurred for coal and cellulose blend (Figure 3-6). Clearly, the synergy appear to be split into two regions, between 450 °C and 800 °C i.e. volatile matter evolution stage, and hence above 800 °C that is during char gasification. This figure confirms two possible synergy mechanisms during co-gasification process; volatile interactions [4,5,14] and the AAEM catalysis [1,2,3]. It can also be observed that lower temperature synergy for coal and cellulose co-gasification case is superior to that observed during co-gasification of either simulated biomass or lignin with coal.

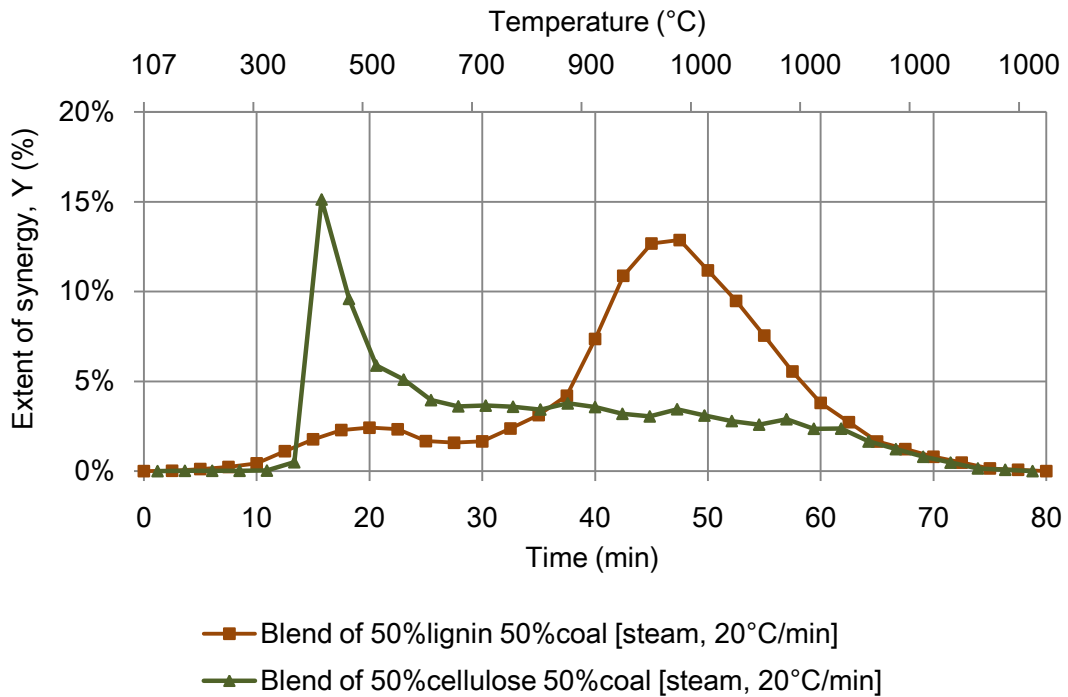


Figure 3-6. Extent of synergy effect during steam co-gasification of coal with cellulose and/or lignin.

3.5 Morphology changes during co-gasification process

3.5.1 Morphology changes in biomass and coal blends

To understand the morphology changes which take place during gasification, morphology of the raw samples as well as partially gasified samples was investigated. Morphology of the raw cedar are presented and discussed as Figure 2-3(a) in chapter 2. Figure 3-7(a) and Figure 3-7(b) shows SEM images of raw coal particle and its magnified surface taken from the solid rectangular inset, respectively. Raw coal has a solid structure and shiny surface [6,13].

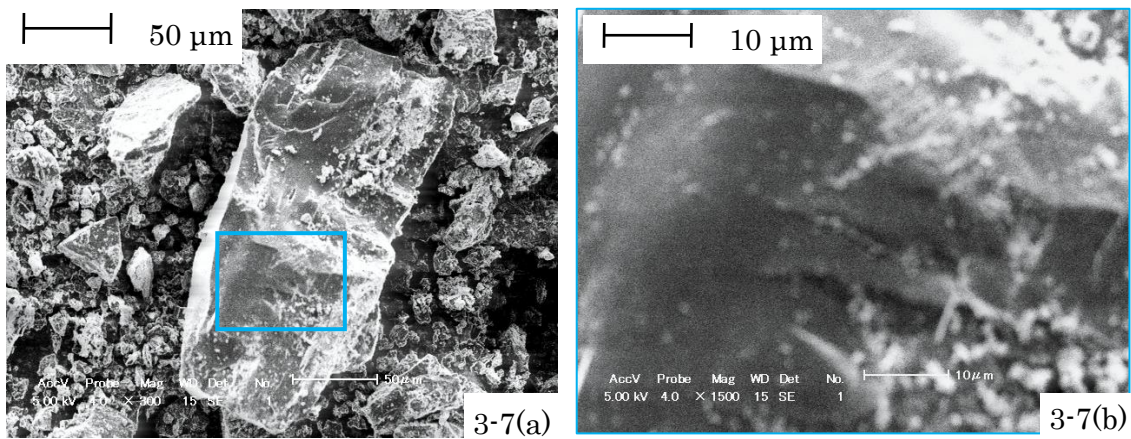


Figure 3-7. SEM images of raw coal; (a) particle morphology, (b) magnified surface taken from solid boundary inset.

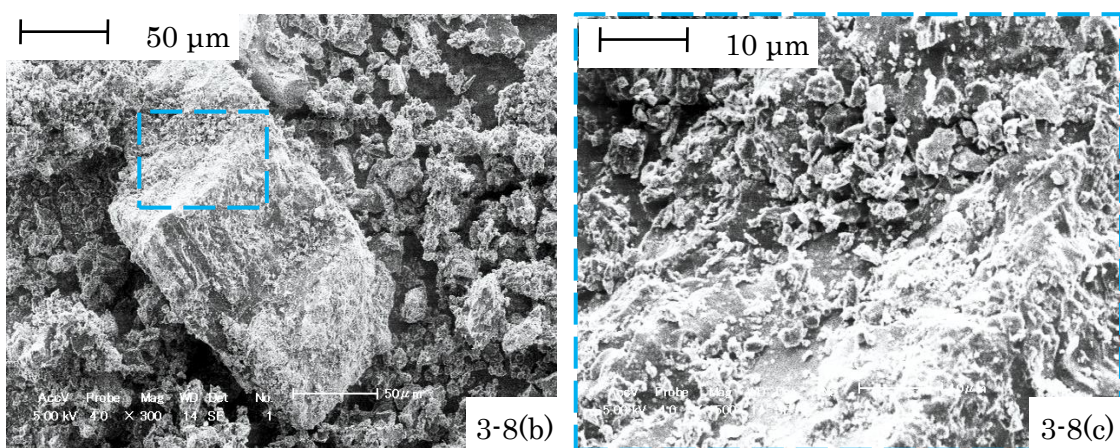
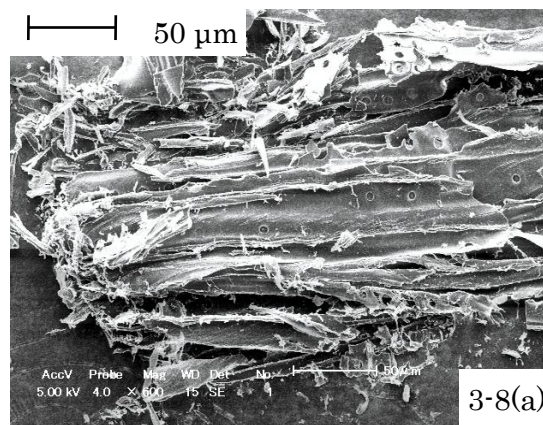


Figure 3-8. SEM images after separate gasification to 800 °C by using steam; (a) cedar particle (b) coal particle (c) coal surface taken from dashed boundary inset.

SEM images for Japanese cedar and coal after separate gasification to 800 °C by using steam are presented in Figure 3-8. Figure 3-8(a) shows longitudinal and cross sectional view of cedar particle that attained 90% conversion (Figure 3-1(b)). Figure 3-8(b) and Figure 3-8(c) shows coal particle and its magnified surface taken within the dashed boundary inset. Slight pore development and slight physical cracking attributed to around 41% conversion can be observed.

Figure 3-9(a) shows cedar coal and blend particles gasified to 800 °C under steam environment. At this stage, the blend reached 73% conversion (Figure 3-1(b)). Figure 3-9(b) and Figure 3-9(c) shows corresponding magnified surface structures of coal and cedar particles taken from solid and dashed boundary insets in Figure 3-9(a). Moderate physical cracking can be observed on coal surface. These features, probably lead to improved steam diffusion and hence gasification reaction improvement [4,5,6], as shown in Figure 3-1(b) between 800 °C and 1,000 °C. Nevertheless, cedar surface structure suggests slightly delayed conversion.

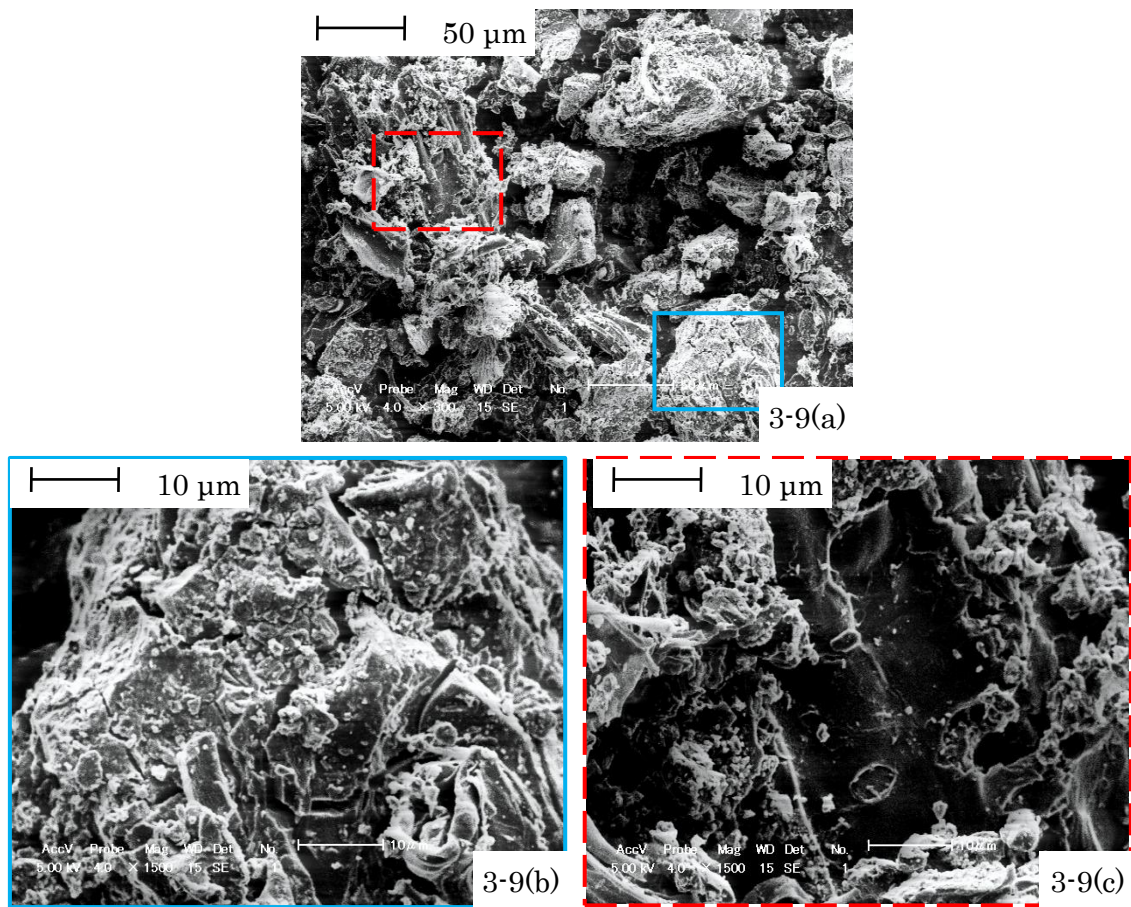


Figure 3-9. SEM images after co-gasification to 800 °C by using steam; (a) cedar and coal blend (b) coal surface taken from solid boundary inset (c) cedar surface taken from dashed boundary inset.

3.5.2 Morphology changes in simulate biomass and coal blends

SEM images for lignin and cellulose are shown in Figure 3-10(a) and Figure 3-10(b), respectively. Raw lignin shows a lumpy solid shape while raw cellulose demonstrates solid fiber based structure.

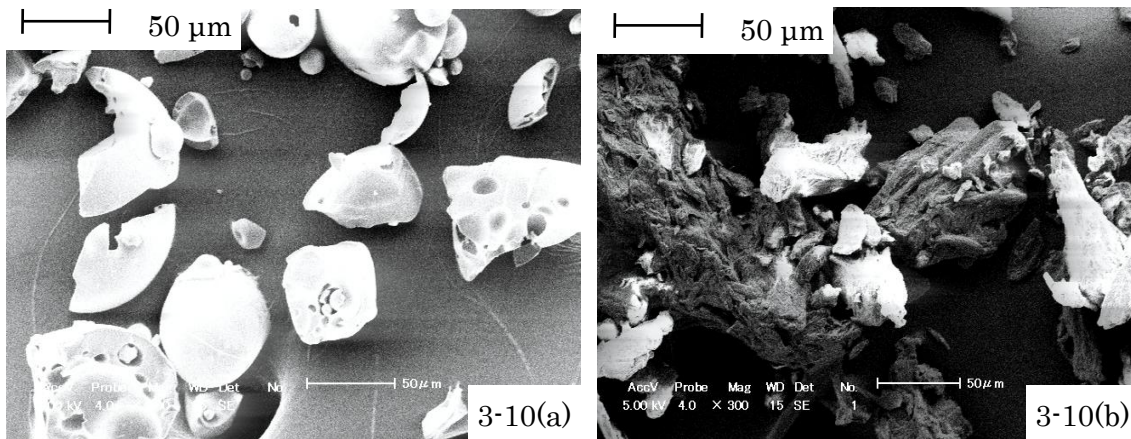


Figure 3-10. SEM images of raw samples; (a) lignin particles (b) cellulose particles.

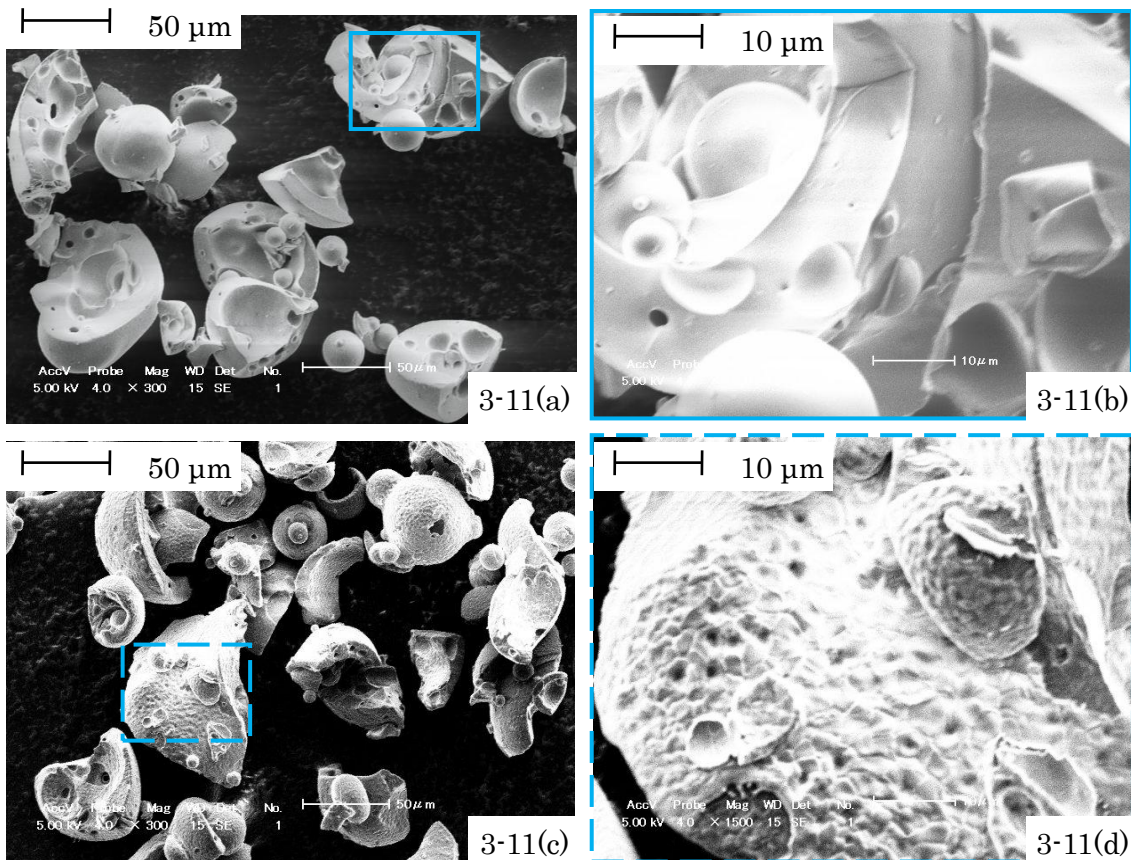


Figure 3-11. SEM images after partial gasification by using steam; (a) lignin particles gasified to 550 °C, (b) surface of lignin gasified to 550 °C, (c) lignin particles gasified to 800 °C, (d) surface of lignin gasified to 800 °C.

After gasification to 550 °C, lignin particles show no significant morphology change as shown in Figure 3-11(a) and in a magnified surface taken from the solid boundary inset (Figure 3-11(b)). This is despite the fact that lignin had attained over 37% conversion (Figure 3-4), that is almost after complete decomposition of its volatile matter (Table 3-1). However, when gasified to 800 °C lignin particles shows spongy surface as shown in Figure 3-11(c) and particularly on the magnified surface taken from a dashed boundary inset (Figure 3-11(d)). Probably, spongy surface offers less steam diffusion resistance [4,5,6], resulting into enhanced gasification of lignin as observed from 800 °C onwards (Figure 3-4).

SEM images for particle surfaces taken from coal and lignin blends gasified to 550 °C and 800 °C are presented in Figure 3-12. Magnified surface of lignin and coal co-gasified to 550 °C are shown in Figure 3-12(a) and Figure 3-12(b), respectively. In comparison to raw lignin, no significant morphology change was noted on lignin surface. Likewise, no considerable pore development was observed on coal surface. Limited morphology changes can be associated with corresponding low volatile matter contents for these samples (Table 3-1), in addition to slow decomposition behaviors (see Figure 3-4). Even after gasification to 800 °C, morphology changes on lignin and coal surface structure remain to be less significant (Figure 3-12(c) and Figure 3-12(d)). Non-interactive relation between lignin and coal is probably due to their similar benzene based molecular structures [23,24]. In addition to that, low reactivity of coal and lignin particles can be associated to their solid shapes maintained even at high temperature, despite of high conversion stages are attained [20].

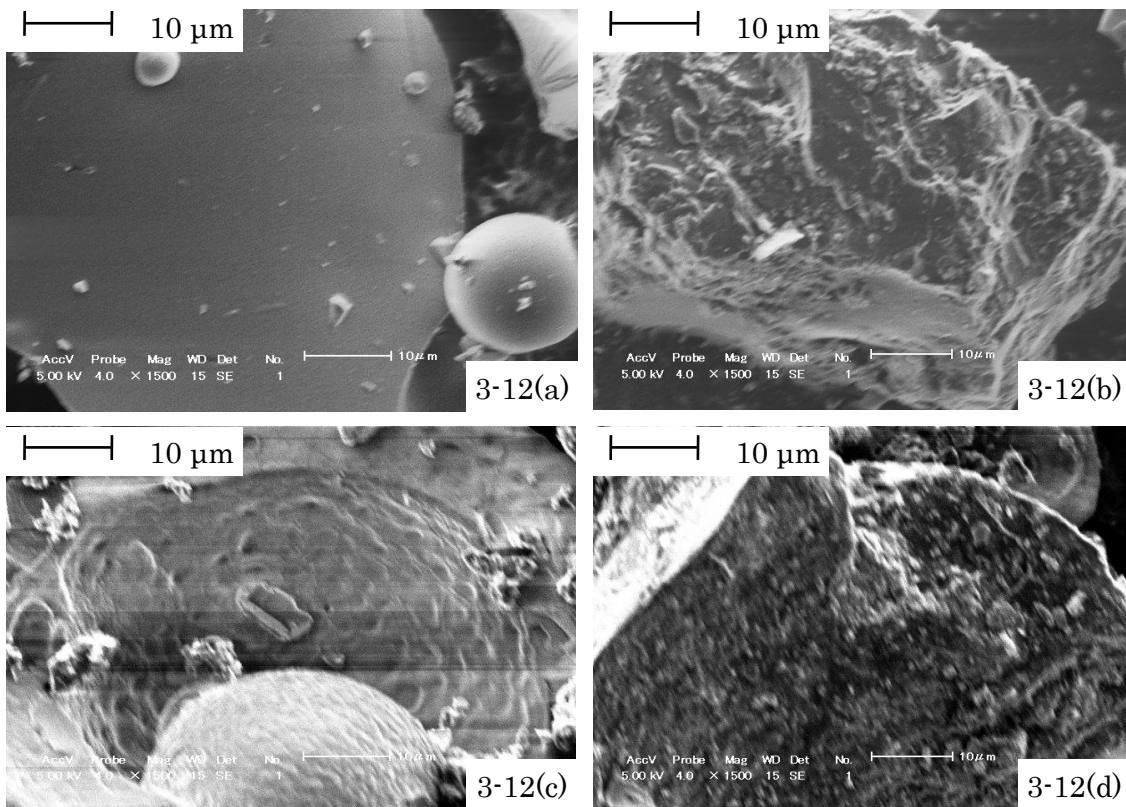


Figure 3-12. Magnified surfaces taken from the gasified lignin and coal blends; (a) lignin in the blend gasified to 550 °C, (b) coal in the blend gasified to 550 °C, (c) lignin in the blend gasified to 800 °C, (d) coal in the blend gasified to 800 °C.

Morphology changes in gasified cellulose are appreciable on fiber shrinkage basis as shown in Figure 3-13(a) and in a magnified surface captured from the solid boundary inset is presented in Figure 3-13(b). This shrinkage observed at 550 °C is attributed to decomposition of volatile matter which accounts for 85% mass of cellulose (Table 3-1). After gasification to 800 °C, further fiber shrinkage was notable (Figure 3-13(b)). A magnified shape of cellulose taken from dashed boundary inset is presented in Figure 3-13(b). The minor fiber shrinkage in cellulose fibers which occurs between 550 °C and 800 °C corresponds to its limited conversion that took place during this interval (Figure 3-5(a)).

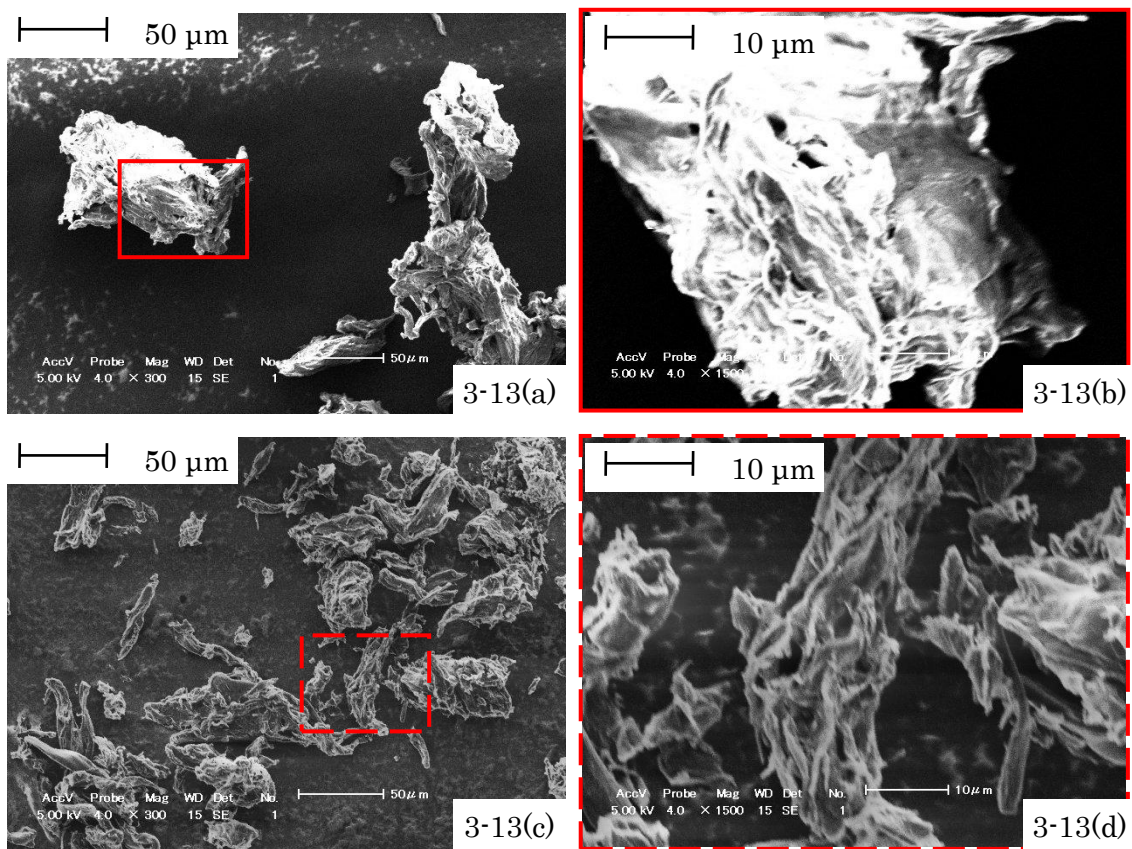


Figure 3-13. SEM images after partial gasification by using steam; (a) cellulose particles gasified to 550 °C, (b) surface of cellulose gasified to 550 °C, (c) cellulose particles gasified to 800 °C, (d) surface of cellulose gasified to 800 °C.

Figure 3-14 shows surfaces of cellulose and coal particles from partially gasified blends. As opposed to lignin and coal blend, it was difficult to differentiate between cellulose and coal particles in this case. Figure 3-14(a) and Figure 3-14(b), shows magnified surfaces of cellulose and coal, after co-gasification to 550 °C. Fiber shrinkage and pore development are significant on cellulose and coal surfaces, respectively. After co-gasification to 800 °C, no further change was observed on cellulose (Figure 3-14(c)) however further development of pores and physical cracking were notable on coal surface (Figure 3-14(d)). These features on coal

surface, demonstrate on occurrence of further conversion in addition to the possible reason for accelerated gasification reactivity owing to the resulting low steam diffusion resistance [4,5].

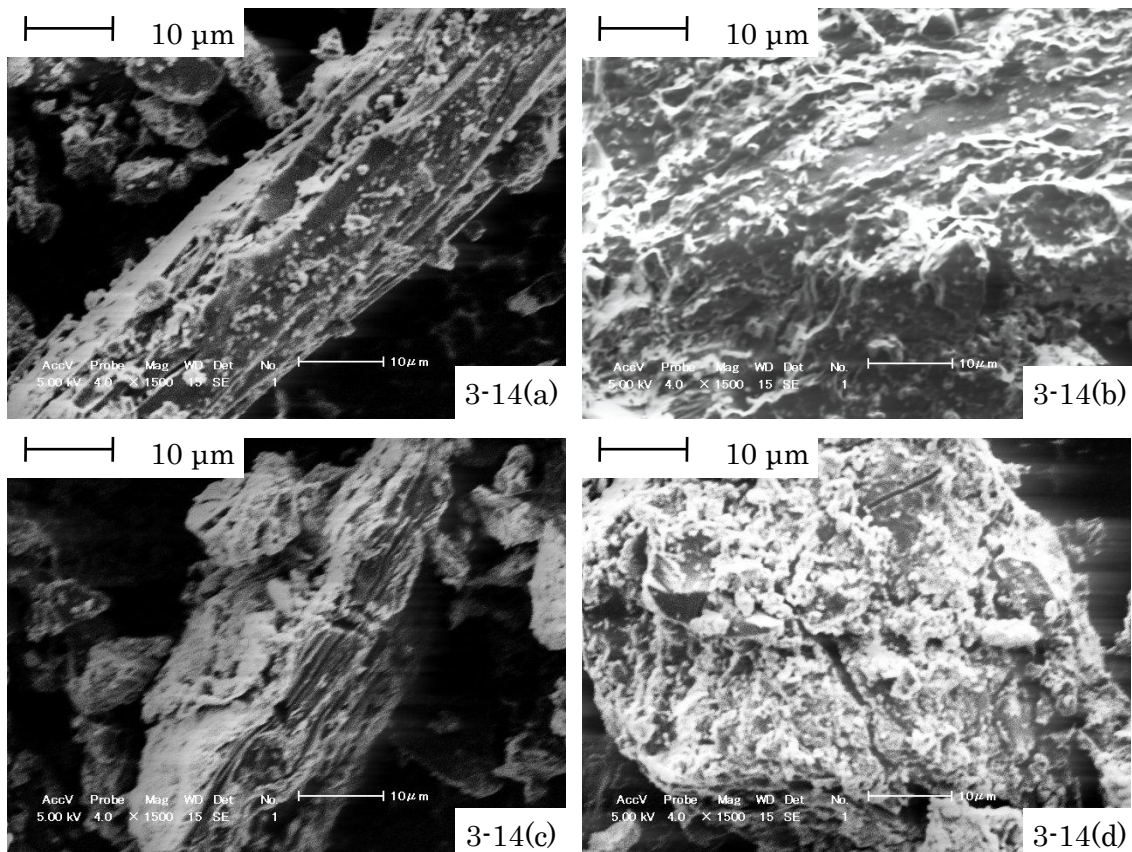


Figure 3-14. Magnified surfaces taken from the gasified cellulose and coal blends; (a) cellulose in the blend gasified to 550 °C, (b) coal in the blend gasified to 550 °C, (c) cellulose in the blend gasified to 800 °C, (d) coal in the blend gasified to 800 °C.

3.6 Summary

In pursuit of confirming, quantified and discussing the underlying synergy mechanism, this chapter presented co-gasification conversion behaviors, gas release patterns and morphology changes. The following results were obtained:

- Two conversion synergetic peaks occurs during co-gasification of biomass with coal;
 - The first peak occurred at around 400 °C while the other peak occurred above 800 °C, and
 - Steam environments yielded significant synergy than CO₂ gasification.
- Below 700 °C, H₂ release from biomass and coal blend was less than the average release from separate gasification of coal and cedar.
 - This result suggests H₂ capture through volatile interactions,
 - Biomass can serve as a hydrogen donor to enhance coal conversion
- Co-gasification of acid washed cellulose with coal resulted into only a single synergy peak between 350 °C and 450 °C.
 - Synergy can occur under the influence of volatiles interactions.
 - However, co-gasification of Na rich lignin with coal proves that synergy which occur above 800 °C is associated with AAEM catalysis.
- Morphology changes which occur during gasification contribute to gasification characteristics.
 - Pore and physical cracking on coal surface favors diffusion of gasifying agent and hence gasification reactions.
 - Low reactivity of coal and lignin particles is associated to their solid shapes maintained even at high temperature.

References

- [1] Lv D, Xu M, Liu X, Zhan Z, Li Z, Yao H, Effect of cellulose, lignin, alkali and alkaline earth metallic species on biomass pyrolysis and gasification. *Fuel Processing Technology*, 2009, 91, 903-909.
- [2] Zhu W, Song W, Lin W, Catalytic gasification of char from co-pyrolysis of coal and biomass. *Fuel Processing Technology*, 2008, 89, 890-896.
- [3] Mitsuoka K, Hayashi S, Amano H, Kayahara K, Sasaoaka E, Uddin A. Gasification of woody biomass char with CO₂: The catalytic effects of K and Ca species on char gasification reactivity. *Fuel Processing Technology*, 2011, 92, 26-31.
- [4] Haykiri-Acma H, Yaman S. Interaction between biomass and different rank coals during co-pyrolysis. *Renewable Energy*, 2010, 35, 288-292.
- [5] Sonobe T, Worasuwanarak N, Pipatmanomai S. Synergies in co-pyrolysis of Thai lignite and corncob. *Fuel Processing Technology* 2008, 89, 1371-1378.
- [6] Xu Q, Pang S, Levi T. Reaction kinetics and producer gas compositions of steam gasification of coal and biomass blend chars, part 1: Experimental investigation. *Chemical Engineering Science* 2011, 66, 2141-2148.
- [7] Meesri C, Moghtaderi B. Lack of synergetic effects in the pyrolytic characteristics of woody biomass/coal blends under low and high heating rate regimes. *Biomass Bioenergy*, 2002, 23, 55-66.
- [8] Kastanaki E, Vamvuka D, Grammelis P, Kakaras E. Thermogravimetric studies of the behavior of lignite–biomass blends during devolatilization. *Fuel Processing Technology*, 2002, 77, 159-166.
- [9] Sigma-Aldrich, product number 22182,

http://www.sigmaaldrich.com/catalog/search?interface=All_JA&term=cellulose&lang=ja®ion=JP&focus=product&N=0 accessed on December 6, 2012.

- [10] M. Sagehashi, N. Miyasaka, H. Shishido, A. Sakoda, Superheated steam pyrolysis of biomass elemental components and Sugi (Japanese cedar) for fuels and chemicals. *Bioresource Technology*, 2006, 97, 1272–1283.
- [11] H. Take, Y. Andou, Y. Nakamura, F. Kobayashi, Y. Kurimoto, M. Kuwahara, Production of methane gas from Japanese cedar chips pretreated by various delignification methods. *Biochemical Engineering Journal*, 2006, 28, 30–35.
- [12] Chung KE, Goldberg IB. Relation of the chemical structure of coal to its hydrolysis. *Fuel*, 1984, 63, 482-487.
- [13] Feng B, Bhatia SK. Variation of the pore structure of coal chars during gasification. *Carbon*, 2003, 41, 507–523.
- [14] Suelves I, La'zaro MJ, Moliner R. Synergetic effects in the co-pyrolysis of coal and petroleum residues: influences of coal mineral matter and petroleum residue mass ratio. *Journal of Analytical and Applied Pyrolysis*, 2000, 55, 29–41.
- [15] Fushimi C, Wada T, Tsutsumi A. Inhibition of steam gasification of biomass char by hydrogen and tar. *Biomass Bioenergy*, 2011, 35, 179-185.
- [16] Crichko AA, Gagarin SG. New ideas of coal organic matter chemical structure and mechanism of hydrogenation processes. *Fuel*, 1990, 69, 885–891.
- [17] Miura K, Mae K, Morikawa H, Hashimoto K. Flash hydrolysis of coal impregnated with catalyst through solvent swelling. *Fuel*, 1994, 73, 443-448.
- [18] Chung KE, Goldberg IB. Relation of the chemical structure of coal to its hydrolysis. *Fuel*, 1984, 63, 482-487.

- [19] Marzec A, Schulten H-R, Bimolecular and radical hydrogenation of coal studied by field ionization mass spectrometry. *Fuel*, 1987, 66, 844-850
- [20] Gani A, Naruse I. Effect of cellulose and lignin content on pyrolysis and combustion characteristics for several types of biomass. *Renewable Energy*, 2007, 32, 649-661.
- [21] Yang H, Yan R, Chen H, Lee DH, Zheng C, Characteristics of hemicellulose, cellulose and lignin pyrolysis. *Fuel*, 2007, 86, 1781-1788.
- [22] Haykiri-Acma H, Yaman S, Kucukbayrak S, Comparison of the thermal reactivities of isolated lignin and holocellulose during pyrolysis. *Fuel Processing Technology*, 2010, 91, 759-764.
- [23] Carrier M, Loppinet-Serani A, Denux D, Lasnier J-M, Ham-Pichavant F, Cansell F, Aymonier C, Thermogravimetric analysis as a new method to determine the lignocellulosic composition of biomass. *Biomass and Bioenergy*, 2011, 35, 298-307.
- [24] Haykiri-Acma H, Yaman S, Kucukbayrak S, Comparison of the thermal reactivities of isolated lignin and holocellulose during pyrolysis. *Fuel Processing Technology*, 2010, 91, 759-764.

Chapter 4

Gasification of biomass in the auto-thermal packed bed reactor

4.1 Introduction

In previous chapters, thermo-gravimetric characteristics of biomass gasification in addition to co-gasification characteristics of biomass with coal were presented. These characteristics provide fundamental knowledge required for setting up a gasification or co-gasification system. However, before putting such fundamental knowledge into practice, bench scale systems can be used to investigate other issues which cannot be assessed by using thermo-gravimetric methods.

Therefore, in this chapter, gasification of biomass was investigated by using an auto-thermal packed bed reactor. Behaviors investigated include temperature profiles, syngas composition, tar generation as well as gas concentration in the reactor. Performance factors such as syngas LHV, cold gas efficiency and carbon conversion are also presented. Results obtained, provide the basis for investigation of co-gasification behavior by using the packed bed reactor (refer to Chapter 5).

4.2 Experimental methods

4.2.1 Properties of the sample

Pellets made from whole body black pine (*pinus thunbergiana*) were used in this study. These pellets were about 8.5 mm long, 6.5 mm in diameter with apparent density of 1.1 g/cm³. Proximate analysis results for these pellets is presented in Table 4-1. Before the experiment, these pellets were dried at 107 °C for 24 hours.

Table 4-1. Proximate and ultimate analysis of the whole black pine pellets

Proximate analysis (<i>wt %</i>)			Ultimate analysis (<i>wt %</i>)					
As received	Dry basis		Dry ash free				Balance	
Moisture	VM	FC	Ash	C	H	N	S	O
4.64	83.58	15.81	0.61	49.25	6.65	0.91	-	43.19

^aVM represents volatile matter

^bFC represents fixed carbon

4.2.2 Experimental set-up

Gasification reactor used in this study was made of 1000 mm long reactor SUS304 stainless steel tube having 114 mm outer diameter and 6 mm wall thickness. Gas sampling ports were located at 50 mm, 100 mm, 200 mm, 300 mm, 400 mm, 500 mm, 600 mm, 700 mm, 800 mm, 900 mm and 950 mm from the bottom of the reactor (Figure 4-1). Correspondingly, 11 temperature thermocouples were located at similar heights with gas sampling ports. These thermocouples were connected to the data logger and hence computer for data storage.

Downdraft and updraft gasification were conducted by using the same reactor. During downdraft gasification, air was supplied from the upper port and therefore gasses inside reactor flow towards the bottom of the reactor as shown in Figure 4-2(a). However, during updraft gasification, air was supplied from the lower port, gasses flow upwards and the syngas exited from the upper port (Figure 4-2(b)).

The biomass hopper at the top of the reactor was packed with pine pellets and purged with N₂ at 1.6 L/min to avoid pre-combustion. The screw feeding mechanism supplied biomass pellets into the reactor, where the pellets were supported by stainless wire mesh located at the bottom of the reactor. The height of biomass packed bed was checked by using metering rod inserted from the top of the

reactor. Ash from the spent biomass passed through the stainless wire mesh and dropped into the ash tray by gravity. The exits for the syngas from the reactor were located at the top and at the bottom of the reactor (Figure 4-2(a) and Figure 4-2(b)). From either of the two exits, syngas was then passed through the water-cooled cooling tower. Part of the syngas was sampled for analysis by using a micro gas chromatograph.

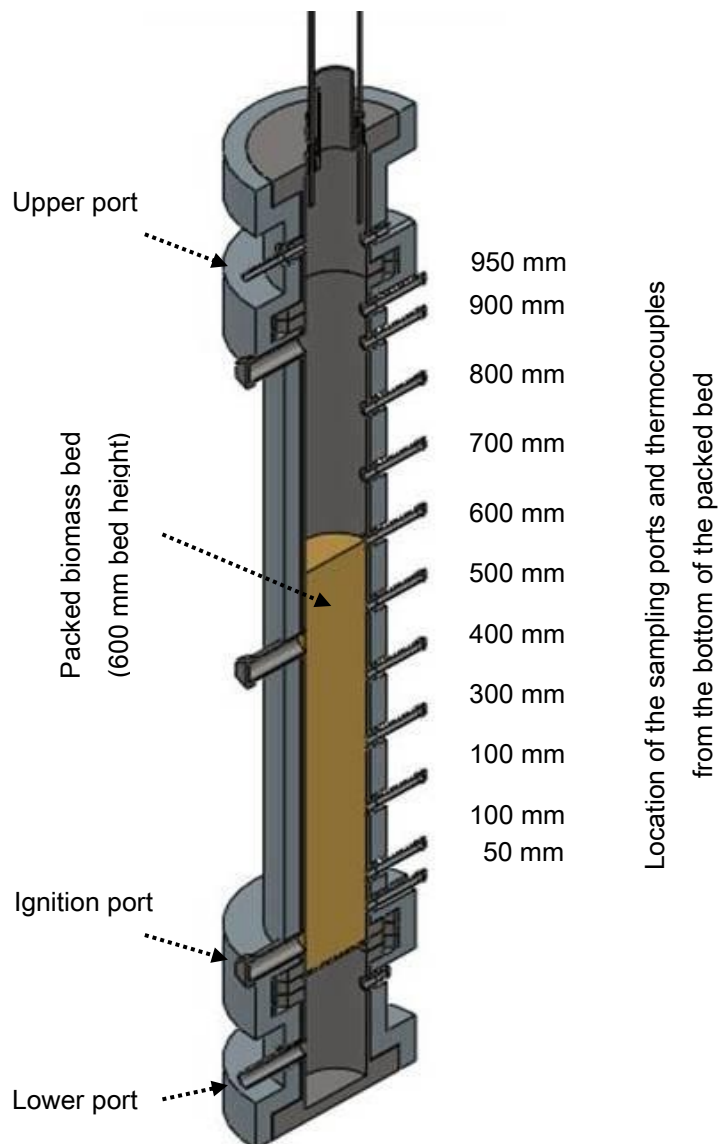


Figure 4-1. The packed bed reactor

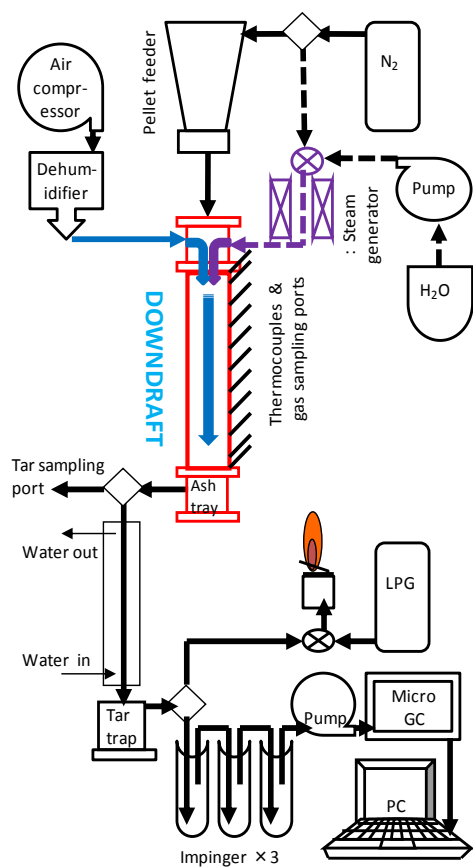


Figure 4-2(a)

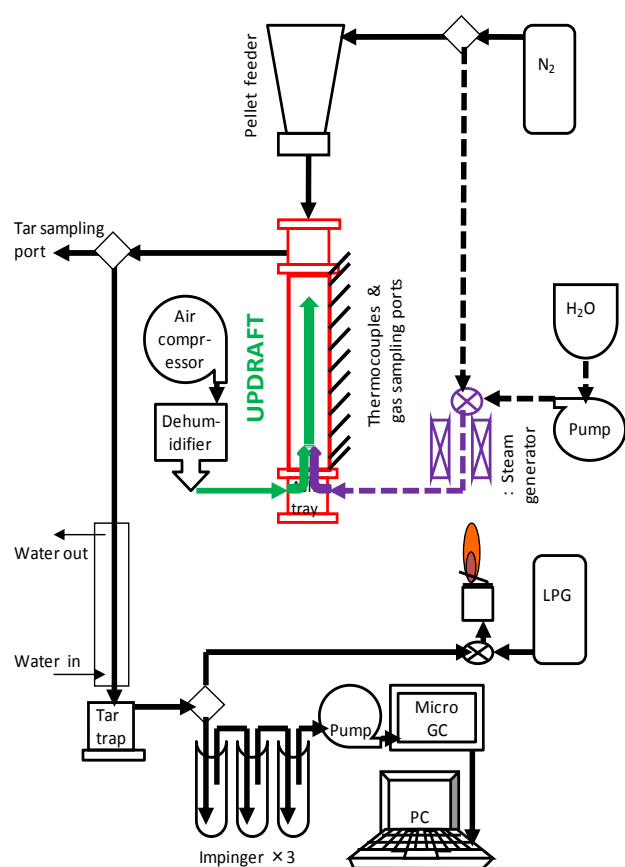


Figure 4-2(b)

Figure 4-2. Schematic diagram for (a) downdraft gasifier (b) updraft gasifier

4.2.3 Gasification and tar sampling procedures

During the start-up period, the reactor was fed with about 0.5 kg of biomass pellets forming about 90 mm bed height (Table 4-2). This amount of biomass was ignited by using a propane burner through the ignition port. Then, air at 20 L/min was supplied from the top or from the bottom of the gasifier resulting into downward or updraft gasification, respectively. When the temperature of about 200 °C was attained, continuous feeding of biomass pellets at 20 g/min was started. Bed heights were checked in every 20 minutes intervals and allowed to rise to 1000

mm. In order to maintain the packed bed height during the continuous operation modes of the reactor, biomass supply was reduced to 9 g/min (Table 4-2). After attaining steady state, i.e. stabilization of reactor temperature and syngas composition, tar and gas sampling was conducted.

Table 4-2. Experimental conditions for downdraft and updraft gasification

Sample	Japanese black pine pellets
Initial packed pellets (weight / bed height)	0.5 kg / 90 mm
Air flow rate	20 L/min
Feeding rate (start up mode)	20 g/min
Feeding rate (continuous running mode)	9 g/min
Target value of packed-bed height	600 mm
Stoichiometric combustion air ratio	0.44

Tar content in the syngas was analyzed by using a set of three impingers cooled in the ice bath. These impingers were set between the tar trap and the micro gas chromatograph (Figure 4-2(a) and Figure 4-2(b)). The first two impingers were filled with 150 mL of dichloromethane to dissolve the tar while the third impinger was packed with cotton wool for tar scavenging. Before tar sampling, an empty beaker in addition to the cotton wool packed impinger and the other two empty impingers, were dried in a constant temperature oven at 107 °C for 3 hours and weighed. During tar sampling, the sampled syngas flowing at the rate of 1 L/min was passed through the three impingers for 1 hour. Then, all the impingers were disconnected from the sampling line. Tar deposited along the tubes in the sampling line, was rinsed by using dichloromethane and poured in to the beaker. Hence impingers and the collected tar in a beaker were dried at 107 °C for 3 hours to

vaporize dichloromethane as well as moisture contents. Weight differences before the tar sampling and after vaporization; indicate tar content in the syngas.

4.2.4 Analysis of performance factors

Lower heating value, LHV [$\text{MJ}/\text{m}^3_{\text{N}}$], of the syngas was calculated as follows [1,2]:

$$\text{LHV} = \sum V_i \times \text{LHV}_i \quad (4-1)$$

where V_i denotes volumetric composition of H_2 , CO or CH_4 in the syngas [%] and LHV_i represents lower heating value [$\text{MJ}/\text{m}^3_{\text{N}}$] of the respective gases.

Cold gas efficiency, CGE [%] was calculated as suggested by Howaniec et al [1]:

$$\text{CGE} = \text{LHV}_{\text{gas}} \times Q_{\text{gas-fuel}} / \text{LHV}_{\text{bio}} \quad (4-2)$$

where LHV_{gas} is the syngas LHV [$\text{MJ}/\text{m}^3_{\text{N}}$], $Q_{\text{gas-fuel}}$ denotes volumetric flow rate of syngas per supplied mass of biomass pellets [$\text{m}^3_{\text{N}}/\text{kg}$] and LHV_{bio} represents biomass LHV [MJ/kg].

Carbon conversion, C_{conv} [%] was estimated as a ratio of carbonaceous gas produced C_{gas} [$\text{mol}_{\text{carbon}}$] to carbon in biomass pellets supplied C_{bio} [$\text{mol}_{\text{carbon}}$] as reported by Kumabe et al [1].

$$C_{\text{conv}} = C_{\text{gas}} / C_{\text{bio}} \quad [\%] \quad (4-3)$$

4.3 Results and discussion

4.3.1 Temperature and gas compositions during downdraft gasification

Figure 4-3(a) shows temperature variations with time during downdraft gasification. Sharp increase in temperature for successive bed heights as packed bed height increases and consequently oxidation of the supplied biomass pellets propagates to the upper parts of the gasifier. After 6 hours, 600 mm packed bed height was attained and therefore biomass feed rate was reduced to 9 g/min (Table 4-2). Temperature profiles indicated a stable trend 2 hours later.

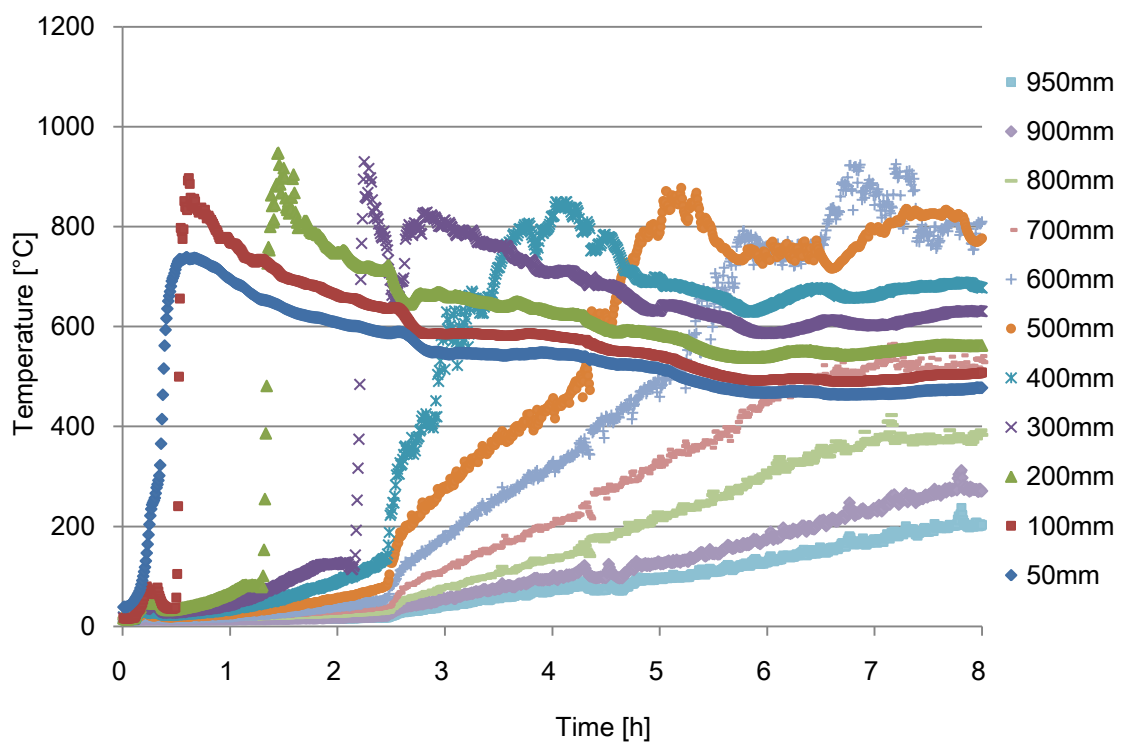


Figure 4-3(a). Temperature variations during downdraft gasification.

Variations of syngas compositions covering a span of 8 hours are presented in Figure 4-3(b). CO increased to surpass CO₂ as bed height increases and O₂ content vanished. With the decrease in biomass and air supply rate at the end of start-up mode and beginning of downdraft operation, volumetric composition of the gaseous species in the syngas also decreased. Under steady state downdraft conditions, syngas was composed of about 14.7% CO, 13.6% CO₂, 12% H₂ and 2.2% CH₄ (Figure 4-3(b)).

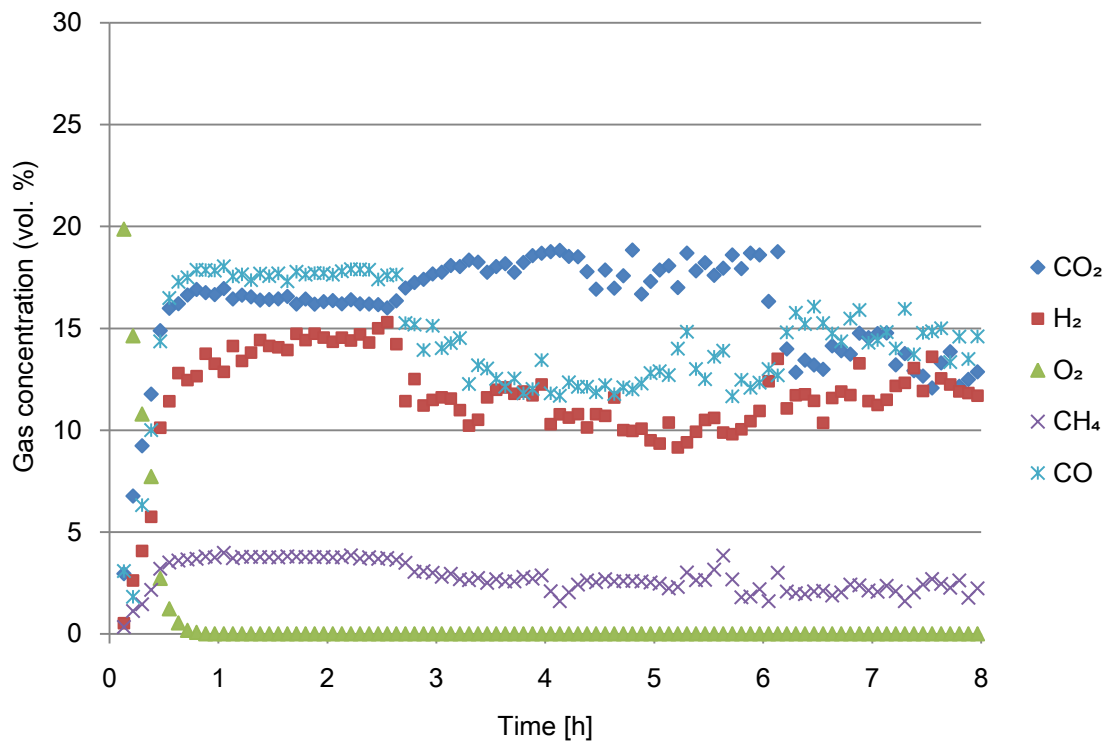


Figure 4-3(b). Syngas compositions during downdraft gasification.

Steady state reactor temperatures and gas compositions at various bed heights during downdraft gasification are presented in Figure 4-4. Maximum temperature was observed at the top of the packed bed i.e. 600 mm, where partial

oxidation takes place. Since no further oxidation occurs, temperature decreases gradually to the lowest temperature at the bottom part. This gradual temperature decrease can also be associated with endothermic char reductions which takes place along this reduction zone [3,4]. The same figure suggests that most of the product gasses were generated at the upper part of the packed bed where due to evolution of volatile matter and partial oxidation. CO, H₂ and CH₄ tend to increase slightly towards the bottom of the reactor owing to the reduction reactions [5].

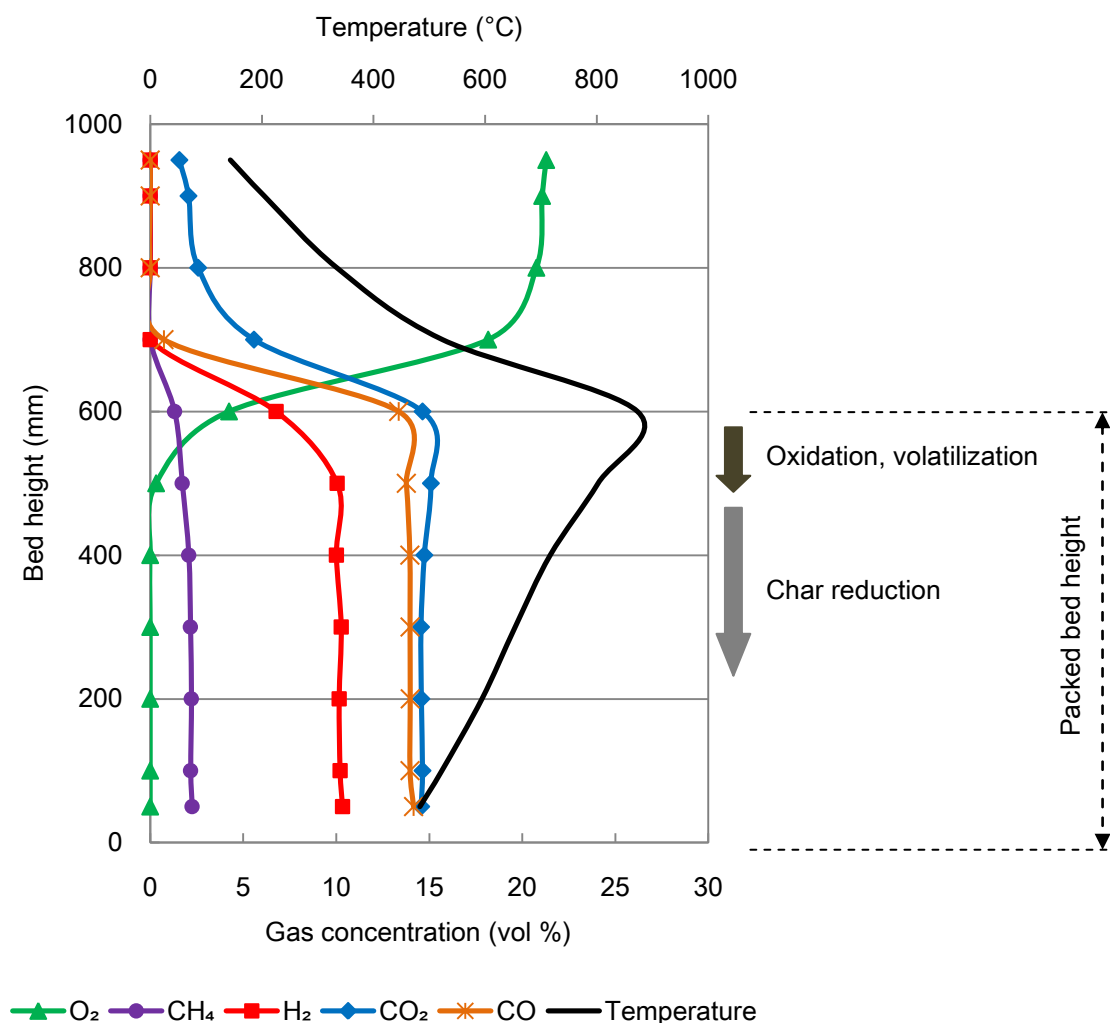


Figure 4-4. Syngas compositions during downdraft gasification.

4.3.2 Temperature and gas compositions during updraft gasification

Figure 4-5(a) shows temperature variations with time during updraft gasification. As opposed to downdraft gasification, high temperature occurs at the lower part of the reactor during updraft gasification. After 3.5 hours bridging phenomena occurred and therefore temperature decreased sharply. Nevertheless, temperature stabilized after breaking up of the bridging biomass. Target bed height of 600 mm was attained after 6.5 hours.

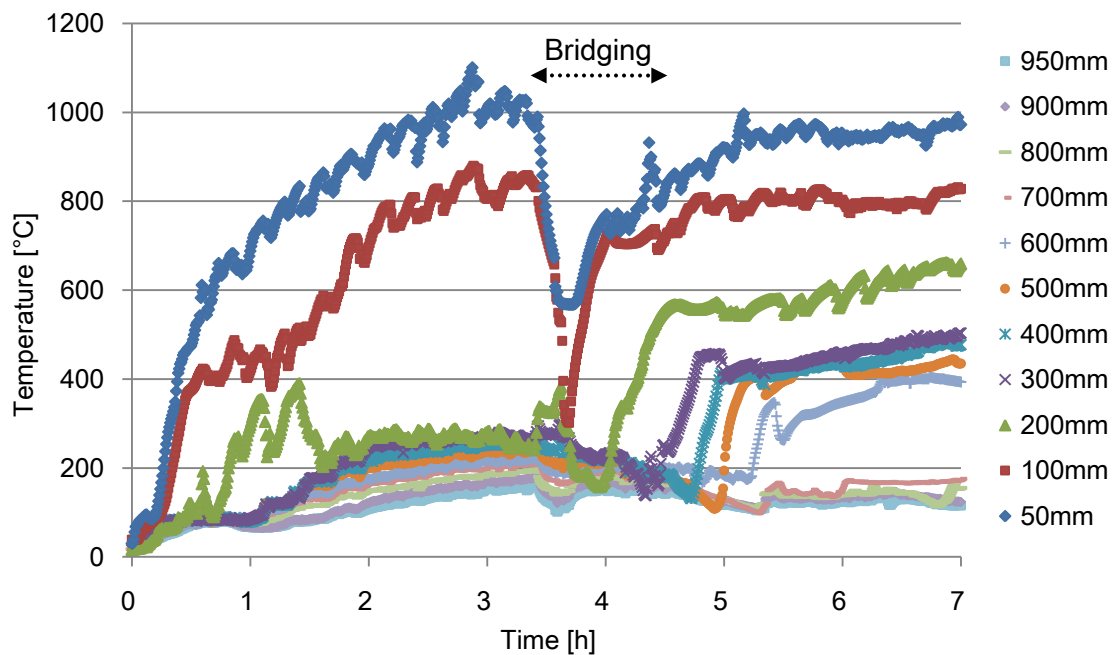


Figure 4-5(a). Temperature variations during updraft gasification.

Syngas compositions during updraft gasification are presented in Figure 4-5(b). CO surpassed CO₂ production 1 hour after starting experiment. The period at which bridging occurred is marked by abrupt increase in CO₂ and decrease in CO and H₂. Under steady state updraft gasification, syngas composition was 26.8% CO, 5.3% CO₂, 4.9% H₂ and 1.4% CH₄ (Figure 4-5(b))

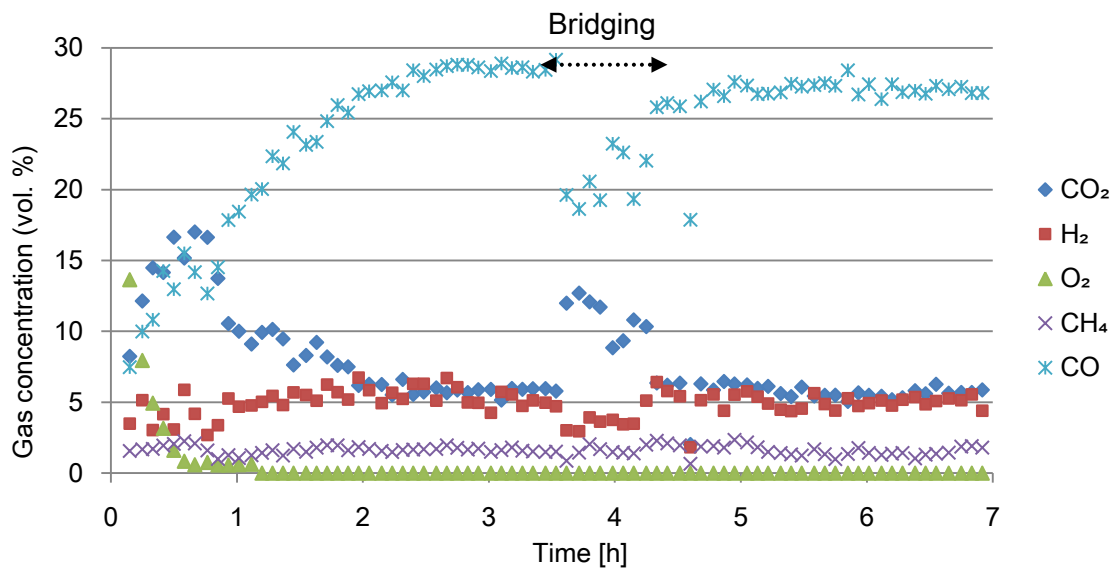


Figure 4-5(b). Syngas compositions during updraft gasification.

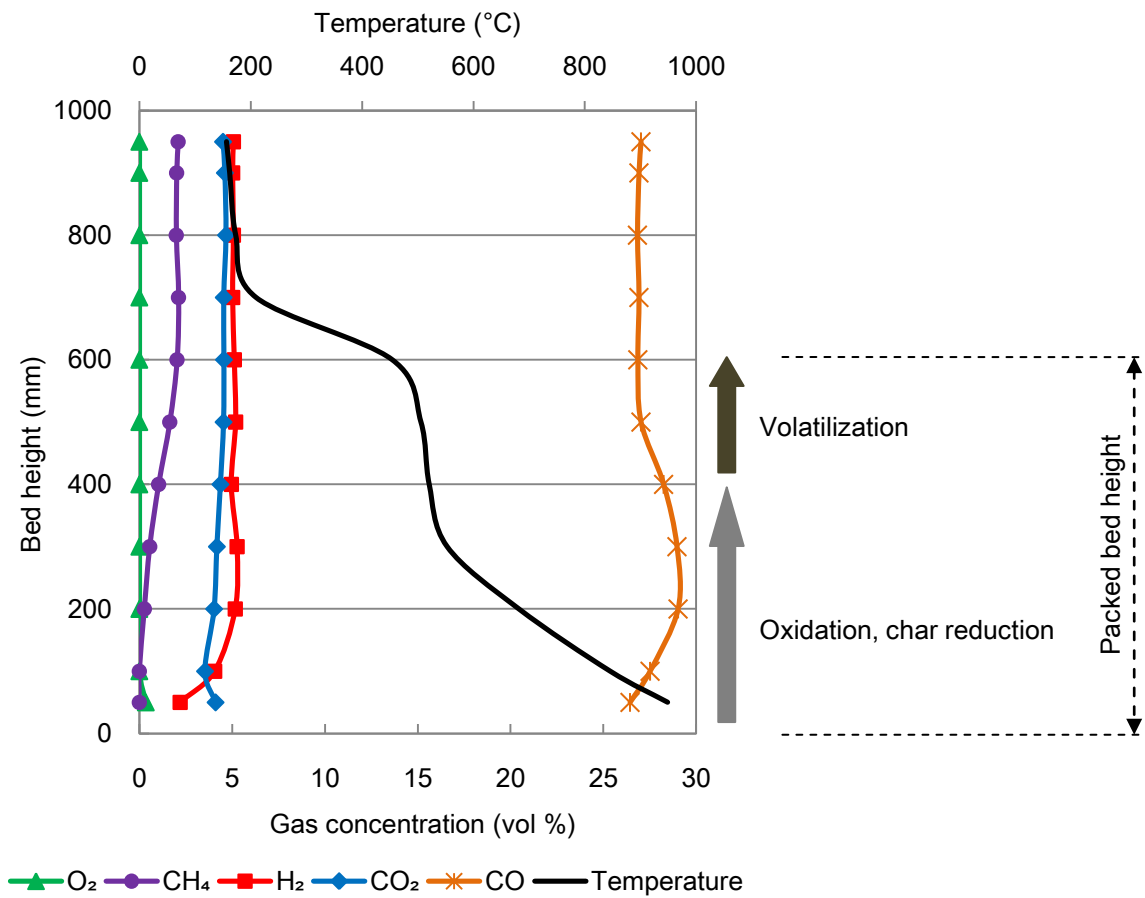


Figure 4-6. Syngas compositions during updraft gasification.

Figure 4-6 shows reactor temperature and gas compositions during updraft gasification. Highest temperature was observed at the bottom of the packed bed where oxidation occurred. Temperature decreases to the upper part of the packed bed and further at the top of the gasifier. CO₂ was generated at the lower part due to oxidation while CO and H₂ were produced by reduction reactions between the bottom and the middle parts of the part of the packed bed. Notably, CO production during updraft gasification was significantly higher than for downdraft case (Figure 4-4 vs. Figure 4-6). CH₄ was mainly produced by evolution of volatile matter at the upper of the part of the packed bed.

4.3.3 Tar contents and performance factors

Tar contents in syngas during downdraft and updraft gasification was derived by using the method described in section 4.2.3. Performance factors such as lower heating value (LHV), cold gas efficiency and carbon conversion were calculated as shown in section 4.2.4. Tar contents and performance factors are presented in Table 4-3. LHV of the syngas produced during downdraft and updraft was 3.9 MJ/m³_N and 4.4 MJ/m³_N, respectively. Corresponding, tar contents for downdraft and updraft syngas were 9.17 g/m³_N and 26.83 g/m³_N. Photos of impinger sets after tar sampling are shown in Figure 4-7. According to these results, updraft favorably produced higher syngas LHV however tar contents were unfavorably very high. On the other side, downdraft generated low tars but also low LHV. Low tar generation during downdraft can be linked to longer residence time taken by the tars to pass through the 600 mm hot packed charred biomass [5,6].

Table 4-3. Tar contents and performance factors

	Downdraft gasification	Updraft gasification
Syngas LHV (MJ/m ³ _N)	3.9	4.4
Tar content (g/m ³ _N)	9.17	26.83
Cold gas efficiency (%)	75%	81%
Carbon conversion (%)	85%	96%



Figure 4-7(a)



Figure 4-7(b)

Figure 4-7. Impingers used for tar analysis; (a) downdraft case (b) updraft case.

Cold gas efficiency and carbon conversion during downdraft and updraft gasification are presented in Table 4-3. For downdraft and updraft, cold gas efficiency was about 75% and 81%, respectively. Corresponding carbon conversions were 85% and 96%. These proportions suggest that updraft gasification is efficient than downdraft gasification due to highly effective conversion of supplied biomass fuel. Higher conversion and efficiency in updraft case is associated to higher CO production (Figure 4-4 vs. Figure 4-6).

4.3.4 Tar reduction by steam injection

Results presented in the previous section, show importance of enhancing syngas LHV and reducing tar generation. Various methods including improvement of gasifier designs, use of catalysts and steam injection have been reported [2,5,6]. Steam injection was chosen as the first hand method. Under such scheme, water-gas shift reaction (Equation 4-4) can also occur to favor H₂ production. However, this reaction will have an adverse effect on CO content. In addition, steam reaction with tar as a typical hydrocarbon can result in production of CO and H₂ and therefore contribute to improvement of syngas LHV as shown in Equation 4-5.

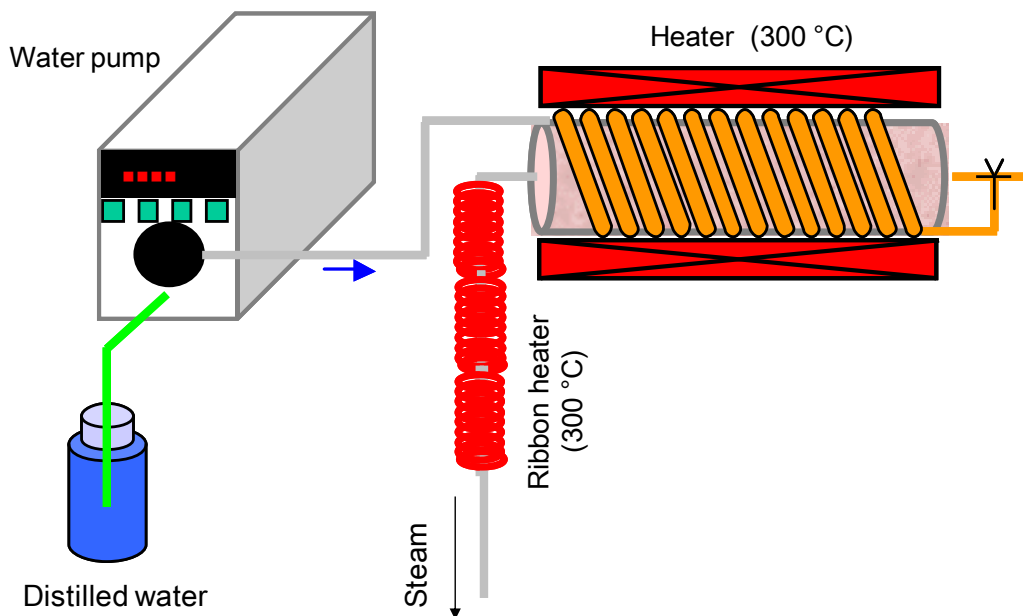
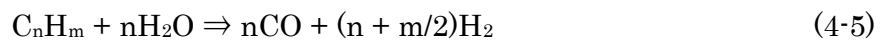


Figure 4-8. Schematic diagram for steam generator.

Steam generated at 300 °C was injected into the reactor at 1.23 g/min during downdraft gasification. The schematic diagram for steam generation is shown in Figure 4-8. As a result, tar content was reduced from 9.17 g/m³_N to 8.5 g/m³_N. Syngas composition changed to 13.2% CO, 16.5% CO₂, 11.1% H₂ and 1.9% CH₄. Therefore, LHV was reduced from 3.9 MJ/m³_N to 3.5 MJ/m³_N.

Although tar reduction was achieved by steam injection method, the observed reduction was very little. Moreover, this reduction came with the sacrifice of syngas LHV. Similarly, Wang *et al.* [7] used a steam tar reformer and concluded a trade-off relation between improvement of syngas LHV and reduction of tar generation. Therefore, another method for tar reduction has to be applied. Gasifier improvement work conducted in this study is presented in Chapter 5.

4.4 Summary

Gasification of biomass in an auto-thermal packed bed reactor was investigated. Temperature profiles, syngas composition, tar generation as well as gas concentration in the reactor have been presented and discussed. Performance factors such as syngas LHV, cold gas efficiency and carbon conversion have also been presented. The following findings were obtained;

- Updraft favorably produced higher syngas LHV however tar contents are unfavorably high.
- Downdraft generated low tars but also low LHV due to longer residence time for tar cracking to occur inside the reactor.
- Higher conversion and efficiency for updraft gasification is due to higher CO production.

- Tar reduction is achievable by steam injection however at the sacrifice of syngas LHV.
 - Therefore, other methods for should be applied.

References

- [1] Howaniec N, Smolinski A, Stanczyk K, Pichlack M. Steam co-gasification of coal and biomass derived chars with synergy effect as way of hydrogen-rich gas production. *International Journal of Hydrogen Energy*, 2011, 36, 14455-14463.
- [2] Kumabe K, Hanaoka T, Fujimoto S, Minowa T, Sakanishi K, Co-gasification of woody biomass with steam. *Fuel*, 2007, 86, 684-689.
- [3] Bunt JR, Waanders FB. Identification of the reaction zones occurring in a commercial-scale Sasol-Lurgi FBDB gasifier. *Fuel* 2008, 87, 1814-1823.
- [4] Gordillo G, Annamalai K, Carlin N. Adiabatic fixed-bed gasification of coal, dairy biomass and feedlot biomass using an air-steam mixture as an oxidizing agent. *Fuel* 2010, 89, 384-391.
- [5] Chen Y, Luo Y-H, Wu W-G, Su Y, Experimental Investigation on Tar Formation and Destruction in a Lab-Scale Two-Stage Reactor. *Energy Fuels* 2009, 23, 4659-4667.
- [6] Brandt P, Larsen E, Henriksen U, High Tar Reduction in a Two-Stage Gasifier. *Energy and Fuels* 2000, 14, 816-819.
- [7] Wang Y, Yoshikawa K, Namioka T, Hashimoto Y, Performance optimization of two-staged gasification system for woody biomass. *Fuel Processing Technology*, 2007, 88, 243-250.

Chapter 5

Co-gasification of biomass and coal in the auto-thermal packed bed reactor

5.1 Introduction

Improvement of syngas LHV and reduction of tar generation remain to be the principal objective for many of biomass gasification researches [1,2,3,4]. Biomass gasification by using air is reported to produce syngas with around 4 MJ/m³_N LHV and tar content of about 20 g/m³_N while the basic requirements for gas application in the engine are LHV of above 3.5 MJ/m³_N and tar concentration of less than 0.02 g/m³_N [1,5]. Although syngas LHV from these results indicate promising results, tar generation is still far above the required values. Primary methods for tar removal from the syngas include improvement of operating parameters, the use of catalysts and system design modifications [1,4,5]. Secondary methods include thermal or catalytic tar cracking and cleaning. Brandt *et al.* reported on remarkable tar reduction after oxidation of pyrolysis gas and passage of the producer gas through the char bed [2]. Cao *et al.*, re-circled part of the syngas into the reactor and introduced secondary air to produce syngas with extremely low tar content [4].

In Chapter 4, gasification of biomass by using an auto-thermal packed bed reactor was investigated. Results obtained show that updraft favorably produced higher syngas LHV however tar contents are unfavorably high. As opposed to that downdraft generated low tars but also low LHV. Tar reduction by steam injection was examined however tar reduction was not so successful and syngas LHV was slightly affected. These results suggest that other methods for should be applied for enhancement of syngas LHV and reduction of tar formation.

Based on the salient differences on performance of downdraft and updraft gasification, as far as tar generation and syngas LHV are concerned, combination of downdraft and updraft gasification was investigated. In this thesis, such a combination will be called *counter-flow gasification*. For the purpose of comparison, gasification of biomass and co-gasification of biomass with coal were conducted by using counter-flow method. Meanwhile, downdraft and updraft air supply were varied to find the optimal operating conditions. Analyses performed include syngas composition, tar generation as well as temperature profiles and gas concentration in the reactor. Performance factors such as syngas LHV, cold gas efficiency and carbon conversion are also presented. In addition to that, some synergetic observations are discussed.

5.2 Experimental methods

5.2.1 Properties of the samples

Pellets made from whole body black pine (*pinus thunbergiana*) and coal were used in this study. Pine pellets were about 8.5 mm long, 6.5 mm in diameter with apparent density of 1.1 g/cm³. Particle size for coal sample used was about 10±0.5 mm. Proximate analysis results for these samples are presented in Table 5-1. Before the experiment, these samples were dried at 107 °C for 24 hours.

Table 5-1. Proximate and ultimate analysis of the samples

Sample			Pine pellets	Coal
Proximate analysis (wt %)	As received	Moisture	4.64	2.2
	Dry basis	Volatile matter	83.58	28.2
		Fixed carbon	15.81	55.8
		Ash	0.61	16.0
Ultimate analysis (wt %)	Dry and ash free basis	C	49.25	83.19
		H	6.65	4.95
		N	0.91	1.73
		S	-	0.21
	Balance	O	43.19	9.92

5.2.2 Improved experimental set-up and stoichiometric air ratio

Gasification reactor used in this study was made of 1000 mm long reactor SUS304 stainless steel tube having 114 mm outside diameter and 6 mm wall thickness. Gas sampling ports were located at 50 mm, 100 mm, 200 mm, 300 mm, 400 mm, 500 mm, 600 mm, 700 mm, 800 mm, 900 mm and 950 mm from the bottom of the reactor (Figure 5-1(a)). Correspondingly, 11 temperature thermocouples were located at similar heights with gas sampling ports. These thermocouples were connected to the data logger and hence computer for data storage.

The biomass hopper at the top of the reactor was packed with either biomass pellets or a mixture of biomass and coal during gasification and co-gasification, respectively. The hopper was purged with N₂ at 1.6 L/min and the screw feeding mechanism supplied fuel into the reactor. The height of the packed bed was checked by using metering rod inserted from the top of the reactor. Ash from the spent fuel passed through the stainless wire mesh and dropped into the ash tray by gravity. The exits for the syngas from the reactor were located at the middle and at the

bottom of the reactor (Figure 5-1(b)). From either of the two exits, syngas was then passed through the water-cooled cooling tower. Part of the syngas was sampled for analysis by using a micro gas chromatograph.

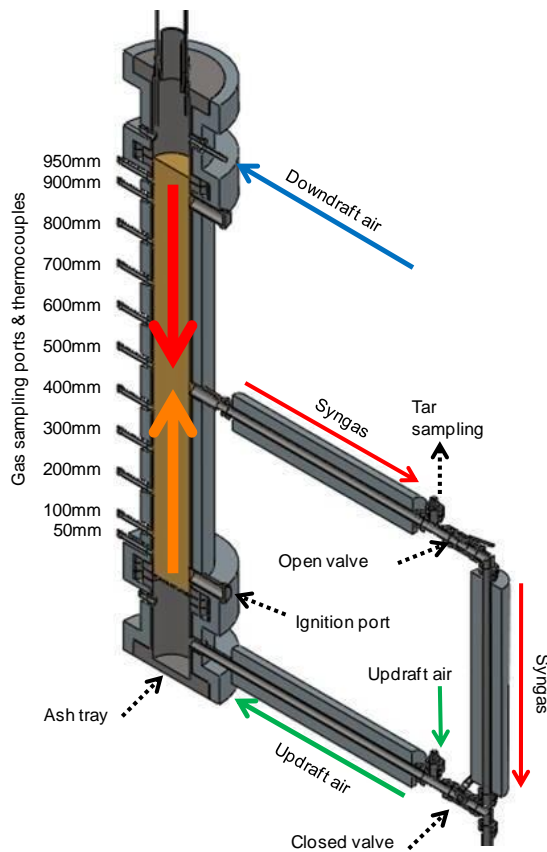


Figure 5-1(a)

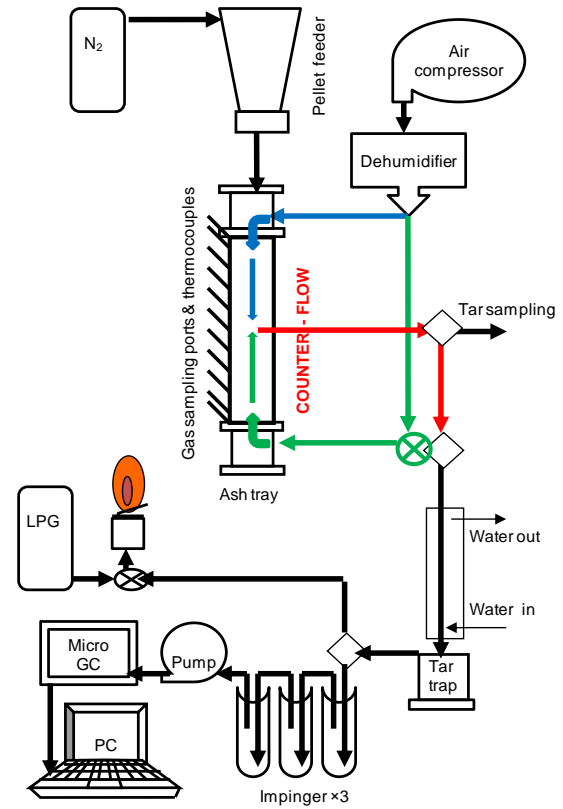


Figure 5-1(b)

Figure 5-1. The counter-flow gasifier (a) reactor (b) schematic system.

The following gasifier modifications were done for counter-flow gasification:

- Air supply lines were set at the top and at the bottom of the reactor.
- Syngas exit was placed at the middle of the gasifier.
- Ball valves designed to withstand 520 °C were positioned at far ends of the middle and bottom syngas exits.

- Based on energy balance analysis of selected endothermic and exothermic reaction for a typical auto-thermal gasification process, air supply was reduced from 20 L/min to 16/min. Therefore, stoichiometric combustion air ratio changed from 0.44 to 0.35.

5.2.3 Gasification and tar sampling procedures

During the *start-up* period, the reactor was fed with about 0.5 kg of biomass pellets forming about 90 mm bed height (Table 5-2). This amount of biomass was ignited by using a propane burner through the ignition port. It can be noted that even for co-gasification of biomass and coal case, 0.5 kg of biomass only was fed for ignition purpose, there after a mixture of biomass and coal was supplied.

Table 5-2. Experimental conditions for gasification and co-gasification experiments

		Gasification	Co-gasification
	Fuel	Biomass only	80%biomass 20%coal
	Target bed height	1,000 mm	
Start-up	Initial packed pellets	0.5 kg / 90 mm	
	Downdraft air supply	20 L/min	
	Fuel feeding rate	20 g/min	
Downdraft	Downdraft air supply	16 L/min	18 L/min
	Fuel feeding rate	9 g/min	9 g/min
Counter-flow	Downdraft/Updraft air (L/min)	12/4 ^g , 8/8 ^h , 4/12 ^k	13.5/4.5 ^g , 9/9 ^h
	Fuel feeding rate	9 g/min	9 g/min
Stoichiometric combustion air ratio		0.35	
	^g CFL-1	^h CFL-2	^k CFL-3

With the bottom syngas exit open and the middle exit closed, downdraft air was supplied at 20 L/min. When the temperature of about 250 °C to 300 °C was attained, continuous feeding of biomass or biomass and coal blend 20 g/min was started. Bed heights were checked in every 20 minutes intervals and allowed to rise to 1,000 mm. In order to maintain the packed bed height during all continuous operation modes, fuel supply was reduced to 9 g/min (Table 5-2). Meanwhile air was reduced to 16 L/min for biomass gasification and 18 L/min during co-gasification of biomass with coal. After attaining steady state, i.e. stabilization of reactor temperature and syngas composition; tar and gas sampling was conducted.

Operation mode of the reactor was changed from downdraft to counter-flow by closing the bottom syngas exit and opening the middle exit (see Figure 5-1(a)). Simultaneously, updraft air was introduced and downdraft air was reduced so that the total air supply was maintained at 16 L/min during biomass gasification and 18 L/min for co-gasification experiments (Table 5-2). With downdraft air supplied at 12 L/min and updraft air at 4 L/min during biomass gasification we refer this counter-flow mode as CFL-1 as shown by a footnote in Table 5-2. Similarly, CFL-1 under co-gasification case was realized by supplying 13.5 L/min downdraft air and 4.5 L/min updraft air. During these counter-flow modes, tar and gas sampling were also conducted after stabilization of reactor temperature and syngas composition. To realize CFL-2 and CFL-3 counter-flow modes; downdraft air was further reduced while updraft air was increased as shown in Table 5-2. Tar and gas sampling were also performed during these operation modes.

Tar content in the syngas was analyzed by using a set of three impingers cooled in the ice bath. These impingers were set between the tar trap and the micro

gas chromatograph (Figure 5-1(b)). The first two impingers were filled with 150 mL of dichloromethane to dissolve the tar while the third impinger was packed with cotton wool for tar scavenging. Before tar sampling, an empty beaker in addition to the cotton wool packed impinger and the other two empty impingers, were dried in a constant temperature oven at 107 °C for 3 hours and weighed. During tar sampling, the sampled sygas flowing at the rate of 1 L/min was passed through the three impingers for 1 hour. Then, all the impingers were disconnected from the sampling line. Tar deposited along the tubes in the sampling line, was rinsed by using dichloromethane and poured in to the beaker. Hence impingers and the collected tar in a beaker were dried at 107 °C for 3 hours to vaporize dichloromethane as well as moisture contents. Weight differences before the tar sampling and after vaporization; indicate tar content in the syngas.

5.2.4 Analysis of performance factors and synergetic aspects

Lower heating value, LHV [MJ/m³N] of the syngas was calculated as [6,7]:

$$\text{LHV} = \sum V_i \times \text{LHV}_i \quad (5-1)$$

where V_i denotes volumetric composition of H₂, CO or CH₄ in the syngas [%] and LHV_{*i*} represents lower heating value [MJ/m³N] of the respective gases.

Cold gas efficiency, CGE [%] was derived as suggested by Howaniec *et al.* [6]:

$$\text{CGE} = \text{LHV}_{\text{gas}} \times Q_{\text{gas-fuel}} / \text{LHV}_{\text{bio}} \quad (5-2)$$

where LHV_{gas} is the syngas LHV [MJ/m³N], $Q_{\text{gas-fuel}}$ denotes volumetric flow rate of syngas per supplied mass of biomass pellets [m³N/kg] and LHV_{bio} represents

biomass LHV [MJ/kg].

Carbon conversion, C_{conv} [%] was estimated as a ratio of carbonaceous gas produced C_{gas} [mol_{carbon}] to carbon in biomass pellets supplied C_{bio} [mol_{carbon}] as reported by Kumabe et al [7].

$$C_{\text{conv}} = C_{\text{gas}} / C_{\text{bio}} \text{ [%]} \quad (5-3)$$

Synergy during co-gasification of biomass and coal indicate unexpected difference in behavior of the blend from the expected behavior that can be calculated from the behavior of separate gasification of the two fuels, biomass and coal [6,7]. Therefore, in order to establish the occurrence of synergy, behavior of the parent samples must be available as shown in Equation (3-2) in the Chapter 3. The packed bed reactor used in this study, was designed for biomass gasification only. Therefore, we could not conduct gasification of coal. However, co-gasification of biomass and coal blends with high biomass to coal ratio were conducted. Despite of this barrier, this chapter discusses on synergetic observations upon availability of reliable assumption on coal behavior.

5.3 Results and discussion

5.3.1 Temperature and gas compositions during biomass gasification

Temperature variations with time during start-up period indicate sharp increase in temperature for successive bed heights as packed bed height increases and consequently oxidation of the supplied biomass pellets propagates to the upper parts of the gasifier (Figure 5-2(a)). After 8 hours, 1000 mm packed bed height was attained and therefore marking the end of start-up mode. Reduction of air flow rate and biomass feed rate (Table 5-2), resulted into low temperatures. While

temperature at the top parts increased, temperature at the bottom parts of the reactor remained low and stable. As from 11 hours, temperature profiles indicated a stable trend for the downdraft gasification operation.

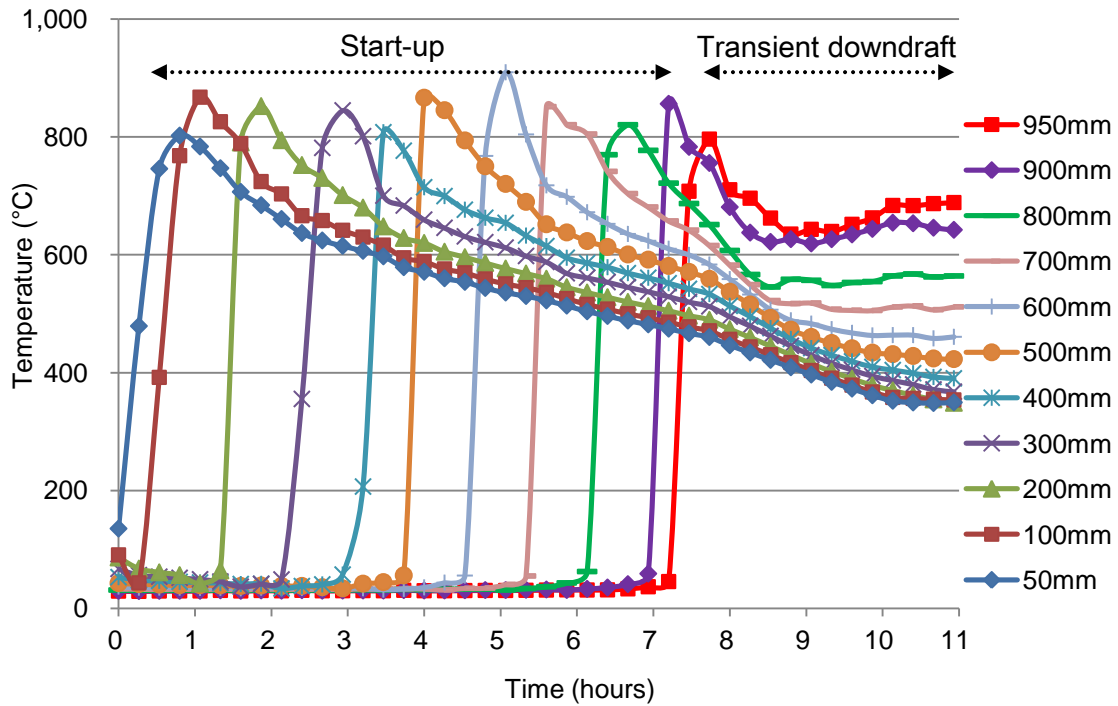


Figure 5-2(a). Temperature variations during start-up and transient downdraft biomass gasification.

During counter-flow operation mode, temperature at the lower parts of the reactor, notably at 50 mm and 100 mm from the bottom of the reactor, increased with the increase of the updraft air supply (Figure 5-2(b)). Steady state downdraft temperature profiles are also shown in this figure. This trend can be observed for all three counter-flow operation modes; *CFL-1*, *CFL-2* and *CFL-3* (Table 5-2). Temperature at the upper parts of the reactor, especially at 950 mm and 900 mm decreased while temperature at the middle parts were less affected.

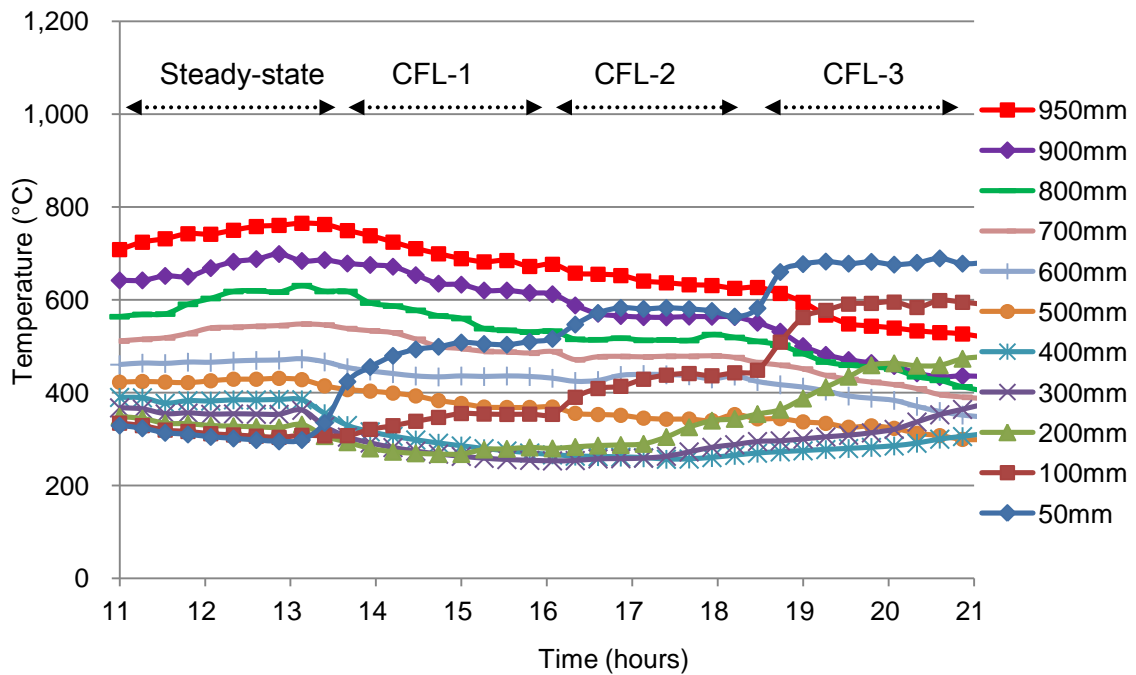


Figure 5-2(b). Temperature variations during downdraft and counter-flow biomass gasification.

Variation of syngas compositions covering a span of initial 11 hours, i.e. the start-up and the transient downdraft operation periods are presented in Figure 5-2(c). At the early stages of the start-up mode, CO₂ production was higher than CO. Then, CO increased to surpass CO₂ as bed height increases and O₂ content vanished. With the decrease in biomass and air supply rate at the end of start-up mode and beginning of downdraft operation, volumetric composition of the gaseous species in the syngas also decreased. Under steady state downdraft conditions, syngas was composed of about 15.9% CO, 12% CO₂, 10.4% H₂ and 2.5% CH₄ (Figure 5-2(c)). It can be noted that during *CFL-1*, composition of CO, H₂ and CH₄ increased slightly, however further increase in updraft air during *CFL-2* and *CFL-3*, resulted in reduction of these combustible gases.

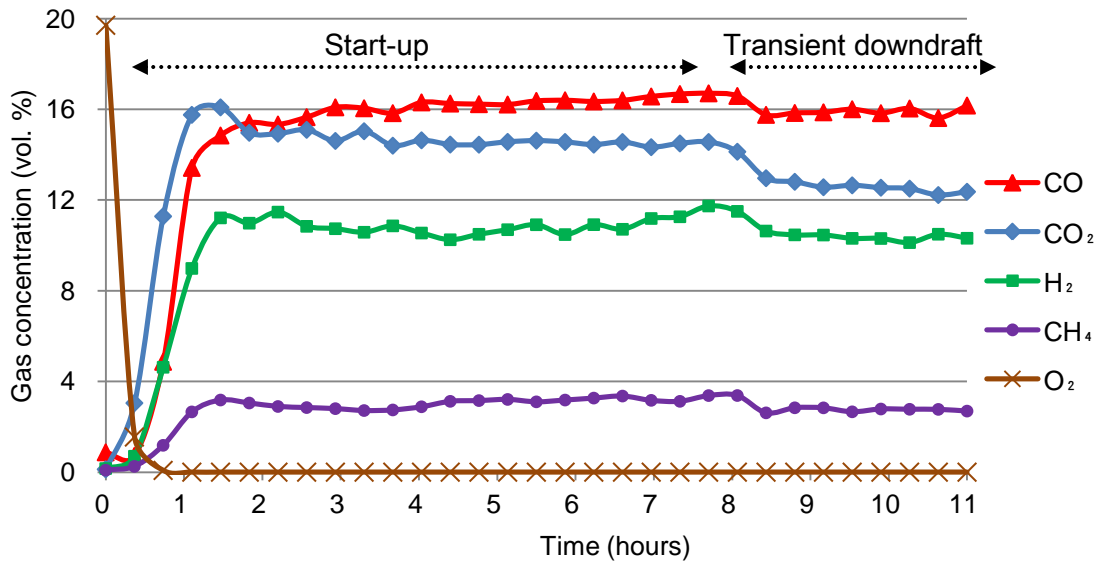


Figure 5-2(c). Syngas compositions during start-up and transient downdraft biomass gasification.

5.3.2 Temperature and gas compositions during co-gasification

As noted during biomass gasification, temperature increased sharply during start-up (Figure 5-3(a)). Peak temperatures reached 1,100 °C on average while maximum temperature during gasification of biomass was around 850 °C. Target bed height of 1000 mm was attained after 10 hours. During stabilization of the downdraft mode, temperature at the top parts increased while temperature at the bottom parts slightly decreased. Steady state condition was attained 2.5 hours later. As indicated in Table 5-2, during counter-flow *CFL-1* and *CFL-2* only were conducted. Temperatures were slightly high during co-gasification, however they followed the similar trend as it was the case for biomass gasification (Figure 5-3(b)).

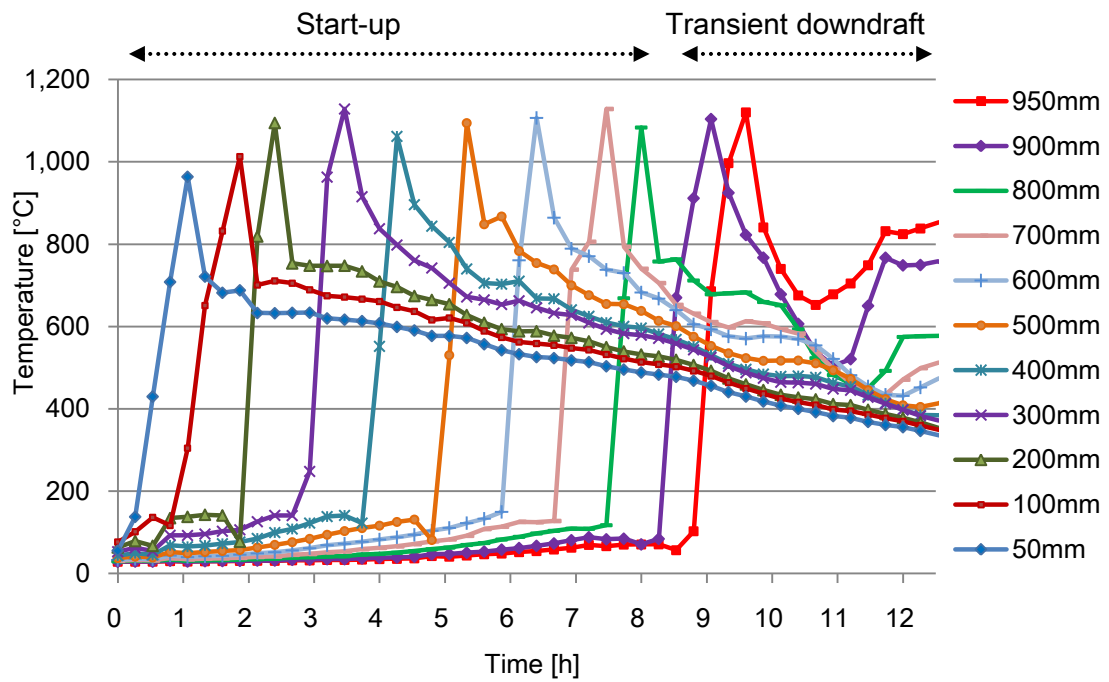


Figure 5-3(a). Temperature variations during start-up and transient downdraft co-gasification of biomass with coal.

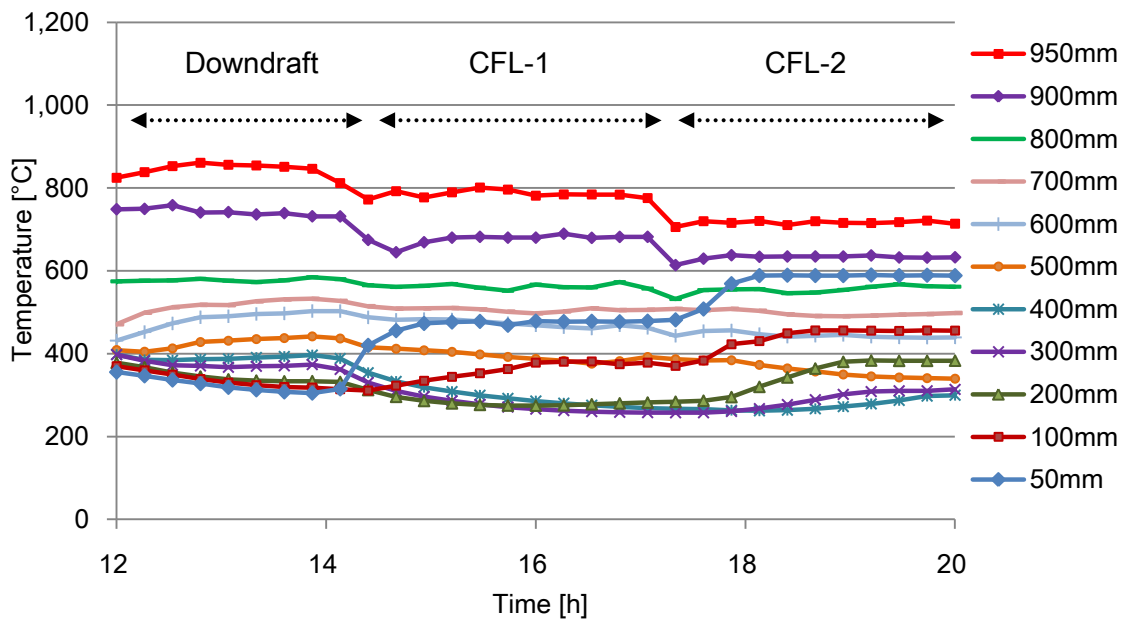


Figure 5-3(b). Temperature variations during downdraft and counter-flow co-gasification of biomass with coal.

Figure 5-3(c) shows syngas compositions during start-up and the transient downdraft operation periods. Syngas concentrations also show the similar trend as syngas for biomass gasification however concentrations of individual gases were slightly low. During downdraft gasification, syngas was composed of about 14% CO, 11.5% CO₂, 10.2% H₂ and 2.4% CH₄ (Figure 5-3(c)). Gas analysis and sampling was also conducted during *CFL-1* and *CFL-2*. As noted during counter-flow biomass gasification, CO, H₂ and CH₄ decreased upon further increase in updraft air.

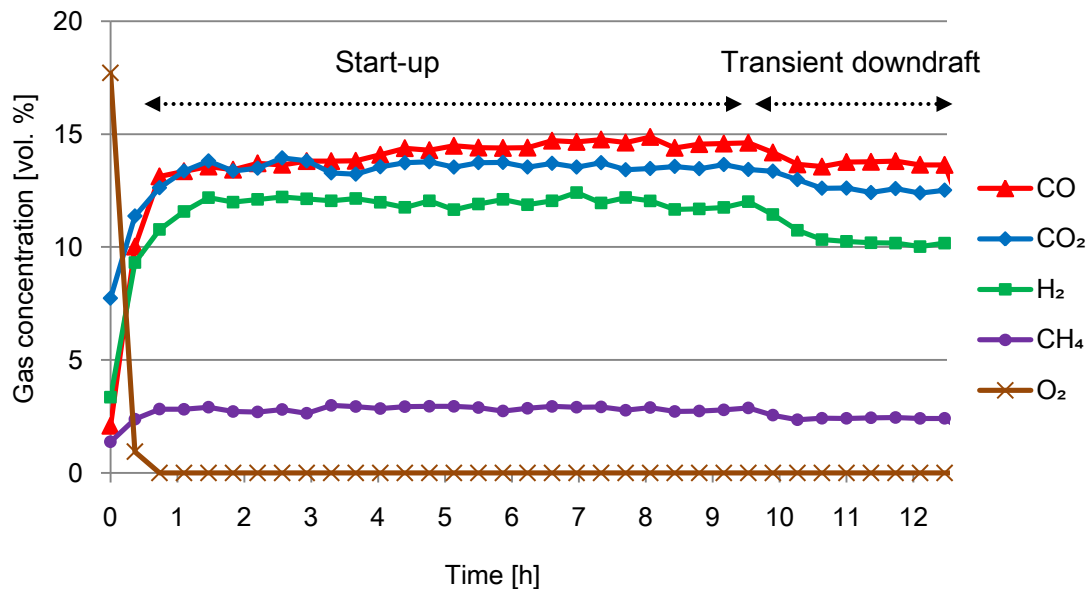


Figure 5-3(c). Syngas compositions during start-up and transient downdraft co-gasification of biomass with coal.

5.3.3 Temperature and gas inside the gasifier

Steady state reactor temperatures at various bed heights during gasification and co-gasification cases are presented in Figure 5-4(a) and Figure 5-4(a), respectively. In both cases, temperature during downdraft mode is shown as a

slanting line with the peak temperature at the top, that's where partial oxidation takes place. The same figure shows bell-type temperature profiles for all counter-flow modes. Temperatures were slightly high during co-gasification. High temperature occurred at the top of the reactor where primary partial oxidation generates heat for driving the pyrolytic reactions and primary reduction of the charred biomass. Likely, the final stage oxidation that occurred at the lower part of the reactor, generated heat for secondary char reduction in addition to heat for thermal cracking of the tars [2,8].

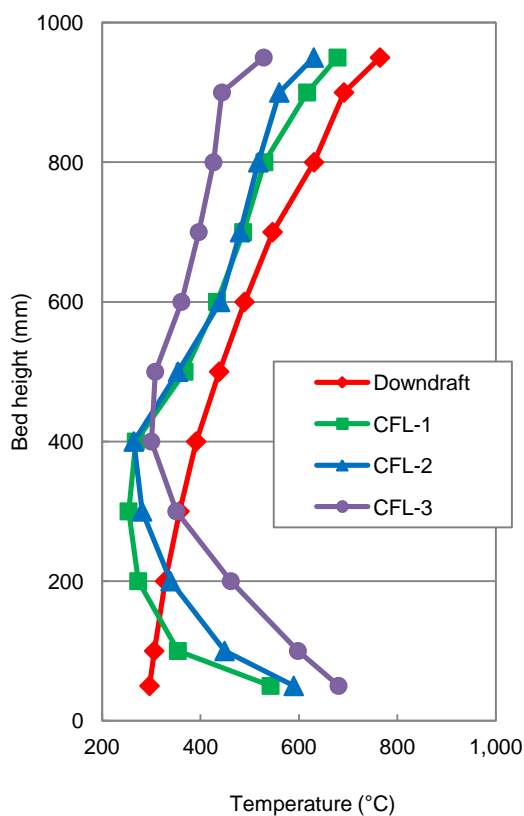


Figure 5-4(a)

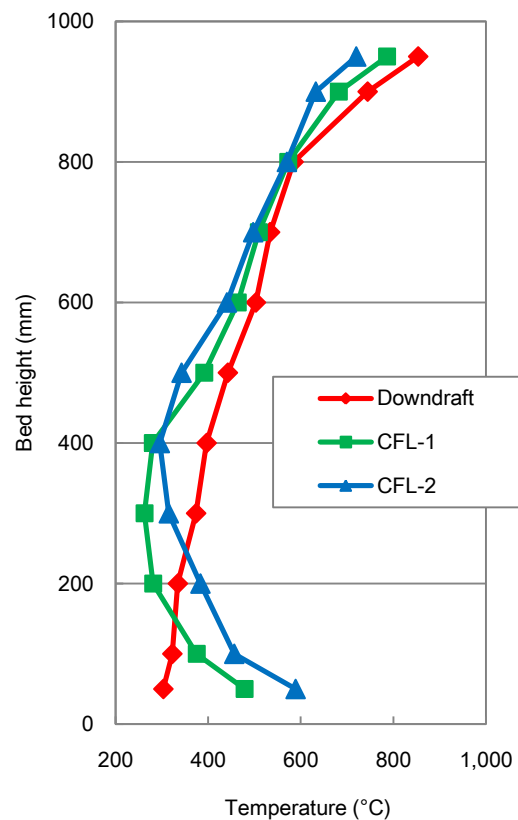


Figure 5-4(b)

Figure 5-4. Temperature profiles inside the reactor during; (a) gasification (b) co-gasification.

Gas composition in the reactor during downdraft gasification and co-gasification, are presented in Figure 5-5(a) and Figure 5-5(b), respectively. These figures indicate that CO_2 , CO , H_2 and CH_4 were generated at the top part of the reactor due to pyrolytic reactions and partial oxidation. Then compositions of CO , H_2 and CH_4 tend to increase slightly up to the middle of the reactor owing to occurrence of the reduction reactions [8,9]. However no significant change in gas compositions occurred between the middle of the reactor and the bottom, signifying that less or no further gasification reactions took place at lower parts. Due to lack of information on coal gasification behavior, it is difficult to discuss synergetic effects.

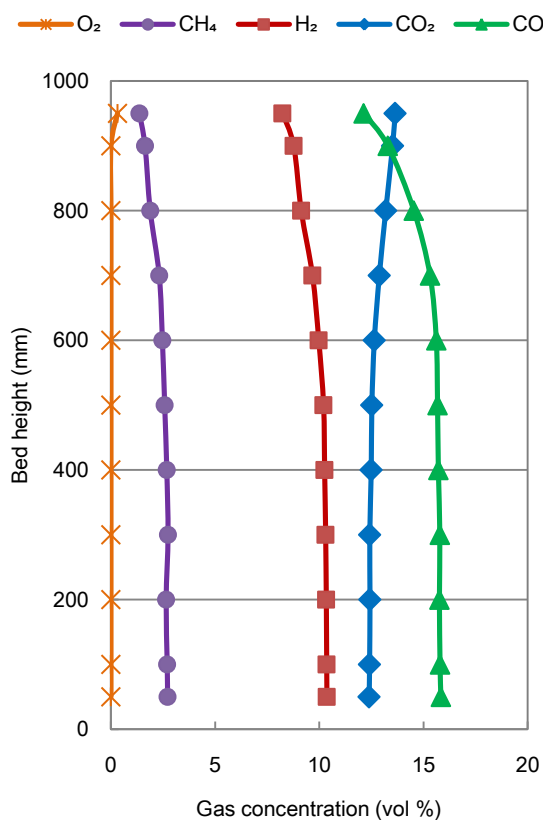


Figure 5-5(a)

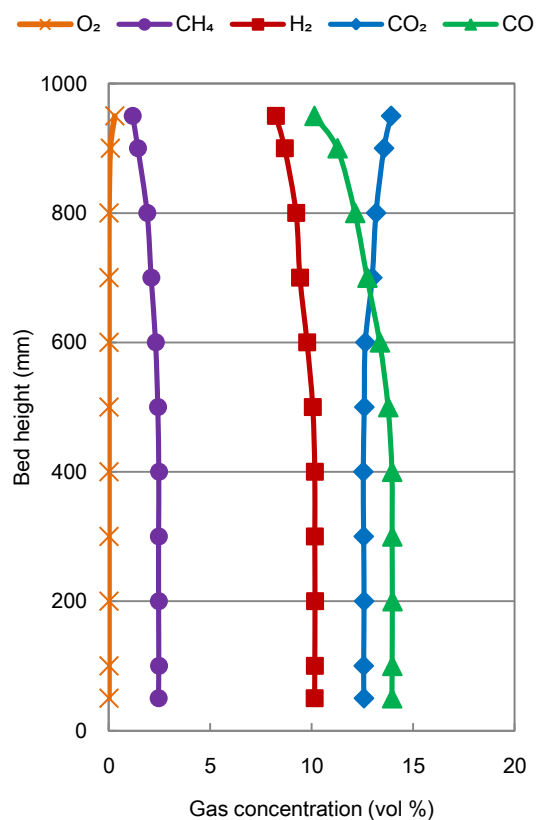


Figure 5-5(b)

Figure 5-5. Syngas compositions inside the reactor during downdraft: (a) gasification (b) co-gasification.

During gasification and co-gasification under CFL-1 conditions, significant generation of CO_2 , CO , H_2 and CH_4 also occurred at the top part of the reactor as it was the case for downdraft operation. Figure 5-6 also suggests that pyrolysis and oxidation zone and reduction zone occurred between the top parts of the reactor. For the lower part of the reactor, gas composition increases with bed height indicating occurrence of secondary oxidation as well as gasification reactions. At the middle of the reactor, say between 400 mm and 600 mm bed heights, gas composition was likely affected by circulating gas flows before the syngas escaped through the exit located at 500 mm. From these results it is also difficult to discuss synergy effects.

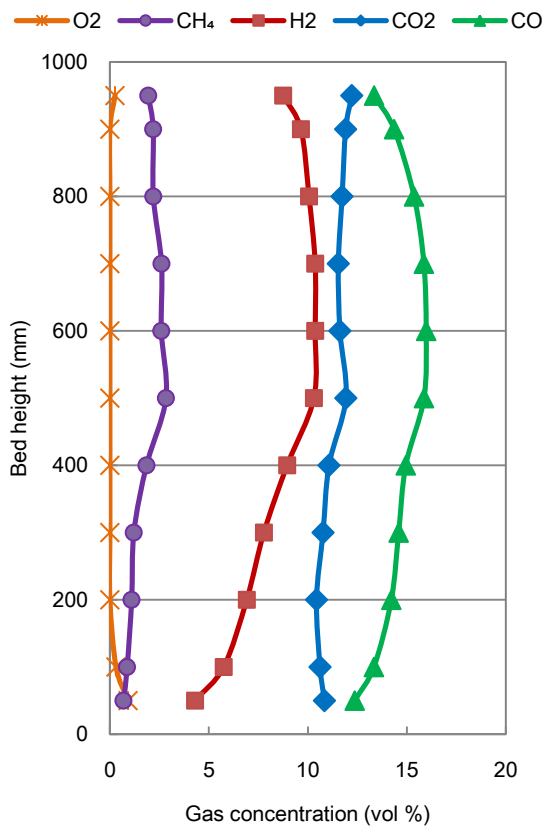


Figure 5-6(a)

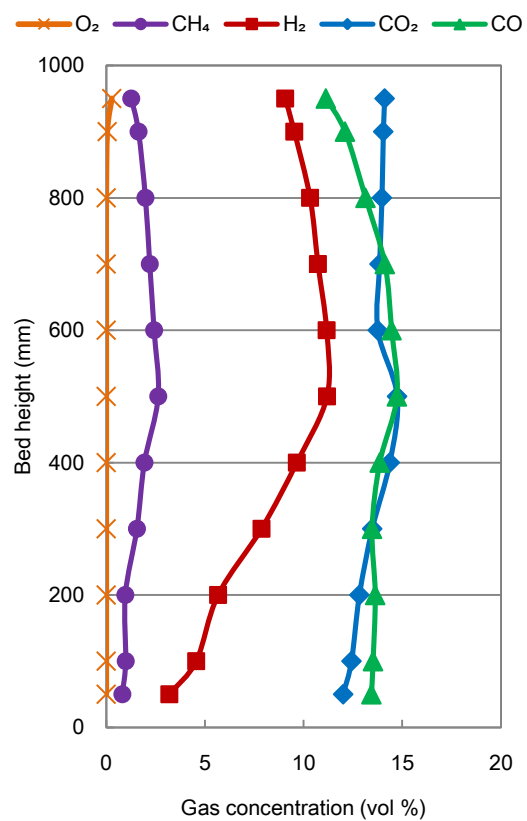


Figure 5-6(b)

Figure 5-6. Syngas compositions inside the reactor during CFL-1 operation; (a) gasification (b) co-gasification.

5.3.4 Tar contents and performance factors

Tar contents during gasification and co-gasification, are presented in Figure 5-7(a). Tar generation during biomass gasification increased slightly after changing from downdraft to CFL-1. Lower tar generation during downdraft can be linked to longer residence time taken by the tars to pass through the 1,000 mm hot packed charred fuel inside the reactor [2,8]. The corresponding reaction path is limited to 500 mm during CFL-1. However, by increasing updraft air, tar was reduced to the lowest value of around $5.17 \text{ g/m}^3_{\text{N}}$, obtained during CFL-3. During co-gasification, tar reduction was achieved in all counter-flow modes. Assuming tar generation from sub-bituminous coal used is negligible compared to biomass [5], averagely expected tar content is also presented in Figure 5-7(a). Apparently, tar generation during co-gasification is less than the expected average tar generation. This difference indicates occurrence of synergetic effect on tar reduction.

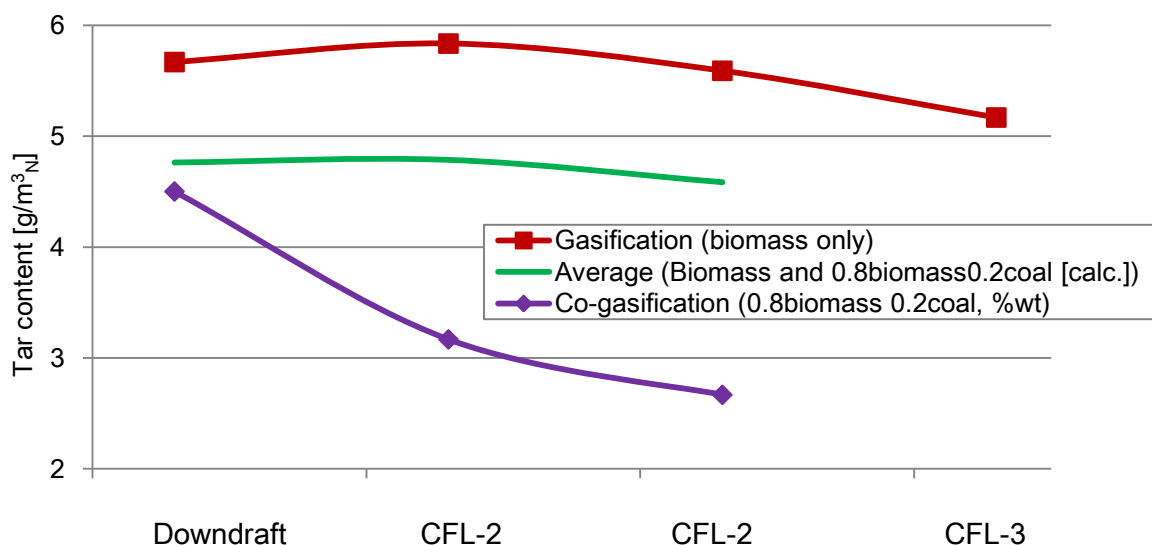


Figure 5-7(a). Tar content during counter-flow gasification and co-gasification.

Lower heating value (LHV) during gasification and co-gasification, are presented in Figure 5-7(b). LHV of the syngas produced during biomass gasification was 4.12 MJ/m³_N for downdraft case and increased to 4.28 MJ/m³_N during CFL-1 operation. However, further increase in updraft air during biomass gasification, lowered the syngas LHV to 3.65 MJ/m³_N realized during CFL-3. This is likely due to undesirable extensive oxidation of the low carbon content charred biomass at the lower part of the reactor. Similarly, during co-gasification experiments, syngas LHV varied from 3.74 MJ/m³_N to 4.01 MJ/m³_N and hence to 3.96 MJ/m³_N during downdraft, CFL-1 and CFL-2, respectively. Syngas LHV obtained under all counter-flow modes, are within the range of syngas LHV produced under normal downdraft and updraft modes [2,10]. Anyhow, synergetic effects cannot be discussed.

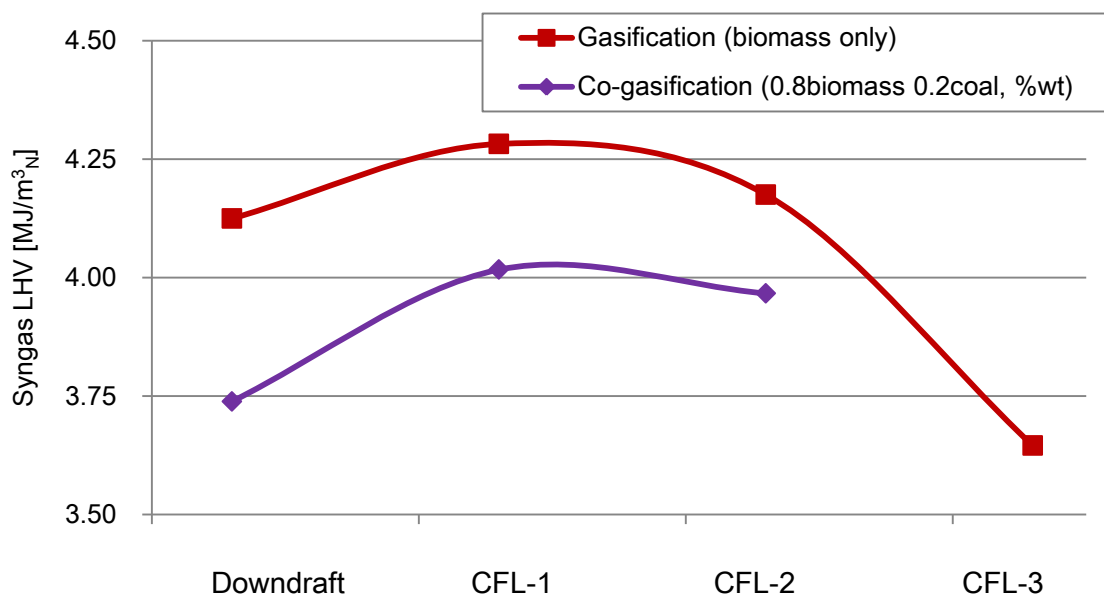


Figure 5-7(b). Syngas LHV during counter-flow gasification and co-gasification.

Figure 5-7(c) and Figure 5-7(d) shows cold gas efficiency and carbon conversion during counter-flow gasification and co-gasification. Due to a direct relationship as given in Equation (5-2), Cold gas efficiency shows a similar trend with syngas LHV. The highest efficiency was realized to be 77% during gasification and 73% during co-gasification (Figure 5-7(c)). On the other hand, carbon conversion increased with updraft air (Figure 5-7(d)). The lowest carbon conversion was about 84% during downdraft gasification and 70% during downdraft co-gasification. These figures suggest that higher carbon conversion does not necessarily result into proportional higher cold gas efficiency [1,11]. As a typical auto-thermal gasification process, the difference between carbon conversion and CGE indicates biomass energy spent for exothermic partial oxidation reactions which supply necessary energy to drive endothermic pyrolytic and reduction reactions. Synergy cannot be discussed from these results.

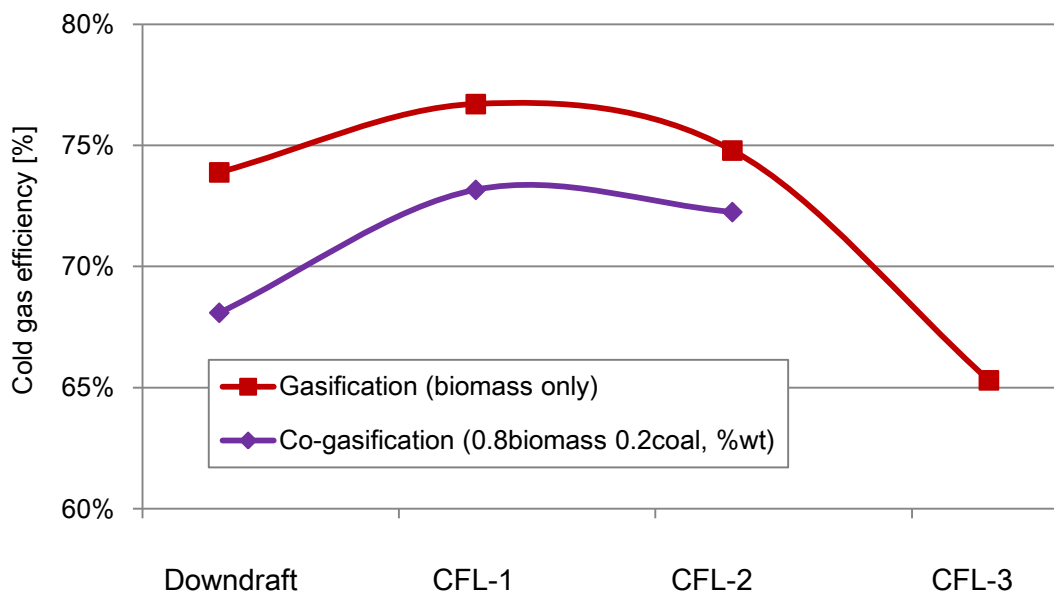


Figure 5-7(c). Cold gas efficiency during counter-flow gasification and co-gasification.

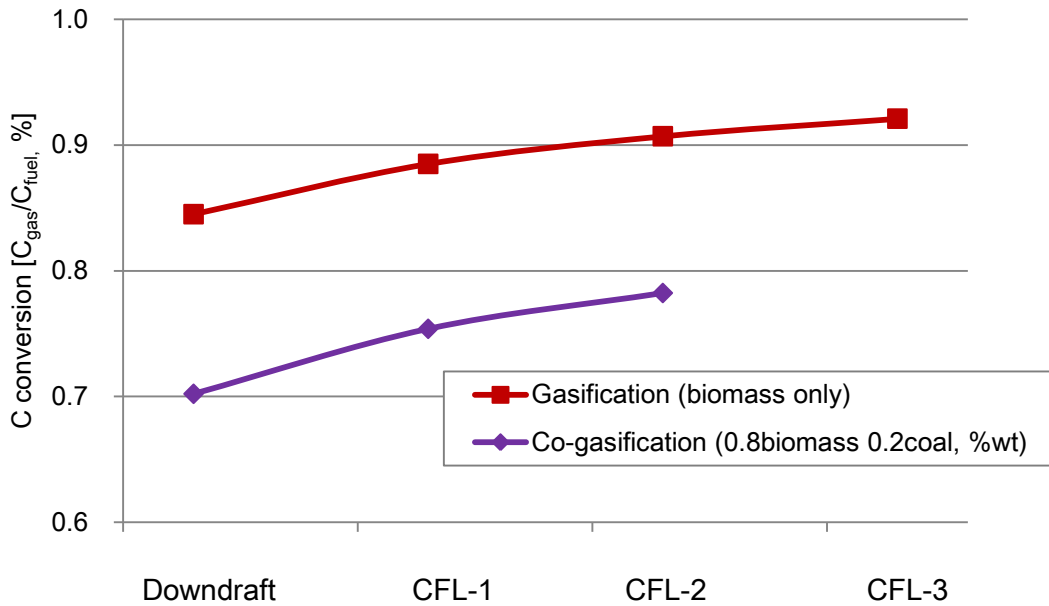


Figure 5-7(d). Carbon conversion during counter-flow gasification and co-gasification.

Consideration of the results presented in Figure 5-7, optimal counter flow can be realized. Figure 5-7(a) shows that increasing the updraft air supply, reduced the tar generation. However, Figure 5-7(b) shows that syngas LHV was adversely affected. A similar trend was observed by Wang *et al.* who concluded that tar cracking and improvement of syngas LHV appear to trade-off each other [1]. CFL-1 mode realized highest syngas LHV during both, gasification and co-gasification experiments and corresponding tar contents were observed to be moderate. Figure 5-7(c) and Figure 5-7(d), also confirms CFL-1 as an optimum counter-flow mode under which the highest cold gas efficiency was realized at a moderate carbon conversion.

5.1 Summary

A combination of downdraft and updraft gasification i.e. *counter-flow gasification* was investigated. Comparison of gasification of biomass and co-gasification of biomass with coal conducted by using counter-flow method was discussed. Analyses performed include syngas composition, tar generation as well as temperature profiles and gas concentration in the reactor. Performance factors such as syngas LHV, cold gas efficiency and carbon conversion are also presented. In addition to that, some synergetic observations are discussed. The results obtained are summarized as follows;

- Tar reduction during counter-flow gasification was realized by increasing the updraft air.
 - However, further increase of updraft air adversely affects syngas LHV.
 - Tar cracking and improvement of syngas LHV compromise each other.
- Optimal counter-flow gasification condition was realized when:
 - Syngas LHV was 4.28 MJ/m³_N LHV and tar content of 5.84 g/m³_N.
 - Cold gas efficiency was about 77% while carbon conversion was 88%.
- Unexpected tar reduction was the synergetic observation during co-gasification of biomass and coal in the packed bed reactor.

References

- [1] Wang Y, Yoshikawa K, Namioka T, Hashimoto Y, Performance optimization of two-staged gasification system for woody biomass. *Fuel Processing Technology*, 2007, 88, 243–250.
- [2] Brandt P, Larsen E, Henriksen U, High Tar Reduction in a Two-Stage Gasifier.

- Energy and Fuels 2000, 14, 816-819.
- [3] Pérez JF, Melgar A, Benjumea PN. Effect of operating and design parameters on the gasification/combustion process of waste biomass in fixed bed downdraft reactors: An experimental study. *Fuel*, 2012, 96, 487-496.
- [4] Cao Y, Wang Y, Riley JT, Pan W-P, A novel biomass air gasification process for producing tar-free higher heating value fuel gas. *Fuel Processing Technology*. 2006, 87, 343 – 353.
- [5] Rezaiyan J, Cheremisinoff NP. *Gasification technologies: a primer for engineers and scientists*. Boca Raton: Taylor and Francis, 2005.
- [6] Howaniec N, Smolinski A, Stanczyk K, Pichlack M. Steam co-gasification of coal and biomass derived chars with synergy effect as way of hydrogen-rich gas production. *International Journal of Hydrogen Energy*, 2011, 36, 14455-14463.
- [7] Kumabe K, Hanaoka T, Fujimoto S, Minowa T, Sakanishi K, Co-gasification of woody biomass with steam. *Fuel*, 2007, 86, 684-689.
- [8] Chen Y, Luo Y-H, Wu W-G, Su Y, Experimental Investigation on Tar Formation and Destruction in a Lab-Scale Two-Stage Reactor. *Energy Fuels* 2009, 23, 4659-4667.
- [9] Bunt JR, Waanders FB. Identification of the reaction zones occurring in a commercial-scale Sasol-Lurgi FBDB gasifier. *Fuel* 2008, 87, 1814-1823.
- [10] Yoon HC, Cooper T, Steinfeld. Non-catalytic gasification of woody biomass. *International Journal of Hydrogen Energy*, 2011, 36, 7852-7860.
- [11] Thunman H, Niklasson F, Johnsson F, Leckner B. Composition of Volatile Gases and Thermochemical Properties of Wood for Modeling of Fixed or Fluidized Beds. *Energy Fuels* 2001, 15, 1488-1497.

Chapter 6

Conclusions

The objective of this research is to investigate co-gasification characteristics of biomass and coal. Thermo-gravimetric methods have been used to study conversion characteristics, gas evolution and morphology changes. Based on the results obtained, occurrence of synergy was confirmed, quantified and the underlying mechanism was discussed. Also, the packed bed reactor has been used for investigating gas composition, temperature variations and tar contents. Syngas LHV, cold gas efficiency and carbon conversion were also analyzed. In addition, this study realized improvement of gasification method targeting at tar reduction and syngas LHV enhancement.

In Chapter 2, effects of gasification agents, i.e. CO₂ and steam, on conversion ratios and morphology changes during biomass gasification were investigated. To realize such effects, pyrolytic characteristics of biomass in N₂ atmosphere was taken as the basis for comparison. Summary of the results obtained is as follows:

- Biomass gasification is faster under steam environment than under CO₂ environment especially during char reduction stage.
- During gasification, enhanced conversion of biomass which occurs above 750 °C is contributed by porosity of well developed char matrix favoring diffusion of the gasifying agent and intrinsic gasification reactions.

In Chapter 3, comparison of co-gasification behavior with the average behavior calculated from the separate biomass gasification and coal gasification was presented. The contribution of volatile interaction and catalytic effects of AAEM were realized by using acid washed cellulose [9] that has high volatile matter and Na rich lignin. The following results were obtained;

- Two conversion synergetic peaks occur during co-gasification of biomass with coal; the first at around 400 °C and other peak occurred above 800 °C.
- Below 700 °C, H₂ release from biomass and coal blend was less than the average, indicating that biomass can serve as a hydrogen donor to coal.
- Co-gasification of acid washed cellulose with coal resulted into synergy confirming that synergy can occur under the influence of volatiles interactions.
- Morphology changes which occur during gasification contribute to gasification characteristics.

In Chapter 4, gasification of biomass in an auto-thermal packed bed reactor was investigated. Temperature profiles, syngas composition, tar generation as well as gas concentration in the reactor have been discussed. Performance factors such as syngas LHV, cold gas efficiency and carbon conversion have also been presented. The following findings were obtained;

- Updraft favorably produced higher syngas LHV though tar contents are unfavorably higher.
- Downdraft generated low tars but also low LHV due to longer residence time for tar cracking to occur inside the reactor.

- Higher conversion and efficiency for updraft gasification is due to higher CO production.
- Tar reduction is achievable by steam injection however at the sacrifice of syngas LHV.

In Chapter 5, a combination of downdraft and updraft gasification i.e. *counter-flow gasification* was investigated. Comparison of gasification of biomass and co-gasification of biomass with coal conducted by using counter-flow method was discussed. Analyses performed include syngas composition, tar generation as well as temperature profiles and gas concentration in the reactor. Performance factors such as syngas LHV, cold gas efficiency and carbon conversion have also been presented. In addition to that, some synergetic observations were discussed. The results obtained are summarized as follows;

- Tar reduction during counter-flow gasification was realized by increasing the updraft air.
 - However, further increase of updraft air adversely affects syngas LHV.
 - Tar cracking and improvement of syngas LHV compromise each other.
- Optimal counter-flow gasification condition was realized when;
 - Syngas LHV was 4.28 MJ/m³_N LHV and tar content of 5.84 g/m³_N.
 - Cold gas efficiency was about 77% while carbon conversion was 88%.
- Unexpected tar reduction was the only synergetic observation during co-gasification of biomass and coal in the packed bed reactor.

Acknowledgements

I would to extend my praises to Holy Lord, God the Almighty, who led me all the way to here.

I would like to dedicate my gratitude to my advisor, Prof. Ichiro Naruse for his generous support, encouragement and guidance throughout the course of this research, in both academic and but also social perspectives. I would express my sincere thanks to Associate Prof. Ryo Yoshiie for his outstanding advice and valuable discussion that kept me on track. I would also like to express my appreciation to Prof. Norihiko Yoshikawa and Prof. Hiroshi Yamashita, who gave distinguished contributions for my thesis.

I am obliged to acknowledge the Ministry of Education, Culture, Sports, Science and Technology (*mombu-kagaku-sho*) for facilitating this research in addition to my stay in Japan. I am thankful to the Japanese Embassy in Dar-es-Salaam for offering me the scholarship. Nagoya University through Graduate School of Engineering and International Student Centre provided a very conducive atmosphere for my study. I would like to acknowledge receiving some research fund from Hori Foundation. I am also grateful to the University of Dar es Salaam for a study leave.

I would like to give thanks to Prof. Iddi Mkilaha for advising and recommending me to study in Japan. I am thankful to Prof. Yadon Kohi for his concern on my career development. Also, Dr. Cuthbert Mhilu mentored me with the fundamental vision for post-graduate studies.

I am indebted to Dr. Yasuaki Ueki, Dr. Yoko Nunome, Dr. Slamet Raharjo, Mr.

Eiji Asakura and Mr. Takahiro Miwa for their support. My colleagues, Mr. Ono Hirofumi, Mr. Ryo Tamba and Mr. Toshiki Shimizu, helped me in conducting packed bed gasification experiments.

Lastly, but not least, I am thankful to my parents, my family, brothers and sisters for their support and consideration over the entire period of my study.

KIHEDU, Joseph

January 18th, 2013

論文目録
(Thesis List)

氏名 KIHEDU, Joseph

(発表した論文)

論文題目	公表の方法及び時期	著者
I. 学会誌等		
1. 木質バイオマスの CO ₂ および H ₂ O との反応特性 Reaction Characteristic of Woody Biomass with CO ₂ and H ₂ O.	鉄と鋼、2010、Vol. 96、No. 4、 pp 150–155 ISSN: 0021-1576	成瀬 一郎、 植木 保昭、 伊佐 山勉、 榛葉 貴紀、 Kihedu J.H., 義家 亮
2. Gasification characteristics of woody biomass in the packed bed reactor.	Proceedings of the Combustion Institute 2011, Vol. 33, pp 1795–1800. ISSN: 1540-7489	Ueki, Y., Torigoe, T., Ono, H., Yoshiie, R., Kihedu, J.H., Naruse, I.,
3. Conversion synergies steam during co-gasification of ligno-cellulosic biomass with coal.	Journal of Sustainable Bioenergy Systems, 2012, Vol. 2, No. 4, pp 97-103. ISSN: 2165-4018	Kihedu, J.H., Yoshiie, R., Nunome, Y., Ueki, Y., Naruse, I.,
4. Contribution of volatile interactions during co-gasification of biomass with coal.	Journal of Technology Innovations in Renewable Energy, 2013, (accepted)	Kihedu, J.H., Yoshiie, R., Nunome, Y., Ueki, Y., Naruse, I.,

II. 国際会議		
1. Co-gasification and co-pyrolysis of coal with biomass.	Proceedings of the 6 th Sino-Japan Symposium on Chemical Engineering, Chemical Industry and Engineering Society of China (CIESC) and Society of Chemical Engineers of Japan (SCEJ), June 2011, Wuhan - China, EN-O-03, pp EN9-EN12.	Kihedu, J.H., Ueki, Y., Yoshiie, R., Naruse, I.,
2. Synergies during co-gasification of biomass and coal; contribution of volatile-char interactions.	Proceedings of the 2011 International Symposium on EcoTopia Science (ISETS '11), November 2011, Nagoya, Japan, 10C02-06(7046) pg 34.	Kihedu, J.H., Yoshiie, R., Ueki, Y., Naruse, I.,
3. Conversion characteristics and particle morphology changes during co-gasification of coal and biomass.	2 nd International Conference on Mechanical and Industrial Engineering, February 2012, University of Dar es Salaam, Arusha, Tanzania, pp 109-116.	Kihedu, J.H., Yoshiie, R., Ueki, Y., Naruse, I.,
4. Counter-flow air gasification of woody biomass pellets in the auto-thermal packed bed reactor.	Proceedings of the 3 rd International Symposium on Gasification and its Application (iSGA-3), Canadian Society of Chemical Engineering, October 2012, Vancouver, Canada.	Kihedu, J.H., Yoshiie, R., Nunome, Y., Ueki, Y., Naruse, I.,

Ⅲ. その他		
1. Steam co-gasification characteristics of coal with biomass.	Proceedings of the 76 th Annual Meeting, Society of Chemical Engineers of Japan (SCEJ), March 2011, Tokyo, Japan I105, pg I-341.	Kihedu, J.H., Ueki, Y., Yoshiie, R., Naruse, I.,
2. Co-gasification of coal with biomass using steam and CO ₂ .	Proceedings of the 20 th Convention, Japan Institute of Energy (JIE), August 2011, Osaka, Japan, 3-7-2, pp 110-111.	Kihedu, J.H., Ueki, Y., Yoshiie, R., Naruse, I.,
3. Air gasification of biomass pellets in the auto-thermal packed bed reactor	Proceedings of the 44 th Autumn Meeting, Society of Chemical Engineers of Japan (SCEJ), Sendai, Japan, September 2012, pg M-217	Kihedu, J.H., Nunome, Y., Ueki, Y., Yoshiie, R., Naruse, I.,